

The thioredoxin redox charge as a measure of cell redox homeostasis in *Schizosaccharomyces pombe*

By

Tejal Bhagwandeem

BSc. (*Hons*) Genetics

Submitted in fulfilment of the academic requirements for the degree of Master of Science in the Discipline of Genetics, School of Life Sciences, College of Agriculture, Engineering and Science, University of KwaZulu-Natal, Pietermaritzburg, South Africa



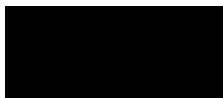
**UNIVERSITY OF
KWAZULU-NATAL**

**INYUVESI
YAKWAZULU-NATALI**

As the candidate's supervisor I, have approved this dissertation for submission

Supervisor: Dr C. S. Pillay

Signature:



Date: 29/9/2022

Preface

The research contained in this dissertation was completed by the candidate from January 2020 to December 2021 while based in the Discipline of Genetics, School of Life Sciences, College of Agriculture, Engineering and Science, University of KwaZulu-Natal, Pietermaritzburg, South Africa under the supervision of Dr C. S. Pillay.

These studies represent original work by the candidate and have not otherwise been submitted in any form to another University. Where use has been made of the work by other authors it has been duly acknowledged in the text.

Supervisor: Dr C. S. Pillay

Signature:



Date: 29/9/2022

College of Agriculture, Engineering, and Science

Declaration of Plagiarism

I, Tejal Bhagwandeem, declare that:

(i) the research reported in this dissertation, except where otherwise indicated or acknowledged, is my original work;

(ii) this dissertation has not been submitted in full or in part for any degree or examination to any other university;

(iii) this dissertation does not contain other persons' data, pictures, graphs or other information, unless specifically acknowledged as being sourced from other persons;

(iv) this dissertation does not contain other persons' writing, unless specifically acknowledged as being sourced from other researchers. Where other written sources have been quoted, then:

a) their words have been re-written but the general information attributed to them has been referenced;

b) where their exact words have been used, their writing has been placed inside quotation marks, and referenced;

(v) where I have used material for which publications followed, I have indicated in detail my role in the work;

(vi) this dissertation is primarily a collection of material, prepared by myself, published as journal articles or presented as a poster and oral presentations at conferences. In some cases, additional material has been included;

(vii) this dissertation does not contain text, graphics or tables copied and pasted from the Internet, unless specifically acknowledged, and the source being detailed in the dissertation and in the References sections.



Signature: Tejal Bhagwandeem

Date: 29/09/2022

Declaration Plagiarism 22/05/08 FHDR Approved

Abstract

Thiol-based redox systems play essential roles in repairing oxidatively damaged proteins, deoxyribonucleotide synthesis, sulfur metabolism, protein folding, and oxidant detoxification and signaling. The principal thiol systems in most cells are the thioredoxin (Trx) and the glutathione/glutaredoxin (GSH/Grx) systems. In the thioredoxin system, reducing equivalents from NADPH are transferred by thioredoxin reductase to thioredoxin, resulting in reduced thioredoxin. Thioredoxin in the reduced form further reduces target proteins and is itself consequently oxidized. Given the system's essential role in cellular physiology, inhibition of the thioredoxin system is an important drug target for communicable and non-communicable diseases. However, measuring the activity of the thioredoxin system *in vivo* is challenging. The thioredoxin redox charge (reduced thioredoxin/total thioredoxin) was proposed as a novel, surrogate measure of the thioredoxin system's activity and could be used as a general measure of the cellular redox state. Indeed, published data showed that the thioredoxin redox charge and cell viability collapsed if a chemical inhibitor directly targeted thioredoxin reductase. To evaluate the utility of the thioredoxin redox charge as a generic indicator of redox stress, the fission yeast *Schizosaccharomyces pombe*, was subjected to various stressors including hydrogen peroxide, heat, cadmium sulfate and potassium ferricyanide and the thioredoxin redox charge and cell viability were measured over time. We found dynamic changes in the thioredoxin redox charge profiles, in response to these stressors, but only obtained weak, positive correlations between the thioredoxin redox charge and cell viability. Thus, and in contrast to our initial hypothesis, the thioredoxin redox charge appeared to be buffered in response to high-stress perturbations, even when cell viability was clearly inhibited. These results show that the redox poise of the thioredoxin system can presumably only be disrupted by direct inhibitors of the system. Future work should aim to elucidate the mechanisms underlying the preservation of the thioredoxin redox charge.

Acknowledgements

My sincere appreciation and gratitude go out to the following people upon completing my MSc thesis:

To my supervisor, Dr Ché Pillay, thank you for your constant support and guidance right from the very beginning, and for patiently nurturing me into the scientist that I am today. The passion and zeal that you have for your field of work are an inspiration to me and I will always fondly remember my years spent in your lab.

My heartfelt thanks to my lab mates of Lab B23, both former and current: Diane and Keli for teaching me the art of western blotting and for always being eager to share in my highs and woes when it came to all things blotting-related, Nolyn for kindly showing me how to produce and purify protein, Limpho and Erin for the interesting discussions and laughs and Chris for useful input on my presentations. I appreciate all the good times and I am so thankful for all your advice, help and contributions to this work. Knowing that I always had supportive people to chat with, made research so much easier. Thank you to the technical team Megan, Jessica, Q and Noma for all the practical help and equipment in the lab, to Pat Joubert for all the lab orders and to Jothi, Sibongile and Charmaine for the admin assistance. Thank you to the Biochemistry department for letting me use their equipment and thank you to the University of KwaZulu-Natal for awarding me scholarships throughout my years of study and the National Research Foundation for the scholarships that supported this research.

To my dogs, Princey, Pixie, Pablo and my late Pooksie, thank you for always welcoming me home with such excitement and unconditional love, and for always brightening up my mood and easing my stress. To my late grandmothers Argie and Nani, thank you for your wisdom, I will always carry your memory with me. To my best friend Jo'Hara, thank you for more than a decade of friendship and for always being so compassionate and caring. To my other half Milesh, thank you for simply being my constant. I cannot imagine my life without you and I am so grateful to have you. I cannot wait for what our future holds. To my baby sisters Payal and Yukta, thank you for adding color to my life and for teaching me how to be selfless and responsible. To my mum Shakti and my dad Vinnay, I am so thankful to come from a family with an unshakable foundation that you built, and for your never-ending support. Thank you for enabling me to pursue my passion. Bab, thank you for always being my moral compass and for being such a superb example of a dedicated work ethic. Mum, thank you for always being present, no matter what, and for loving all of us so fiercely. Everything I am, I owe to you.

Table of Contents

Preface.....	i
Declaration of Plagiarism	ii
Abstract.....	iii
Acknowledgements.....	iv
Table of Contents.....	v
List of Abbreviations	x
List of Tables	xiii
List of Figures.....	xiv
Chapter 1: Literature Review.....	1
1.1 Introduction.....	1
1.2 Major thiol based redox signaling systems	3
1.3 The thioredoxin system is a key intracellular redox regulatory system.....	3
1.3.1 Thioredoxin and thioredoxin reductase structure and activity	5
1.4 General functions of the thioredoxin system.....	6
1.4.1 Oxidative stress response.....	6
1.4.2 Methionine sulfoxide reduction.....	7
1.4.3 Ribonucleotide reductase synthesis	8
1.5 Thioredoxin system functions limited to bacteria, yeast and bacteriophages	9
1.5.1 Sulfate assimilation.....	9
1.5.2 Filamentous phage assembly in bacteriophages	10
1.5.3 DNA metabolism in bacteriophage T7	10
1.6 Thioredoxin system functions in mammals	10
1.7 The glutathione/glutaredoxin system is an alternate redox regulatory system to the thioredoxin system in microbes.....	12
1.7.1 The glutathione/glutaredoxin system.....	12

1.7.2 Glutathione/glutaredoxin and the thioredoxin systems' functional overlap in <i>E. coli</i>	14
1.7.3 Glutathione/glutaredoxin and the thioredoxin systems' functional overlap in <i>S. cerevisiae</i> and <i>S. pombe</i>	14
1.8 The thioredoxin system as a drug target	15
1.8.1 Auranofin	17
1.8.2 Ebselen	19
1.9 System-level properties of the thioredoxin system	21
1.10 The thioredoxin redox charge – A novel assay to quantify the thioredoxin system?	21
1.11 Aims of study	23
Chapter 2: Quantifying the thioredoxin redox charge	24
2.1 Introduction	24
2.1.1 DTNB and insulin reduction assays	24
2.1.2 Genetically encoded fluorescent redox biosensors	25
2.1.3 Gel-shift assays and immunoblotting	26
2.2 Materials	29
2.2.1 Culture media and stock reagent preparation	29
2.2.1.1 Luria-Bertani (LB) broth and agar	29
2.2.1.2 Edinburgh Minimal Medium (EMM) broth	30
2.2.1.3 Yeast extract with 5 amino acid supplements (YE5S) agar	31
2.2.1.4 Kanamycin stock	31
2.2.1.5 Isopropyl β -D-1-thiogalactopyranoside (IPTG) stock	31
2.2.1.6 Dithiothreitol (DTT) stock	31
2.2.1.7 Ammonium persulfate (APS) solution	31
2.2.1.8 SDS-PAGE loading buffer (4 \times)	31
2.2.1.9 (1 \times) Laemmli SDS-PAGE tank buffer	31
2.2.1.10 Laemmli SDS-PAGE - Tris lower gel buffer	31
2.2.1.11 Laemmli SDS-PAGE - Tris upper gel buffer	32

2.2.1.12	Coomassie blue stain.....	32
2.2.1.13	Destaining solution one.....	32
2.2.1.14	Destaining solution two	32
2.2.1.15	Lysis buffer	32
2.2.1.16	Equilibration buffer.....	32
2.2.1.17	Wash buffer.....	32
2.2.1.18	Dialysis buffer.....	33
2.2.1.19	IAM alkylation buffer	33
2.2.1.20	NEM alkylation buffer	33
2.2.1.21	PEG-maleimide alkylation buffer	33
2.2.1.22	AMS alkylation buffer	33
2.2.1.23	AIS alkylation buffer	33
2.2.1.24	(1×) Tris-Tricine SDS-PAGE anode tank buffer	33
2.2.1.25	(1×) Tris-Tricine SDS-PAGE cathode tank buffer	34
2.2.1.26	Tris-Tricine SDS-PAGE gel buffer	34
2.2.1.27	Acrylamide stock solutions.....	34
2.2.1.28	(1×) Transfer buffer	34
2.2.1.29	Ponceau S stain	34
2.2.1.30	Tris-buffered saline with TWEEN 20 (TBST)	34
2.2.1.31	BSA stock solution	34
2.2.1.32	Primary antibody dilution (0.5 µg/ml).....	34
2.2.1.33	Secondary antibody dilution (1:20 000)	35
2.3	Methods.....	35
2.3.1	Induction and production of recombinant <i>S. pombe</i> Trx1	35
2.3.2	Sonication	36
2.3.3	Ni-NTA affinity purification	36
2.3.4	Dialysis	37

2.3.5 Alkylation of purified, recombinant <i>S. pombe</i> Trx1	37
2.3.6 Harvesting concentrated <i>S. pombe</i> protein	38
2.3.7 Protein extraction from <i>S. pombe</i>	39
2.3.8 Western blotting of <i>S. pombe</i> Trx1	40
2.4 Results	42
2.4.1 Production and purification of recombinant <i>S. pombe</i> Trx1	42
2.4.2 Alkylation optimization of recombinant <i>S. pombe</i> Trx1	45
2.4.3 Optimization of the redox western blotting assay for <i>S. pombe</i> Trx1 for <i>in vivo</i> stressor experiments	48
2.5 Discussion	53
Chapter 3: Conservation of the thioredoxin redox charge in <i>Schizosaccharomyces pombe</i> ...	56
3.1 Introduction	56
3.2 Materials.....	59
3.3 Methods.....	59
3.3.1 <i>S. pombe in vivo</i> stress test experiments.....	59
3.3.2 Protein extraction and redox western blotting of <i>S. pombe</i> JB35 Trx1	60
3.3.3 Measuring <i>S. pombe</i> cell viability using the 3-(4,5-dimethylthiazol-2-yl)-2,5- diphenyltetrazolium bromide (MTT) reduction assay	60
3.3.4 Computational analyses of data	61
3.4 Results	62
3.4.1 Evidence of potential correlation from the literature between the thioredoxin redox charge and cell viability.....	62
3.4.2 Cell viability and the thioredoxin redox charge quantified in unstressed <i>S. pombe</i> JB35	64
3.4.3 Cell viability and the thioredoxin redox charge quantified in <i>S. pombe</i> JB35 stressed with hydrogen peroxide (H ₂ O ₂).....	67
3.4.4 Cell viability and the thioredoxin redox charge quantified in <i>S. pombe</i> JB35 stressed with heat, cadmium sulfate (CdSO ₄) and potassium ferricyanide [K ₃ Fe(CN) ₆]	72

3.5 Discussion	78
Chapter 4: General discussion and conclusion	83
Reference List	84
Appendix.....	111

List of Abbreviations

AIS	4-acetamido-4'-[(iodoacetyl)amino]stilbene-2,2'-disulfonic acid
AMS	4-acetamido-4'maleimidylstilbene-2,2'-disulfonic acid
AP-1	Activator protein-1
APS	Ammonium persulfate
ASK1	Apoptosis signal-regulating kinase-1
ATP	Adenosine triphosphate
BCA	Bicinchoninic acid
BSA	Bovine serum albumin
DTNB	5,5-dithio-bis-(2-nitrobenzoic acid)
DTT	Dithiothreitol
ELISA	Enzyme-linked immunosorbent assay
EMM	Edinburgh minimal medium
ETC	Electron transport chain
FAD	Flavin adenine dinucleotide
GAPDH	Glyceraldehyde 3-phosphate dehydrogenase
GR	Glutathione reductase
Grx	Glutaredoxin
GSH	Glutathione
Hif-1	Hypoxia-inducible factor 1
IAM	Iodoacetamide
IPTG	Isopropyl β -D-1-thiogalactopyranoside
LUCA	Last universal common ancestor
MAPK	Mitogen-activated protein kinase

Met	Methionine
MetO	Methionine sulfoxide
MRSA	Methicillin-resistant <i>Staphylococcus aureus</i>
Msrs	Methionine sulfoxide reductases
MTT	3-(4,5-dimethylthiazol-2-yl)-2,5-diphenyltetrazolium bromide
MWCO	Molecular weight cut-off
MWM	Molecular weight marker
NADPH	Nicotinamide adenine dinucleotide phosphate
NEM	N-Ethylmaleimide
NF- κ B	Nuclear factor-kappa B
Ni-NTA	Nickel-charged nitriloacetic acid affinity resin
Ox.	Oxidized
PAPS	3'-phosphoadenylylsulfate
PEBP2/CBF	Polyomavirus enhancer-binding protein 2/core binding factor
PEG-mal	Methoxypolyethylene glycol maleimide
Prx	Peroxiredoxin
PSH	Protein thiols
PSS	Protein disulfides
Red.	Reduced
Ref-1	Redox factor-1
RNR	Ribonucleotide reductase
ROS	Reactive oxygen species
rxRFP1	Redox-sensitive red fluorescent protein
SAPK	Stress-activated protein kinase

SDS	Sodium dodecyl sulfate
SELEX	Systematic Evolution of Ligands
Srx1	Sulfiredoxin
TBST	Tris-buffered saline with TWEEN 20
TCA	Trichloroacetic acid
TEMED	N, N, N', N'-Tetramethylethylenediamine
TGR	Thioredoxin glutathione reductase
TNB	5-thio-2-nitrobenzoic acid
Tpx1	Thiol-specific peroxidase 1
Trx	Thioredoxin
Trx1	Thioredoxin 1
TrxR	Thioredoxin reductase
TrxSH	Reduced thioredoxin
TrxSS	Oxidized thioredoxin
TSA	Thiol-specific antioxidant
YE5S	Yeast extract with 5 amino acid supplements

List of Tables

Table 1.1 Diseases and therapeutics involving the thioredoxin system.....	16
Table 2.1 Preparation of 23% (w/v) Laemmli SDS-PAGE acrylamide gel	38
Table 2.2 Preparation of 25% (w/v) Tris-Tricine SDS-PAGE acrylamide gel.....	38
Table 2.3 Preparation of 22% (w/v) Urea Tris-Tricine SDS-PAGE acrylamide gel.....	40
Table 3.1 Correlation analyses and their coefficients calculated between the thioredoxin redox charge and cell death for ebselen and silver treated <i>E. coli</i> DHB4 (Zou <i>et al.</i> , 2017)	63
Table 3.2 Stressors and concentrations used in the <i>S. pombe</i> stressor experiments	64
Table 3.3 Correlation analyses and their coefficients calculated between the thioredoxin redox charge and cell viability for unstressed <i>S. pombe</i> JB35.....	66
Table 3.4 Correlation analyses and their coefficients calculated between the thioredoxin redox charge and cell viability for <i>S. pombe</i> JB35 stressed with hydrogen peroxide (H ₂ O ₂)	72
Table 3.5 Correlation analyses and their coefficients calculated between the thioredoxin redox charge and cell viability for <i>S. pombe</i> JB35 stressed with heat, cadmium sulfate (CdSO ₄) and potassium ferricyanide [K ₃ Fe(CN) ₆].....	77

List of Figures

Figure 1.1 Causes and consequences of reactive oxygen species (ROS) within cells.....	3
Figure 1.2 Thioredoxin (Trx) system mediated redox reactions from the reduced substrate to targeted proteins.....	4
Figure 1.3 Hydrogen peroxide (H ₂ O ₂) sensing mechanisms	7
Figure 1.4 The thioredoxin (Trx) system provides reducing equivalents for methionine sulfoxide reductases (Msrs) to catalyze methionine sulfoxide (MetO) reduction to methionine (Met).	8
Figure 1.5 Difference in mammalian thioredoxin reductase and <i>E. coli</i> thioredoxin reductase catalysis mechanisms	11
Figure 1.6 Glutathione/glutaredoxin (GSH/Grx) system mediated redox reactions from reduced substrate to targeted proteins	13
Figure 1.7 Chemical structure of auranofin	17
Figure 1.8 Chemical structure of ebselen	19
Figure 2.1 Reduction of 5,5-dithio-bis-(2-nitrobenzoic acid) (DTNB, also known as Ellman's reagent) by a free thiol group.....	24
Figure 2.2 Mechanism of action of alkylation on thioredoxin 1 (Trx1)	27
Figure 2.3 Recombinant <i>S. pombe</i> Trx1 protein sequence confirmation.....	42
Figure 2.4 Successful production and purification of His-tagged, recombinant <i>S. pombe</i> Trx1	44
Figure 2.5 Testing different alkylating agents to determine the most suitable alkylating agent to separate oxidized and reduced, <i>S. pombe</i> thioredoxin 1	47
Figure 2.6 Investigating the optimal combination of primary antibody concentrations and secondary antibody dilutions for linear signal detection of <i>S. pombe</i> JB35 Trx1, to be used in the redox western blotting assay	49
Figure 2.7 Control experiments for the redox western blotting assay to detect <i>S. pombe</i> JB35 Trx1.....	51
Figure 3.1 Experimental approach used to investigate the role of the thioredoxin system in response to stressors in <i>S. pombe</i> and its relation to cell viability.....	57

Figure 3.2 Evidence of a correlation between the thioredoxin (Trx) redox charge and cell death from data extrapolated from the literature..	63
Figure 3.3 Quantification of the thioredoxin (Trx) redox charge and cell viability (562 nm) of unstressed <i>S. pombe</i> JB35 over a 60-minute time course	65
Figure 3.4 Quantification of the thioredoxin (Trx) redox charge of <i>S. pombe</i> JB35 stressed with 100, 300, 500 and 1250 μ M hydrogen peroxide (H_2O_2), over 60-minute time courses	68
Figure 3.5 Quantification of the thioredoxin (Trx) redox charge and cell viability (562 nm) of <i>S. pombe</i> JB35 stressed with a range of hydrogen peroxide (H_2O_2) concentrations, over 60-minute time courses	70
Figure 3.6 Quantification of the thioredoxin (Trx) redox charge of <i>S. pombe</i> JB35 stressed with heat, cadmium sulfate ($CdSO_4$) and potassium ferricyanide [$K_3Fe(CN)_6$] over 60-minute time courses.....	73
Figure 3.7 Quantification of the thioredoxin (Trx) redox charge and cell viability (562 nm) of <i>S. pombe</i> JB35 stressed with heat, cadmium sulfate ($CdSO_4$) and potassium ferricyanide [$K_3Fe(CN)_6$], over 60-minute time courses	75
Figure 3.8 Summary phase plot of thioredoxin (Trx) redox charge and cell viability (measured at an absorbance of 562 nm) for all stressors tested.	78
Figure 3.9 Analysis of trends in the phase plot results of the thioredoxin redox charge and cell viability in <i>S. pombe</i> JB35 for potential correlations, in response to stress.....	80

Chapter 1: Literature Review

1.1 Introduction

Reduction oxidation (redox) biology is intrinsically involved in life. It encompasses the transfer of electrons between “electron-donating” (reductant) chemical species and “electron-receiving” (oxidant) chemical species (Franco and Vargas, 2018). In a more biological sense, redox reactions are involved in metabolism, cellular respiration, DNA replication and detoxification through protein modifications and cellular signaling. Redox reactions form part of essential systems within a cell that contribute to redox control and balance (Franco and Vargas, 2018, Sies, 2015).

Many models have been proposed to explain how life began, including RNA, metabolism-first, thermal vent, membrane and clay worlds (Lanier and Williams, 2017). However, all these models are unanimous in that they all lead to the emergence of the Last Universal Common Ancestor (LUCA). LUCA appeared 3.8 billion years ago when the Earth’s atmosphere was still anoxic. LUCA was anaerobic and depended on inorganic iron-sulfur oxidation that yielded electrons to serve in metabolic redox reactions (Cody, 2004, Miller *et al.*, 2018, Weiss *et al.*, 2018). Later, at around 3.5 to 3.2 billion years ago, evolution resulted in photosynthetic organisms splitting water and fixing carbon dioxide into carbohydrates using radiant energy from light. This process also released oxygen, which led to the Great Oxidation Event resulting in a surge in atmospheric oxygen levels as high as 35%, putting extraordinary pressure on life to adapt (Sessions *et al.*, 2009). The Great Oxidation Event was a milestone event in Earth’s history. Many existing microorganisms at the time did not have proper detoxification mechanisms to deal with toxic oxygen-derived reactive molecules. Some perished, others were forced to populate small anoxic niches in the environment or were pushed to evolve and strengthen detoxification mechanisms (Taverne *et al.*, 2018). Although the rapid increase in oxygen was deleterious for many microbes, it also facilitated aerobic respiration, which is far more energy-efficient than anaerobic respiration; the Great Oxidation Event was therefore, a double-edged sword. This primordial cataclysm, albeit detrimental to most life at the time, allowed for a new kind of aerobic life and initiated the development of eukaryotes (Miller *et al.*, 2018).

It is interesting to note that although LUCA developed in an anoxic environment, sequence analysis shows that LUCA could detoxify reactive oxygen species (ROS) (Slesak *et al.*, 2012). A lack of ozone in the atmosphere caused significant ultraviolet radiation exposure of the Earth, which split water leading to ROS formation. Therefore, the ability to react to

oxygen-derivatives is ancient and developed before the surge in atmospheric oxygen (Briehl, 2015).

Organisms able to withstand the detrimental effects of ROS-generating reactions could also efficiently generate energy with oxygen (Bailey, 2019, Murphy, 2009). The newly adapted eukaryotic cells utilized mitochondria specialist organelles to generate energy by oxidative phosphorylation. However, the by-products of this process were carbon dioxide and ROS (Bailey, 2019).

ROS are oxygen-containing chemical species such as superoxide anion (O_2^-), hydrogen peroxide (H_2O_2) and hydroxyl radicals ($\cdot OH$). These species can be generated by xenobiotics or intracellularly from oxidative metabolism and they can damage cellular constituents like DNA, lipids and proteins (Glasauer and Chandel, 2013). With excess ROS exposure, cells can become oxidatively stressed and damaged (Figure 1.1) (Cencioni *et al.*, 2013, Espinosa-Diez *et al.*, 2015, Kawagishi and Finkel, 2014). This stressed cellular state is counteracted by cellular antioxidant redox systems to combat the deleterious effects of high ROS levels (Davies, 2005, Forman *et al.*, 2009). A major shift in the redox biology field was the discovery that ROS in moderate concentrations play essential roles in eukaryotic cell signaling and metabolism; therefore antioxidant systems must be calibrated to maintain these species within specific limits (He *et al.*, 2017). This constant balancing act in a cell is carried out by essential systems that generate and eliminate ROS (Lennicke and Cochemé, 2021).

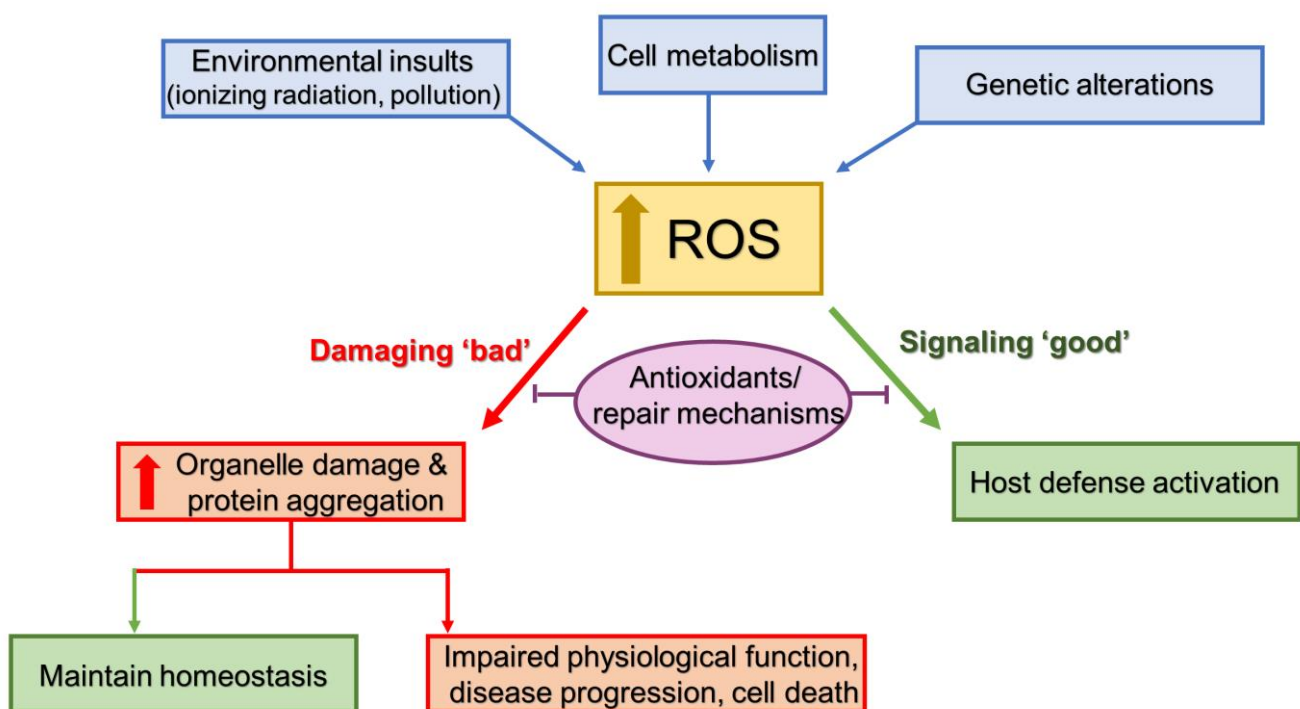


Figure 1.1 Causes and consequences of reactive oxygen species (ROS) within cells. *At low to moderate concentrations, intracellular oxidants act as signaling molecules that can initiate metabolism, host defense pathways, and intracellular signaling activation. On the other hand, cellular damage is caused by high, uncontrolled ROS levels (Adapted from Cencioni et al., 2013, Kawagishi and Finkel, 2014).*

Thiol-based redox systems have evolved to play essential roles in DNA synthesis, protein folding, and protein transport, in addition to cellular detoxification and signaling in the presence of ROS (Toledano *et al.*, 2007). ROS were shown to impact various amino acids with methionine, cysteine, histidine, tyrosine and tryptophan being particularly vulnerable to oxidative modifications (Davies, 2005, Sies *et al.*, 2017, Wang *et al.*, 2018). The principal sulfur-containing amino acids, cysteine and methionine are important redox facilitators because of their thiol group (Poole, 2015). The thiol group of cysteine is ionizable and this therefore increases cysteine's reactivity compared to the less reactive thioether form in methionine (Held, 2020, Poole, 2015). Thiol-based systems funnel reducing equivalents to protein targets to carry out the protein's specific function e.g. ribonucleotide reductase synthesis and the reduction of peroxiredoxins (Banerjee *et al.*, 2008). The principal thiol systems in most cells are the thioredoxin (Trx) and the glutathione/glutaredoxin (GSH/Grx) systems (Go and Jones, 2013).

1.2 Major thiol based redox signaling systems

The thioredoxin and the glutathione/glutaredoxin systems are near-universal, principal systems responsible for intracellular disulfide reduction, that drive a variety of essential cellular functions (Toledano *et al.*, 2013). These systems often have overlapping functions, although they also importantly occupy their own niche in basic life processes in various organisms (Carmel-Harel and Storz, 2000). It is important to understand how these systems complement and compare to one another, to fully shed light on the functioning of a single system. These systems will be discussed individually and also how their functions and roles intertwine.

1.3 The thioredoxin system is a key intracellular redox regulatory system

The thioredoxin system consists of thioredoxin (Trx), thioredoxin reductase (TrxR) and NADPH and is an integral intracellular antioxidant system (Balsera and Buchanan, 2019). It

also participates in thiol-disulfide reaction exchanges with many proteins and can affect multiple pathways such as ribonucleotide reductase synthesis and signaling pathways (Collet and Messens, 2010, Davies, 2005). Proximal cysteine residues may form disulfide bridges by a two-electron oxidation that leads to the reduced sulfhydryl (thiol) cysteines becoming oxidized cysteine residues i.e. S-H becoming S-S groups (Wiedemann *et al.*, 2020). It should be noted that a variety of intermediate oxidative post-translational modifications exist for the thiol group of cysteine including S-nitrosothiols, sulfenic acids, sulfinic acids, sulfonic acids, sulfenamides, persulfides and various disulfides (Alcock *et al.*, 2018, Fra *et al.*, 2017). Most oxidation modifications can be reversed and are generally attributed to thiol-based redox systems such as the thioredoxin system (Balsera and Buchanan, 2019). In the thioredoxin system, reducing equivalents are transferred from NADPH (generated from the pentose phosphate pathway) to thioredoxin in a reaction catalyzed by thioredoxin reductase (Figure 1.2). In turn, thioredoxin reduces specified target proteins via thiol-disulfide exchange resulting in functional and structural changes of the protein (Figure 1.2) (Balsera and Buchanan, 2019, Monteiro *et al.*, 2017).

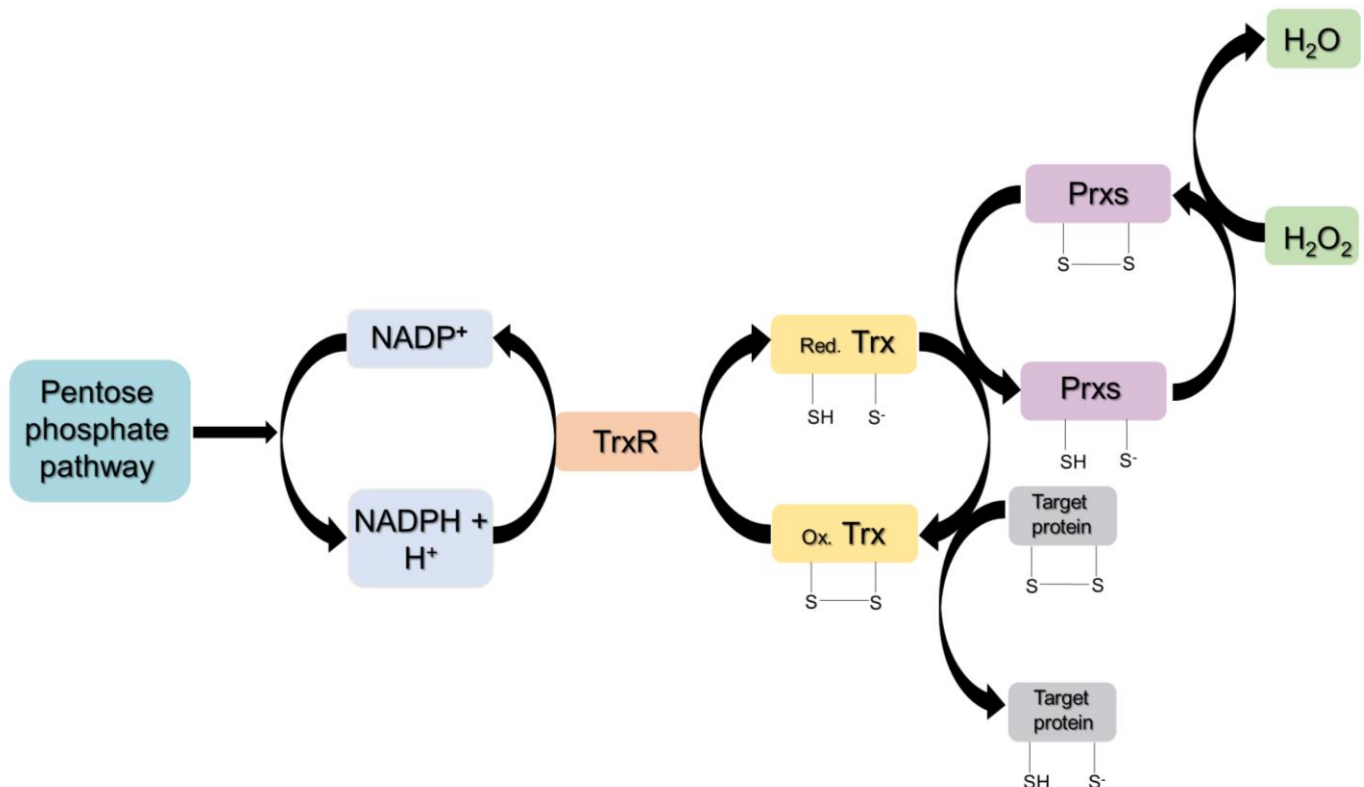


Figure 1.2 Thioredoxin (Trx) system mediated redox reactions from the reduced substrate to targeted proteins. Reducing equivalents are transferred from NADPH via thioredoxin reductase (TrxR) to oxidized thioredoxin (Ox. Trx) which becomes reduced

thioredoxin (Red. Trx). Reduced thioredoxin can then reduce oxidized disulfides in protein targets such as peroxiredoxins (Prxs) (Adapted from Balsera and Buchanan, 2019, Monteiro et al., 2017).

1.3.1 Thioredoxin and thioredoxin reductase structure and activity

Thioredoxin was first discovered in 1964 in *Escherichia coli* and was shown to be an electron source for reducing ribonucleotide reductase (Laurent *et al.*, 1964, Rollins *et al.*, 2010). Thioredoxins are 12 kDa redox proteins that may be cytosolic or mitochondrial and belong to the ubiquitous thioredoxin oxidoreductase protein family (Monteiro *et al.*, 2017, Nishinaka *et al.*, 2001). The protein core consists of five β strands, surrounded by four α helices and the sequence of the active site is cysteine-glycine-proline-cysteine (Arnér and Holmgren, 2000, Branco and Carvalho, 2019). The active attacking nucleophile in disulfide protein reduction is the N-terminal cysteine residue of the active site (Holmgren, 1995).

In the reduced form (Trx-(SH)₂), two thiol groups are present and thioredoxin can catalyze a single exposed disulfide reduction and then becomes oxidized (Pedrajas *et al.*, 1999). During its catalytic cycle, a mixed disulfide intermediate with a substrate is formed followed by thiol-disulfide exchange resulting in thioredoxin oxidation and reduction of the target substrate (Holmgren, 1995). The oxidized form of thioredoxin (Trx-S₂) contains an intramolecular disulfide bond, and undergoes reduction by flavoenzyme thioredoxin reductase and NADPH (Figure 1.2) (Koháryová and Kolárová, 2008). Thioredoxin regulates redox-sensitive molecules that govern critical cellular processes such as proliferation, apoptosis and metabolism by the reversible oxidation of thiols to disulfides, and some of these functions will be discussed below (Lee *et al.*, 2013).

Thioredoxin reductases are enzymes that are part of the pyridine nucleotide-disulfide oxidoreductase flavoprotein family and can be either high molecular weight (55 kDa - higher eukaryotes, mammals, protozoa) or low molecular weight (35 kDa - lower eukaryotes, yeasts, bacteria) (Banerjee *et al.*, 2008, Lu and Holmgren, 2014, Williams *et al.*, 2000). Members of this protein family are homo-dimeric and each monomer contains a flavin adenine dinucleotide (FAD) prosthetic group, a redox-active disulfide active site and an NADPH binding site (Mustacich and Powis, 2000). Electrons from NADPH, are transferred via FAD, to the disulfide of thioredoxin reductase (active-site), which can then reduce thioredoxin (Mustacich and Powis, 2000). Because the only enzymes known to reduce oxidized thioredoxins are thioredoxin reductases, it is believed that changes in thioredoxin reductase activity mediates

the activity of thioredoxin (Becker *et al.*, 2000). Other endogenous substrates (in addition to thioredoxin) have been identified for mammalian thioredoxin reductases, including vitamin K₃ and also lipids and lipoic acid hydroperoxides (Arnér *et al.*, 1996, Björnstedt *et al.*, 1995).

1.4 General functions of the thioredoxin system

Various cellular functions are attributed to the thioredoxin system. Some functions are common in almost all organisms, while others are unique to specific organisms. The thioredoxin system functions that are common in all organisms include oxidative stress response through protein disulfide reduction (Cunniff *et al.*, 2014, Holmgren, 1984), methionine sulfoxide reduction (Arnér and Holmgren, 2000, Banerjee *et al.*, 2008) and DNA synthesis (Muller, 1995).

1.4.1 Oxidative stress response

The detoxifying activity of the thioredoxin system is carried out by transferring electrons to peroxiredoxins and methionine sulfoxide reductases through protein-disulfide reduction (Banerjee *et al.*, 2008). Peroxiredoxins are a large family of highly conserved peroxidases that reduce peroxides and were initially described in baker's yeast in 1987 (Kim *et al.*, 1988). A peroxiredoxin that utilized a thiol-containing electron donor was initially discovered and was named thiol-specific antioxidant (TSA) (Chae *et al.*, 1993, Kim *et al.*, 1988, Lu and Holmgren, 2014, Rhee, 2016). It was believed that the function of TSA was to remove reactive sulfur species, but subsequent sequence analyses revealed homology of TSA with peroxidases that detoxify ROS within cells (Tartaglia *et al.*, 1990). TSA reduced peroxides with thioredoxin as the hydrogen donor and TSA was then named thioredoxin peroxidase (Rhee, 2016). Further analyses showed that not all members of the TSA family used thioredoxin as an electron source and therefore peroxiredoxin was used to denote this family of proteins (Chae *et al.*, 1994, Rhee, 2016). The thioredoxin system can transfer electrons to peroxiredoxins to detoxify and remove ROS like peroxynitrite, hydrogen peroxide and hydroperoxides (Day *et al.*, 2012). Peroxiredoxin recycling is performed when the thioredoxin system reduces the disulfide bonds of peroxiredoxin for it to be in an active state once again (Figure 1.3) (Day *et al.*, 2012, Lu and Holmgren, 2014).

Thioredoxin/peroxiredoxin redox reactions are involved in cellular signaling and transduction. Peroxiredoxins mediate hydrogen peroxide signaling through three mechanisms (Figure 1.3). Hydrogen peroxide may react directly with a target signaling protein as

peroxiredoxins regulate hydrogen peroxide tone in cells (Figure 1.3, blue). In addition, hydrogen peroxide reacting with peroxiredoxin can transmit oxidation from oxidized peroxiredoxin to a target signaling protein (such as a phosphatase or transcription factor) (Figure 1.3, green). Finally, peroxiredoxin-mediated thioredoxin oxidation can lead to signaling protein oxidation by thioredoxin (Figure 1.3, orange) (Netto and Antunes, 2016).

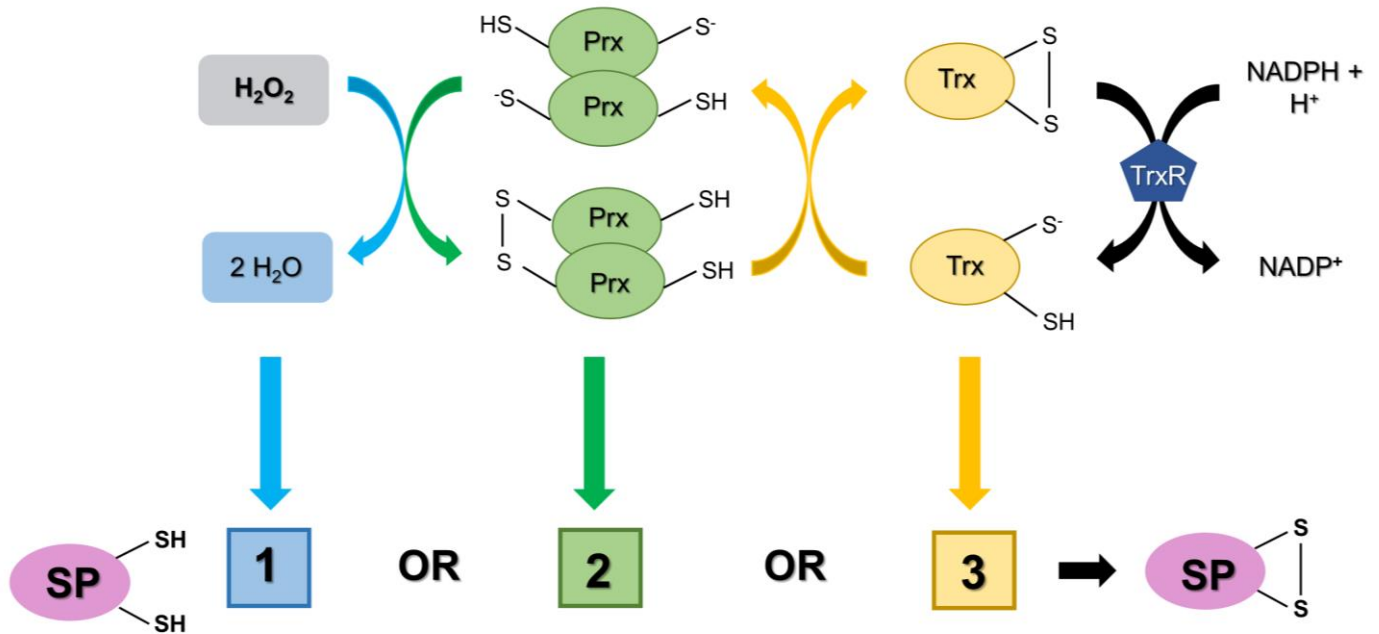


Figure 1.3 Hydrogen peroxide (H_2O_2) sensing mechanisms. Three mechanisms are shown: (1) direct signaling protein (SP) oxidation by H_2O_2 ; (2) signaling protein oxidation is mediated by oxidized peroxiredoxin (Prx) or (3) thioredoxin (Trx). Details in text (Adapted from Netto and Antunes, 2016).

1.4.2 Methionine sulfoxide reduction

Post-translational modifications alter a protein's function, structure and solubility. ROS are responsible for the oxidation of methionine residues, changing the amino acid structure (Lourenço Dos Santos *et al.*, 2018). Methionine is a sulfur-containing amino acid involved in protein synthesis initiation and shares similar functions with cysteine in ROS detoxification, redox signaling and disease (Kaya *et al.*, 2015, Kim *et al.*, 2014, Lim *et al.*, 2019). Methionine sulfoxide (MetO) is the oxidized form of methionine and methionine sulfoxide reductases (Msrs) are enzymes that catalyze the reduction of MetO back to methionine (Figure 1.4) (Ejiri *et al.*, 1979, Lourenço Dos Santos *et al.*, 2018, Oien and Moskovitz, 2007). Msrs reduce MetO at the expense of becoming oxidized, but are reduced by the thioredoxin and the

glutathione/glutaredoxin systems, thus restoring their activity (Figure 1.4) (Kim, 2013, Lourenço Dos Santos *et al.*, 2018, Porqué *et al.*, 1970).

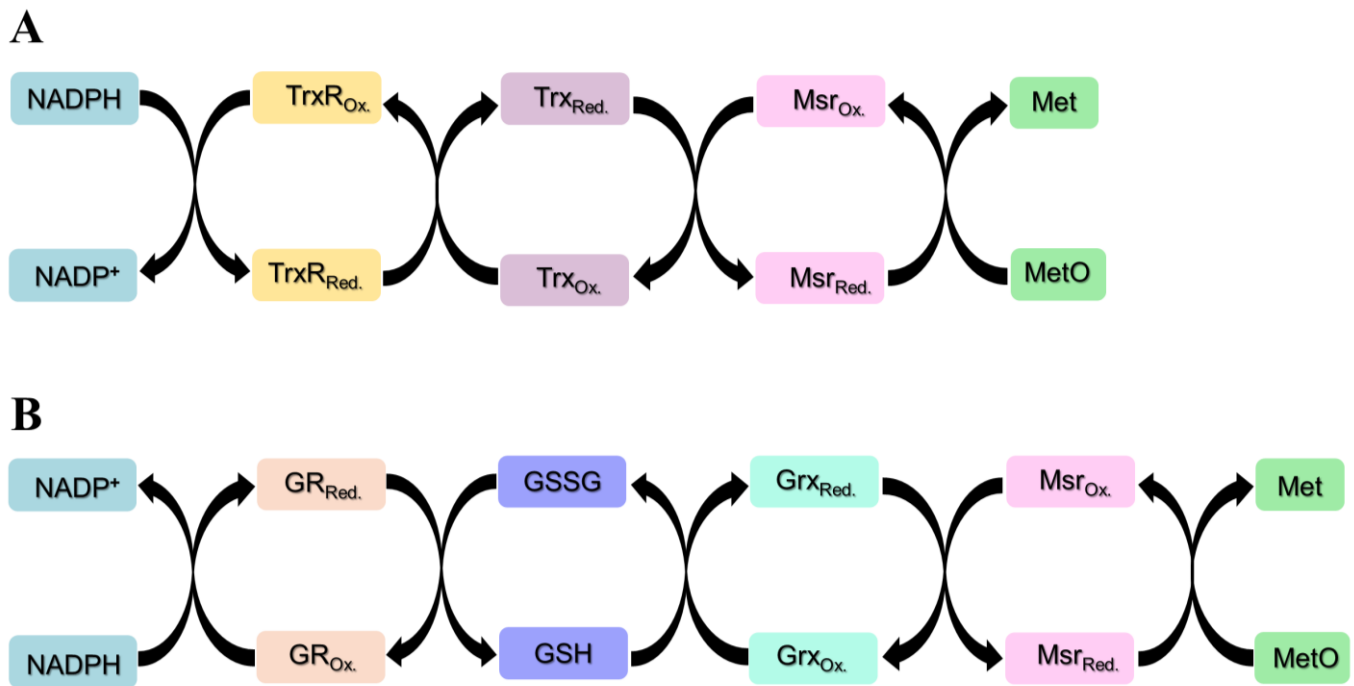


Figure 1.4 The thioredoxin (Trx) system provides reducing equivalents for methionine sulfoxide reductases (Msrs) to catalyze methionine sulfoxide (MetO) reduction to methionine (Met). (A) Msrs reduce MetO to methionine (Met) with the Trx system providing reducing equivalents. (B) The glutathione/glutaredoxin (GSH/Grx) system has been newly identified as providing reducing equivalents for Msrs to reduce MetO, with electron transfer moving from NADPH to glutaredoxin (Grx) via glutathione reductase (GR) and glutathione (GSH) (Adapted from Kim *et al.*, 2013).

Methionine sulfoxide reductases are known for protection against apoptosis and oxidative stress (Kim, 2013, Noh *et al.*, 2017). This protection rendered by methionine residues is attributed to their cyclic reduction by methionine sulfoxide reductases (Lourenço Dos Santos *et al.*, 2018, Luo and Levine, 2009).

1.4.3 Ribonucleotide reductase synthesis

Ribonucleotide reductase participates in DNA synthesis and catalyzes the rate-limiting step in which reduced ribonucleotides form deoxyribonucleotides (Sengupta and Holmgren, 2014). Ribonucleotide reductase catalysis utilizes reducing equivalents from the thioredoxin

system, and its activity is modulated by the expression of various protein subunits, subcellular localisation, post-translational modifications and allosteric regulation (Koc *et al.*, 2006, Sengupta and Holmgren, 2014). Increased ribonucleotide reductase activity during DNA replication is associated with cancer formation and malignancy, because of an imbalance in deoxyribonucleotide levels within cells (Hashemy *et al.*, 2006). On the other hand, blocking ribonucleotide reductase activity, commonly through thioredoxin system inhibition, prevents DNA synthesis as well as cellular repair and this eventually results in apoptosis in eukaryotic cells, showing that ribonucleotide reductase dysregulation is detrimental to cells (Lee *et al.*, 2013, Schallreuter *et al.*, 1990, Sengupta and Holmgren, 2014).

1.5 Thioredoxin system functions limited to bacteria, yeast and bacteriophages

In addition to functions of the thioredoxin system mentioned above; some functions are limited only to bacteria, yeast and bacteriophages.

1.5.1 Sulfate assimilation

Mammals obtain essential amino acids and cofactors from their diet. Unlike mammals, microorganisms can use inorganic sulfate as the sole sulfur supply for cysteine biosynthesis (Finkelstein and Mudd, 1967, Lillig *et al.*, 1999). Inorganic sulfates are converted to sulfide, which forms part of the carbon backbone of cysteine (Kopriva and Koprivova, 2003). Sulfate assimilation occurs in microorganisms in five enzymatic steps. First, due to adenosine triphosphate (ATP) sulfurylase and 5'-adenylylsulfate kinase, sulfate is activated to 5'-adenylylsulfate and 3'-phosphoadenylylsulfate (PAPS). PAPS undergoes reduction to sulfite by PAPS reductase, and sulfite is then reduced by sulfite reductase to sulfide (Bick *et al.*, 2000, Lillig *et al.*, 1999). The last step involves cysteine formation when sulfide integrates into two carbon skeleton type molecules i.e. O-acetyl-L-serine and O-acetyl-L-homoserine. These skeleton molecules are used to produce the organic sulfur molecules cysteine and L-homocysteine (Brzywczy *et al.*, 2002, Kawano *et al.*, 2018, Lillig *et al.*, 1999, Mendoza-Cozatl *et al.*, 2005). To reduce PAPS to free sulfite, the thioredoxin and glutathione/glutaredoxin systems are used as hydrogen donors (Lillig *et al.*, 1999). In baker's yeast, the thioredoxin system is the main hydrogen donor because cells with defective thioredoxins were also defective in sulfate assimilation and could only grow under specific, controlled conditions (Draculic *et al.*, 2000, Muller, 1991).

1.5.2 Filamentous phage assembly in bacteriophages

The thioredoxin system plays a role in filamentous bacteriophage assembly which is the process of membrane construction around the bacteriophage genome (Russel, 1991, Russel and Model, 1985). Reduced thioredoxin is required as a reductant during membrane construction and thioredoxin reductase is needed to ensure thioredoxin is in the reduced conformation (Russel and Model, 1986). Thioredoxin may participate in other components of phage assembly and may not only be a reductant, such as the DNA-handling role of thioredoxin (Loh *et al.*, 2019). This is because thioredoxin mutants that had cysteine residues replaced with serine residues were still functional and supported phage assembly (Russel and Model, 1985, Russel and Model, 1986).

1.5.3 DNA metabolism in bacteriophage T7

Bacteriophage T7 is a phage that infects most strains of *Escherichia coli*. Thioredoxin plays a role in its DNA metabolism as a host-specific subunit of the phage T7 DNA polymerase. This makes thioredoxin essential for T7 DNA replication and thus phage viability (Bedford *et al.*, 1997, Mark and Richardson, 1976). Bacteriophage T7 DNA polymerase shares extensive sequence homology with *E. coli* DNA polymerase I (Bedford *et al.*, 1997), which is primarily involved in the repair of DNA, whereas T7 DNA polymerase is responsible for replicating the viral genome (Mark and Richardson, 1976). Accordingly, T7 DNA polymerase is highly processive, while *E. coli* DNA polymerase I has low processivity (Mark and Richardson, 1976). The high processivity of T7 DNA polymerase is attributed to its tight binding to *E. coli* thioredoxin, which is its processivity factor (Bedford *et al.*, 1997, Ghosh *et al.*, 2008).

1.6 Thioredoxin system functions in mammals

The mammalian thioredoxin system shows differences to the microbial thioredoxin system (Lee *et al.*, 2013). Mammalian thioredoxin reductase is a selenoprotein containing a penultimate C-terminal selenocysteine (glycine–cysteine–selenocysteine–glycine) essential for its catalytic activity (Figure 1.5) (Lillig and Holmgren, 2007, Ren *et al.*, 2018). This highly reactive, openly accessible selenolate active site allows for a broader substrate specificity than the microbial thioredoxin system (Figure 1.5) (Lillig and Holmgren, 2007, Ren *et al.*, 2018). Mammalian cytosolic thioredoxins also contain additional cysteine residues outside their active

site. These residues can be oxidized, resulting in protein inactivation (Lillig and Holmgren, 2007, Powis and Montfort, 2001).

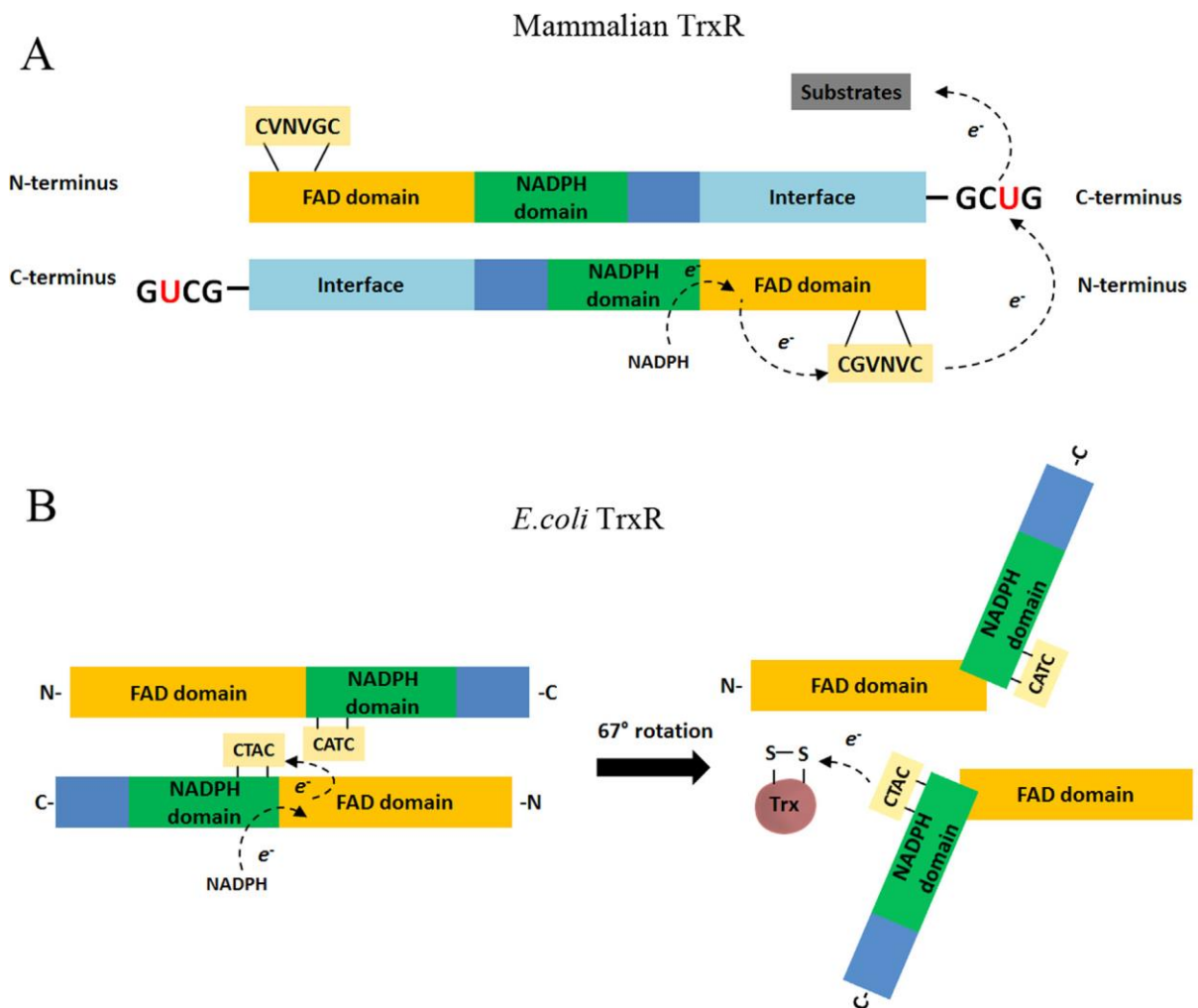


Figure 1.5 Difference in mammalian thioredoxin reductase and *E. coli* thioredoxin reductase catalysis mechanisms. (A) The reactivity of the C-terminal selenocysteine (U) of mammalian thioredoxin reductase can catalyze multiple substrates. Binding occurs between NADPH and the NADPH domain. Electrons move from NADPH to FAD, then to the cysteine active site at the N-terminal and then to the C-terminal selenocysteine. (B) With *E. coli* thioredoxin reductase, the hidden active site is exposed to its specific substrate due to a conformational rotation. Then electrons move from NADPH to FAD, and lastly to the cysteine active site (Ren et al., 2018). Permission to reproduce this figure was obtained from Rightslink/Elsevier.

The functions of the thioredoxin system in mammals are also more varied and complex when compared to the microbial thioredoxin system. In mammals, two thioredoxin isoforms

exist; cytosolic thioredoxin 1 and mitochondrial thioredoxin 2 (Nakamura, 2005). Thioredoxin plays a vital role in intracellular signal transduction and maintains a reduced environment within cells (Nordberg and Arnér, 2001). When exposed to oxidative stress, thioredoxin 1 translocates from the cytosol into the nucleus where it changes the DNA-binding capability and activity of various transcriptional factors including nuclear factor-kappa B (NF- κ B), activator protein-1 (AP-1) and p53 (Lee *et al.*, 2013, Nakamura, 2005, Nordberg and Arnér, 2001). In association with redox factor-1 (Ref-1), thioredoxin 1 also induces p53-dependent, p21 transactivation leading to DNA repair and cell cycle inhibition (Ueno *et al.*, 1999). Reduced thioredoxin 1 regulates apoptosis signaling by binding to and suppressing apoptosis signal-regulating kinase-1 (ASK1) activation (Matsuzawa, 2017). Some transcription factors that are directly activated by thioredoxin 1 include hypoxia-inducible factor 1 (Hif-1) (Zhou *et al.*, 2007), the tumor suppressor p53 (Ueno *et al.*, 1999), the glucocorticoid receptor (Grippeo *et al.*, 1985), the estrogen receptor and polyomavirus enhancer-binding protein 2/core binding factor (PEBP2/CBF) (Lillig and Holmgren, 2007). An interesting fusion protein unique to mammals is thioredoxin glutathione reductase (TGR), which reduces both thioredoxin 1 and glutathione and is present in the testes (Su *et al.*, 2005). Thioredoxin 2 is an essential regulator of the release of mitochondrial cytochrome *c* and apoptosis (Masutani *et al.*, 2005).

1.7 The glutathione/glutaredoxin system is an alternate redox regulatory system to the thioredoxin system in microbes

The glutathione/glutaredoxin and the thioredoxin systems are two primary biological thiol-disulfide redox systems that provide overlapping, but complementary functions in detoxification and intracellular redox state maintenance (Watson *et al.*, 2003). The glutathione/glutaredoxin system protects against various oxidants and electrophiles and plays a significant role in cellular iron homeostasis (Hanschmann *et al.*, 2013, Meyer *et al.*, 2009).

1.7.1 The glutathione/glutaredoxin system

The glutathione/glutaredoxin system is a critical disulfide reduction system in cells and consists of glutathione, glutaredoxin, glutathione reductase and NADPH. Like the thioredoxin system, the glutathione/glutaredoxin system aids in oxidative stress responses (Prieto-Álamo *et al.*, 2000), cellular differentiation, transcription regulation (Takashima *et al.*, 1999), apoptosis (Chrestensen *et al.*, 2000) and DNA synthesis and repair (Sengupta and Holmgren, 2014).

In the glutathione/glutaredoxin system, reducing equivalents from NADPH are shuffled via glutathione reductase to reduce oxidized glutathione (Figure 1.6). Glutathione reductase is a 100-120 kDa, substrate-specific enzyme belonging to the pyridine-nucleotide disulfide oxidoreductase family of flavoenzymes (FAD) and is involved in reducing oxidized glutathione into reduced glutathione. Glutathione is a ubiquitous peptide whose cellular concentrations are maintained at relatively high levels (approximately 10 mM in *Saccharomyces cerevisiae*) and which acts as a buffer for cellular redox homeostasis (Ithayaraja, 2011, Sato *et al.*, 2011). Reduced glutathione reduces ROS and glutaredoxins, which in turn can reduce target proteins (Figure 1.6) (Berndt *et al.*, 2008, Fernandes and Holmgren, 2004, Ukuwela *et al.*, 2018).

Glutaredoxins are small 9–15 kDa proteins and belong to the thioredoxin protein family (Berndt *et al.*, 2008). Glutaredoxins can be divided into two active site motif categories viz. the dithiol glutaredoxins (cysteine-proline-tyrosine-cysteine) and the monothiol glutaredoxins (cysteine-glycine-phenylalanine-serine) (Berndt *et al.*, 2008, Herrero and de la Torre-Ruiz, 2007). This means that in addition to disulfide/dithiol reactions and mechanisms, glutaredoxins can also catalyze substrate reduction reactions via a monothiol mechanism, which plays a key role in iron-sulfur cluster assembly involved in the mitochondrial electron transport chain (Berndt *et al.*, 2021, Mashamaite *et al.*, 2014, Ren *et al.*, 2017).

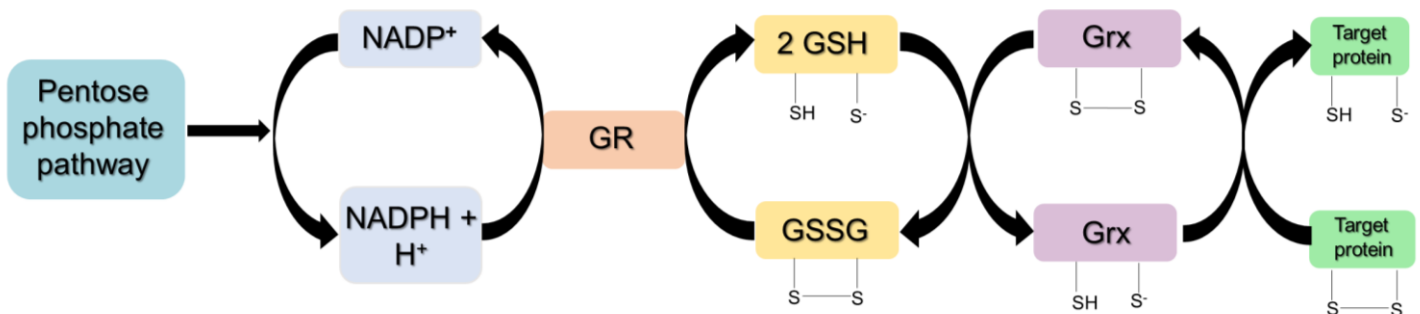


Figure 1.6 Glutathione/glutaredoxin (GSH/Grx) system mediated redox reactions from reduced substrate to targeted proteins. *Glutathione reductase (GR) catalyzes the electron transfer from a reduced substrate (NADPH) to the disulfide bridge of oxidized glutathione (GSSG). Reducing equivalents from reduced glutathione (GSH) are then passed to the disulfide bridge of glutaredoxin (Grx), reducing the oxidized Grx form. Target protein reduction via a dithiol/disulfide reaction exchange occurs due to reduced Grx (Adapted from Fernandes and Holmgren, 2004).*

1.7.2 Glutathione/glutaredoxin and the thioredoxin systems' functional overlap in *E. coli*

The thioredoxin and glutathione/glutaredoxin systems are functionally redundant in *E. coli*, although the inactivation of both or one of the pathways renders cells unviable (Carmel-Harel and Storz, 2000, Toledano *et al.*, 2007). The causes of lethality could be attributed to the accumulation of harmful disulfide bonds in the cell cytoplasm (disulfide stress), defective protein reduction that is important for cell viability or insufficient DNA replication (Toledano *et al.*, 2007). Studies where mutant *E. coli* strains have both thioredoxin 1 and glutaredoxin 1 or thioredoxin 1 and glutathione 1 protein genes deleted, were rendered unviable due to the accumulation of harmful 3'-phosphoadenosine 5'phosphosulfate (PAPS), a crucial metabolite in sulfur assimilation (Russel *et al.*, 1990). This unviable phenotype was rescued by repression of the sulfate assimilation pathway, usually by adding a high organic sulfate concentration to the growth medium or by deleting the *cysA* or *cysC* genes (Thomas *et al.*, 1990). Another study analyzed mutant *E. coli* that had all thioredoxin genes deleted and these cells were rendered unviable (Russel *et al.*, 1990). Concerning the glutathione/glutaredoxin system in *E. coli*, the deleted glutathione 1 strain was both aerobically and anaerobically unviable, with growth only occurring when glutathione was added (Grant *et al.*, 1996). In *E. coli*, glutathione has an essential function that is not shared with the thioredoxin system and this may be because of iron-sulfur cluster assembly (Fernandes *et al.*, 2005, Spector *et al.*, 2001). These studies show that the thioredoxin and glutathione/glutaredoxin systems in *E. coli* are complementary.

1.7.3 Glutathione/glutaredoxin and the thioredoxin systems' functional overlap in *S. cerevisiae* and *S. pombe*

Unlike *E. coli*, in *S. cerevisiae* single and double mutants of thioredoxin 1 and thioredoxin 2 proteins were viable. However, thioredoxin double mutants had a prolonged S phase in their cell cycle because glutaredoxin 1 and glutaredoxin 2 are less efficient reductants of ribonucleotide reductase, compared to the thioredoxin system (Camier *et al.*, 2007, Muller, 1991). On the other hand, *S. cerevisiae* is unviable without glutathione (Grimaud *et al.*, 2001). The glutathione/glutaredoxin system plays an essential role in iron metabolism and iron-sulfur cluster formation (Toledano *et al.*, 2007). Curiously, in *S. cerevisiae*, glutathione reductase is not essential, and reduced glutathione makes up approximately 40% of the total glutathione amount in glutathione reductase mutant cells (Collinson and Dawes, 1995, Meyer *et al.*, 2009, Muller, 1996). Here, the thioredoxin system acts as a replacement reducing system of oxidized glutathione (Bao *et al.*, 2009). Thus, thioredoxin 1 or thioredoxin 2 over-expression in cells

lacking glutathione reductase, decreased oxidized glutathione accumulation and increased reduced glutathione levels (Tan *et al.*, 2010).

These studies show that in *S. cerevisiae*, the thioredoxin and glutathione/glutaredoxin systems occupy their own functions in the cell with some overlap. One system may substitute for the other, although the functional efficiency may not always be optimal. In *S. cerevisiae*, the thioredoxin system is most suited to reducing ribonucleotide reductase and PAPS reductase and plays an essential role in hydrogen peroxide metabolism. The glutathione/glutaredoxin system is most suited to controlling redox buffering and plays a critical role in operating an iron-sulfur metabolism shuttle (Toledano *et al.*, 2007).

In the fission yeast, *S. pombe*, the multicopy suppressor that restored cell growth in glutathione reductase depleted cells was found to be mitochondrial thioredoxin 2. This suggests that glutathione reductase could be necessary for mitochondrial function (Song *et al.*, 2006). The functional overlap could also be seen by the total iron content in glutathione reductase depleted cells being brought to a lower level by thioredoxin 2 (Song *et al.*, 2006).

In summary, these thiol/disulfide redox systems have some overlapping functions, but are still distinct from one another. If one system is disrupted, the remaining system may compensate, but this could lead to slow cell growth and maturity and possibly cell death. The interplay between these systems needs to always be considered in the specific organism when investigating these systems.

1.8 The thioredoxin system as a drug target

The thioredoxin system is an essential redox cellular system in almost all organisms and its dysregulation has been related to various disease conditions and pathologies (Table 1.1). This also leads to the thioredoxin system being a target for certain therapies (Table 1.1). In recent literature among other therapies for various illnesses, thiol-based systems have been proposed as drug targets in microorganisms (Andrade and Reed, 2015, Jeelani and Nozaki, 2016, May *et al.*, 2018). Microbial thioredoxin reductase is structurally and functionally different from mammalian thioredoxin reductase, making microbial thioredoxin reductase suitably druggable from a clinical aspect. In line with this, drugs to inhibit the thioredoxin system have been developed.

Table 1.1 Diseases and therapeutics involving the thioredoxin system

Diseases associated with thioredoxin system imbalances:	Comments:	References:
Viral diseases – HIV & AIDS	Increased thioredoxin detected in blood plasma, could be correlated to increased oxidative stress at certain disease stages and thioredoxin reductase 1 was found to negatively regulate an HIV-encoded transactivating protein	(Kalantari <i>et al.</i> , 2008, Nakamura <i>et al.</i> , 1996)
Cancer	Thioredoxin over-expression has been detected in tumors, initially being expressed to overcome oxidative stress, but ultimately at later disease stages contributing to tumor growth, due to anti-apoptotic properties	(Arnér and Holmgren, 2006, Jia <i>et al.</i> , 2019)
Rheumatoid arthritis	Serum concentrations contained an elevated thioredoxin concentration in patients, contributing to augmented inflammation pathway activation	(Maurice <i>et al.</i> , 1999, Yoshida <i>et al.</i> , 1999)
Disease treatments involving the thioredoxin system:	Comments:	References:
Antimicrobial resistance	Thioredoxin system inhibition has been proposed as a novel therapy to overcome drug resistance in microbial infections	(Felix <i>et al.</i> , 2021, May <i>et al.</i> , 2018, O'Loughlin <i>et al.</i> , 2021)
Diabetes	Thioredoxin-interacting protein binds and inhibits thioredoxin and inhibiting thioredoxin-interacting protein may lead to better β -cell survival	(Chong <i>et al.</i> , 2014, Wondafrash <i>et al.</i> , 2020)
Ischemia-reperfusion injury	Thioredoxin 1 treatment increased the survival of renal and lung ischemia-reperfusion injured mice	(Fukuse <i>et al.</i> , 1995, Nishida <i>et al.</i> , 2020)

1.8.1 Auranofin

Auranofin [2,3,4,6-tetra-*o*-acetyl- β -D-glycopyranp-sato-*S*-(triethyl-phosphine)-gold] is an approved rheumatoid arthritis drug (Roder and Thomson, 2015). This chemical compound comprises gold (I) with phosphine and thiol ligands arranged linearly (Figure 1.7). Auranofin has been prescribed to treat rheumatoid arthritis to slow the disease progression by suppression of inflammation and also promoting cell-mediated immunity (Finkelstein *et al.*, 1976). The mechanism of action of auranofin involves inhibition of thioredoxin reductase and it exhibits proteasome activity inhibition (Fan *et al.*, 2014, Zhang *et al.*, 2019a). Auranofin has thiol ligands and these constituents have a high affinity for thiol and selenol groups, upon which stable and irreversible bonds form (Fan *et al.*, 2014, Roder and Thomson, 2015). It has been suggested that thioredoxin reductase may not be the sole target of auranofin (Thangamani *et al.*, 2016). In an *E. coli* strain (Origami™ 2 Competent Cells – Novagen), with the thioredoxin reductase and glutathione reductase genes mutated to enhance disulfide bond formation, auranofin treatment of these cells exhibited the same antibacterial activity as on the wild-type *E. coli* strain (Thangamani *et al.*, 2016). Thus, auranofin might also target other cell constituents and biosynthetic pathways.

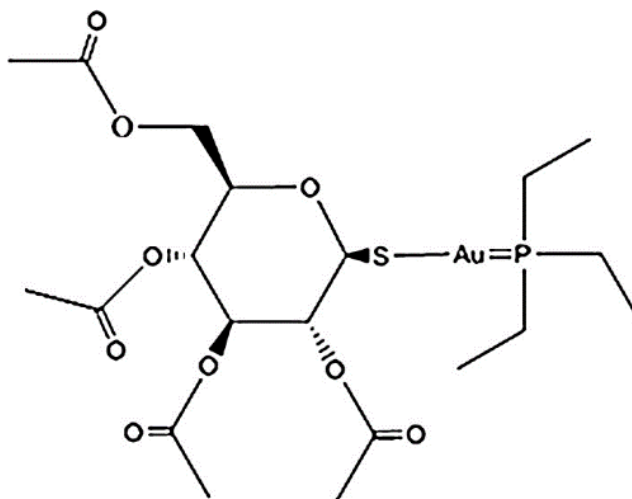


Figure 1.7 Chemical structure of auranofin. Auranofin consists of gold(I) with phosphine and thiol ligands arranged linearly (Roder and Thomson, 2015). Permission to reproduce this figure was granted under the Creative Commons license (Attribution-Noncommercial).

ESKAPE is an acronym for *Enterococcus faecium*, *Staphylococcus aureus*, *Klebsiella pneumoniae*, *Acinetobacter baumannii*, *Pseudomonas aeruginosa* and *Enterobacter* spp. These pathogens are some of the most common microbial pathogens that are highly resistant

to routinely used antimicrobial therapies (Rice, 2008, Santajit and Indrawattana, 2016). Common resistance mechanisms include drug binding site modifications, prevention of drug accumulation through efflux pumps, porin loss and biofilm formation (Mulani *et al.*, 2019).

Caenorhabditis elegans infected with *S. aureus* were treated with auranofin. The auranofin treatment resulted in a 95% survival rate in *C. elegans* (Fuchs *et al.*, 2016). This study also investigated other ESKAPE pathogens and found that auranofin inhibited *E. faecium* and *A. baumannii* (Fuchs *et al.*, 2016). In another study, auranofin and various other gold compounds were also shown to significantly inhibit methicillin-resistant *S. aureus* (MRSA) (Hokai *et al.*, 2014).

Studies have concluded that the minimum inhibitory concentration in response to auranofin for Gram-negative bacteria is higher than for Gram-positive bacteria. The reasons attributed to Gram-negative bacteria requiring a higher concentration of auranofin for inhibition might be the redundancy of both the thioredoxin and glutathione/glutaredoxin systems in these cells and the lack of permeability of the outer membrane (Cassetta *et al.*, 2014, Fuchs *et al.*, 2016, Thangamani *et al.*, 2016). Nonetheless, using *in vitro* enzymatic assays, auranofin was highly bactericidal against replicating and non-replicating *Mycobacterium tuberculosis* and auranofin was able to inhibit *Bacillus subtilis*, *Enterococcus faecalis*, drug-resistant and sensitive strains of *E. faecium* and methicillin-resistant *S. aureus* (all Gram-positive strains) (Harbut *et al.*, 2015).

Fungal and yeast strains were tested using micro dilutions and it was determined that auranofin inhibited *Candida albicans*, *Cryptococcus neoformans*, *Candida tropicalis* and *Candida glabrata* with varying minimum inhibitory concentrations (Fuchs *et al.*, 2016). Interestingly, auranofin was active against many fluconazole-resistant strains of fungi like *C. albicans* and *Candida krusei* and even inhibited *C. neoformans* more efficiently than fluconazole (Fuchs *et al.*, 2016). In another study that dealt with moulds, auranofin was active against *Aspergillus fumigatus*, *Scedosporium apiospermum* and *Lomentospora prolificans* (Wiederhold *et al.*, 2017).

Auranofin also strongly inhibited the malarial parasite growth of *Plasmodium falciparum* (Sannella *et al.*, 2008), the procyclic and bloodstream phases of *Trypanosoma brucei* (Lobanov *et al.*, 2006), the promastigote phase of *Leishmania infantum* (Ilari *et al.*, 2012) and was active against *Echinococcus granulosus* larval worms (Bonilla *et al.*, 2008). It is important to note that auranofin doses were in the nanomolar range, which is within the concentration range given to rheumatoid arthritis patients (Andrade and Reed, 2015). *Entamoeba histolytica* trophozoites were shown to be considerably more sensitive (10 times)

to auranofin compared to metronidazole (antiprotozoal drug) (Debnath *et al.*, 2012). It was proposed that thioredoxin reductase was inhibited by auranofin in strains of *Giardia lamblia* that were metronidazole resistant and vastly decreased trophozoite numbers within the small intestine of newly born and adult mice and gerbils (Tejman-Yarden *et al.*, 2013).

1.8.2 Ebselen

Ebselen [2-phenyl-1,2-benzisoselesazol-3(2H)-one] is a prescribed selenium-containing antioxidant and anti-inflammatory drug (Figure 1.8) that is a substrate for mammalian thioredoxin reductase and thioredoxin. It has been involved in clinical trials to treat acute ischemic stroke and psychiatric disorders (Azad and Tomar, 2014, Lu *et al.*, 2013, Medhi *et al.*, 2013, Sharpley *et al.*, 2020).

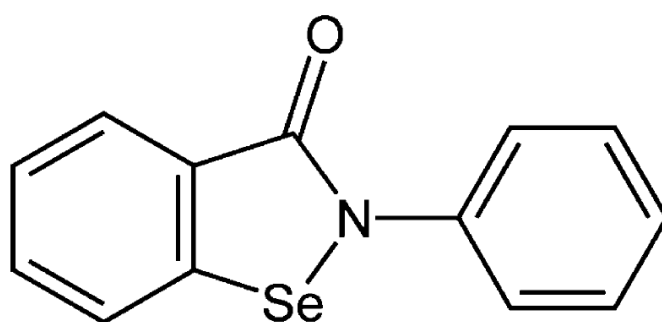


Figure 1.8 Chemical structure of ebselen. *Ebselen contains a selenium molecule (Azad and Tomar, 2014). Permission to reproduce this figure was obtained from Rightslink/ Springer Nature.*

Ebselen is highly effective and bactericidal against methicillin-resistant *Staphylococcus aureus* and was identified as a competitive inhibitor of *E. coli* thioredoxin reductase, due to a reaction with the active site dithiol (Lu *et al.*, 2013). *E. coli* treatment with ebselen resulted in thioredoxin 1 and thioredoxin 2 being oxidized, indicating blockage of the thioredoxin redox cascade via thioredoxin reductase (Lu *et al.*, 2013).

Thioredoxin reductase in bacterial and mammalian cells has different reaction mechanisms as previously described and this is responsible for ebselen affecting bacterial thioredoxin reductase, but not mammalian thioredoxin reductase. Ebselen acts as a glutathione peroxidase and as a peroxiredoxin mimic via thioredoxin and thioredoxin reductase in mammalian cells which decreases reactive oxygen species and is beneficial for mammalian cells (Ren *et al.*, 2018). On the other hand, in prokaryotic cells, ebselen inhibits *E. coli*

thioredoxin reductase due to the selenium atom in ebselen that forms a selenosulfide bond with thioredoxin reductase, making reduction difficult and leading to inhibition of thioredoxin reductase activity (Ren *et al.*, 2018). This selenosulfide bond is situated within the thioredoxin reductase active site, which detrimentally inhibits thioredoxin reductase from reducing thioredoxin, leading to cell death (Lu *et al.*, 2013, Pannala and Dash, 2015, Ren *et al.*, 2018).

Ebselen and ebselen derivatives have bactericidal effects against methicillin-resistant *S. aureus*, *E. coli*, and macrolide-resistant *Helicobacter pylori* by inhibiting the electron transfer chain structure to thioredoxin (Younis *et al.*, 2015). Ebselen, like auranofin, is highly active against bacteria that lack the glutathione/glutaredoxin system and is not as effective on Gram-negative bacteria (Lu *et al.*, 2013, Pietka-Ottlik *et al.*, 2008). A study tested ebselen against drug-resistant pathogens and in a staphylococcal skin infection mouse model using methicillin-resistant *S. aureus*. It was determined that the inhibitory effect of ebselen could be compared to other antibiotic treatments, such as using vancomycin and linezolid (Thangamani *et al.*, 2015). It was also shown that it is generally difficult for bacteria such as *B. subtilis* and *S. aureus* to develop resistance against ebselen (Gustafsson *et al.*, 2016, Ren *et al.*, 2018, Thangamani *et al.*, 2015). To determine if inhibition of both the glutathione/glutaredoxin and the thioredoxin systems could impede bacterial growth in Gram-negative strains, a study investigated the use of ebselen and silver nitrate on *E. coli* (Zou *et al.*, 2017). It was shown that silver and ebselen when used together, had no significant toxicity on mammalian cells at concentrations that would be enough to inhibit *E. coli* cells. Silver ions were described as efficient inhibitors of both the *E. coli* thioredoxin and the glutathione/glutaredoxin systems (Zou *et al.*, 2017). Impaired DNA synthesis likely led to bacterial death. This study also showed that combined treatment allowed for greater survival from sepsis attributed to *E. coli* infection in the mouse model.

In yeasts and fungi, ebselen is known to inhibit *S. cerevisiae* and fluconazole-resistant *C. albicans* (Billack *et al.*, 2010). Ebselen derivatives and related compounds have also exhibited activity against *Aspergillus* spp. (Ngo *et al.*, 2016). It has also been shown that ebselen can regulate and influence fungal glutathione and the production of reactive oxygen species (Thangamani *et al.*, 2017). Ebselen was able to strongly inhibit *Candida* and *Cryptococcus* spp. in a *Caenorhabditis elegans* infection model compared to commonly prescribed antifungal drugs like flucytosine, fluconazole and amphotericin (May *et al.*, 2018, Thangamani *et al.*, 2017). Compared to bacterial thioredoxin reductase and ebselen, there may be a similar association between fungal thioredoxin reductase and ebselen, as fungi also have the lower molecular weight thioredoxin reductase (Ren *et al.*, 2018).

1.9 System-level properties of the thioredoxin system

The thioredoxin system is an interconnected, complex system that affects many different pathways. Systems biology is an approach that aims to model and interpret complicated biological systems using mathematical and computational analyses. Using a computational model of the thioredoxin system from *Escherichia coli*, it was shown that specific modes of kinetic regulation exist within the thioredoxin system (Pillay *et al.*, 2011). Four kinetic behaviours were identified and were proposed as potentially regulating flux through the system. First, it was shown that the system was adaptable, as changes in the system can affect the kinetic profiles of reactions dependent on the thioredoxin system. Second, the reduced thioredoxin concentration responded in an ultrasensitive way to fluctuations in the thioredoxin reductase concentration. Third, distinct reactions dependent on the thioredoxin system affected each other, because of their joined influence on the redox cycle. Finally, it was demonstrated that reactions dependent on the thioredoxin system may be sensitive or insulated to disturbances in the thioredoxin redox cycle (Pillay *et al.*, 2011). However, demonstrating these behaviours *in vivo* was challenging as measuring the fluxes through the thioredoxin system is not trivial.

1.10 The thioredoxin redox charge – A novel assay to quantify the thioredoxin system?

Many methods have been used to measure the thioredoxin system. Enzyme assays like the insulin reduction assay measures thioredoxin, while the 5,5-dithio-bis-(2-nitrobenzoic acid) (DTNB) assay measures thioredoxin reductase using Ellman's Reagent (Cunniff *et al.*, 2013). These spectrophotometrically detectable assays as well as other newer fluorescence assays are relatively easy to carry out and interpret, however they are not always suited to cell lysate samples as there may be interfering enzymes and constituents of the lysate that could skew results and contribute to higher a background detection (Montano *et al.*, 2014). Methods involving calculating the concentrations of thioredoxin and thioredoxin reductase have also been used like the enzyme-linked immunosorbent assay (ELISA), but these methods can only quantify protein concentrations and not the protein's redox states (Lundberg *et al.*, 2014). Mass spectrophotometry has been a valuable tool to analyze a variety of proteins, allowing for easier proteomic studies, although a drawback may be that it is costly and requires specialized equipment and cannot be used routinely for a large number of samples (Winther and Thorpe, 2014). Redox states and redox potentials are another widely used method to measure the thioredoxin system and its redox status using the Nernst equation (Schafer and Buettner, 2001).

The redox state is used to describe the ratio between the oxidized and reduced fractions of a redox couple and the reduction/ redox potential describes the voltage and reducing ability of the redox couple (Schafer and Buettner, 2001). A way to measure the redox state of a cell would be to calculate redox potentials from the Nernst equation (Åslund *et al.*, 1997, Schafer and Buettner, 2001):

$$\text{Redox potential} = E_{trx}^{\circ} + \frac{RT}{nF} \log \frac{Trx_{oxidized}}{Trx_{reduced}} \quad (1)$$

E_{trx}° is the species-specific standard potential of thioredoxin, R is the universal gas constant, T is the temperature in kelvin, n is the number of moles of electrons, F is Faraday's constant, $Trx_{oxidized}$ and $Trx_{reduced}$ are the oxidized and reduced fractions of thioredoxin respectively. Redox potentials are a relatively accessible way to measure the thioredoxin redox poise within the cell. However, changes in the redox potential are difficult to interpret, and the relevance of this using thermodynamic measures in far-equilibrium systems has been questioned (Pillay *et al.*, 2013).

The current methods of quantifying the thioredoxin system are useful, although they do not offer insight into the thioredoxin system as a whole, and instead measure components of the system. A whole system measure that tracks changes in the system may be preferred, considering how interconnected and essential the system is. The thioredoxin redox charge was a proposed novel thioredoxin system measure and is calculated from the concentration of reduced thioredoxin/ total thioredoxin protein concentration (Padayachee *et al.*, 2020):

$$\text{Thioredoxin (Trx) redox charge} = \frac{\text{Reduced thioredoxin}}{\text{Total thioredoxin}} \quad (2)$$

This measure is useful because it is a simple, but accurate descriptor of the thioredoxin flux instead of other more abstruse measures like redox potentials that require species-specific reference values and whose interpretation is unclear (Åslund *et al.*, 1997, Cheng *et al.*, 2007). The redox charge is practical in that it does not require the monitoring of many variables or require expensive equipment or techniques. A useful aspect of the redox charge is that it is a dimensionless, fractional measurement that is bounded between 0 and 1. It can therefore be calculated and compared between different species which is convenient in large scale studies.

The thioredoxin redox charge was initially proposed as a surrogate thioredoxin system measure for flux in the system, along with the thioredoxin redox potential (Padayachee *et al.*, 2020). This novel measure, the thioredoxin redox charge, could also be suitably used to measure cell redox homeostasis and health in thioredoxin system inhibition studies, offering a more straightforward, standard measurement upon which inhibition studies could use as an indicator of various inhibitors' efficacy (Padayachee *et al.*, 2020). However, it remains to be

established if there is a clear correlation between the thioredoxin redox charge and cell viability. If so, the thioredoxin redox charge could be used as a system measure and possible cell health and homeostasis indicator. Additionally, the thioredoxin redox charge is not only limited to microbial thioredoxin system inhibition studies but can also be applied to other areas of study in which thioredoxin is measured e.g. sports science and cancer and tumor therapies in humans. There is a growing interest in the relationship between cellular thioredoxin concentrations and physical activity and its effect on human health within sports science (Hattori *et al.*, 2009, Marumoto *et al.*, 2010, Sugama *et al.*, 2015, Wadley *et al.*, 2015). Thioredoxin is involved in tumor formation and cancers through its role in apoptosis and using the thioredoxin redox charge as a total measure of the thioredoxin system would be helpful to allow for routine and intensive research (Bhatia *et al.*, 2016, Lu *et al.*, 2007, Shabani *et al.*, 2014, Ye *et al.*, 2019, Zhang *et al.*, 2017).

Schizosaccharomyces pombe, or fission yeast has been an extremely useful model organism across many fields. In redox biology research, *S. pombe* has been used to investigate how peroxiredoxins affect cell responses to hydrogen peroxide-induced oxidative stress and has been well characterized. *S. pombe* is suitable because it contains a single two-cysteine peroxiredoxin, that is thiol-specific peroxidase 1 (Tpx1), which is part of a simple pathway to follow. Other model organisms have a more complex eukaryotic system with many peroxiredoxins (Veal *et al.*, 2014). *S. pombe* is also amenable to genetic alteration, allowing easier investigation such as epitope tagging genes (Noguchi *et al.*, 2008).

1.11 Aims of study

The aim of this study was to evaluate whether the thioredoxin redox charge could be used as a general measure of the cellular redox state. To address this question, we first developed and optimized a suitable assay for quantifying the thioredoxin redox charge and thereafter evaluated the utility of the thioredoxin redox charge by stressor investigations using *S. pombe*.

Chapter 2: Quantifying the thioredoxin redox charge

2.1 Introduction

In order to calculate the thioredoxin redox charge, the reduced and oxidized thioredoxin isoforms must be determined. The methods to measure oxidized and reduced thioredoxin fractions from biological samples involve enzymatic assays, genetically encoded fluorescent redox biosensors and analyzing redox states through gel shift assays and immunoblotting (Eaton, 2006, Ying *et al.*, 2007). These different quantification methods will be discussed further.

2.1.1 DTNB and insulin reduction assays

Thiol detection can be carried out using Ellman's reagent, 5,5-dithio-bis-(2-nitrobenzoic acid) (DTNB) (Riddles *et al.*, 1979). The highly oxidizing disulfide bond present in DTNB, is stoichiometrically reduced by the free thiol group, present in thiol-containing molecules like thioredoxin reductase, thioredoxin and glutathione (Winther and Thorpe, 2014). The selenol group on selenocysteine that is only found in mammalian thioredoxin reductase, is also capable of reducing DTNB. The resulting reduction reaction forms a mixed disulfide, in addition to the release of 5-thio-2-nitrobenzoic acid (TNB) (Figure 2.1) (Nieri *et al.*, 2017, Riddles *et al.*, 1979). TNB is a spectrophotometrically detectable leaving group measured at 412 nm, with one TNB molecule released for every thiol that undergoes oxidation when treated with DTNB (Winther and Thorpe, 2014).

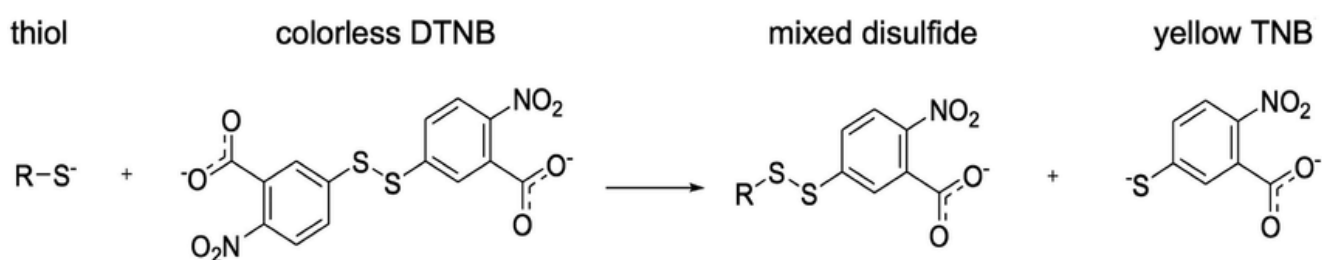


Figure 2.1 Reduction of 5,5-dithio-bis-(2-nitrobenzoic acid) (DTNB, also known as Ellman's reagent) by a free thiol group. The free thiol group reduces DTNB in a sample to produce a mixed disulfide and the release of yellow 5-thio-2-nitrobenzoic acid (TNB) (Nieri *et al.*, 2017). Permission to reproduce this figure was granted under the Creative Commons CC BY license.

Some limitations of this method are that DTNB may be sensitive to hydrolysis at high temperatures and pH values greater than 7. Sulfite and other cell constituents that reduce DTNB may also affect quantification of target protein concentrations like thioredoxin or thioredoxin reductase, as these compounds interact and attack disulfide bonds. Further, DTNB is light sensitive and cannot detect low thioredoxin reductase concentrations (Winther and Thorpe, 2014).

With the insulin reduction assay, thioredoxin catalyzes the reduction of insulin disulfide bonds. Turbidity occurs as free insulin β -chains precipitate which can be spectrophotometrically detected at 650 nm (Holmgren, 1979). A discontinuous, endpoint assay involving both DTNB and insulin can also be used to indirectly measure thioredoxin reductase. Thioredoxin reduces the disulfide bonds of insulin and thioredoxin then undergoes reduction by thioredoxin reductase, using up NADPH as an electron source (Cunniff *et al.*, 2013). The thiol groups of insulin that have been newly reduced can react with DTNB producing a detectable yellow color (TNB molecules), that is spectrophotometrically measured (Winther and Thorpe, 2014). This assay does not monitor NADPH consumption continuously and the reaction can be quenched with a chaotropic agent like guanidinium hydrochloride (Cunniff *et al.*, 2013). However, discontinuous assays only measure fixed time points, without information about reaction progress between the selected time points.

2.1.2 Genetically encoded fluorescent redox biosensors

For most common biosensors that detect redox perturbations, a fluorescent signal comes from the fluorescent protein that serves as a reporting molecule for the activity of the promoter region of a target gene. Therefore, fluorescent protein expression is under the control of the promoter gene region. When cellular changes are experienced, that involve the target gene, the promoter region will be activated and will subsequently result in expression of the fluorescent protein along with the target gene. An increase in fluorescence intensity is interpreted as an increase in gene expression of the specific gene (Kostyuk *et al.*, 2018). More recently, technology involving fusion proteins consisting of redox-active proteins and redox-sensitive fluorescent proteins have been investigated as potential redox probes (Meyer and Dick, 2010). These genetically encoded fluorescent redox biosensors are a type of redox probe that utilizes recombinant fluorescent proteins as an indicator of cellular redox reactions *in vivo*, through real-time imaging of cells (Bilan *et al.*, 2015).

An interesting example of this type of redox probe to detect a target protein's redox status was developed for mammalian cytosolic thioredoxin. This biosensor used genetically encoded red fluorescent protein with reversible disulfide bridges to monitor thioredoxin oxidation *in vivo* (Fan *et al.*, 2017). A redox relay was engineered between the active-site cysteines of human thioredoxin 1 and the red fluorescent protein (rxRFP1). In this study, the biosensor was designed such that with an appropriate rearrangement, the active sites of the cysteine residues of thioredoxin 1 were linked to the redox-sensitive cysteine pair of the fluorescent protein. This would allow redox coupling because of the proximity of the fusion construct, leading to fluorescent protein oxidation becoming an indicator of thioredoxin 1 oxidation. Thus, an increase in fluorescence intensity of the red fluorescent protein due to oxidation would be indicative of thioredoxin 1 oxidation (Fan *et al.*, 2017).

Some advantages of genetically encoded fluorescent redox biosensors are that they allow continuous, real-time monitoring of the redox status of proteins *in vivo*. Several biosensors may be engineered to monitor various redox species in different subcellular compartments and can all be tracked at once. Using biosensors also negates artefacts that may arise due to sample processing when using traditional techniques (Kostyuk *et al.*, 2020). Some disadvantages of these biosensors may be that the fluorescent signal could sometimes be poor and this method still gives semi-quantitative or sometimes qualitative results. Redox biosensors can also be affected by physiological pH changes, the construction and monitoring of biosensors can be expensive requiring specialized equipment and most notably it is unknown what effect the expression of the fluorescent protein has on a cell and whether it interferes with biological functioning (Sin *et al.*, 2014).

2.1.3 Gel-shift assays and immunoblotting

Redox western blotting is a technique that uses gel electrophoresis and immunoblotting to determine a proteins' thiol/ disulfide redox status. Various alkylating reagents are available that react with free thiol groups on proteins, by adding molecular mass to the reduced free thiol groups, which can be differentiated from oxidized isoforms by electrophoresis (Figure 2.2). Western blotting can then be used to quantify these reduced and oxidized isoforms (Rudyk and Eaton, 2014).

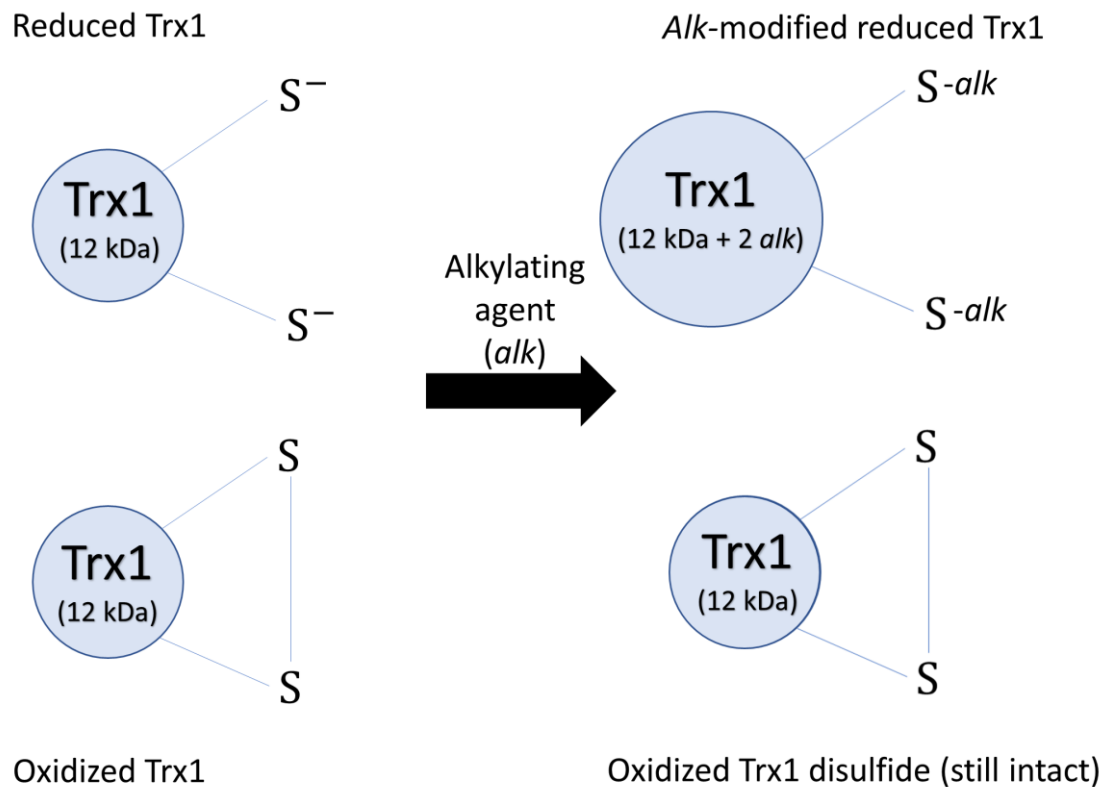


Figure 2.2 Mechanism of action of alkylation on thioredoxin 1 (Trx1). Alkylating agents are used to alkylate Trx1 to resolve and separate oxidized and reduced Trx1. Alkylating agents work by binding to the free thiol groups on reduced Trx1, leading to a mobility shift detected on a gel (Adapted from Rudyk and Eaton).

Alkylation is an important step in the redox western blotting assay that requires careful optimization for reliable quantification of the target protein isoforms. 4-acetamido-4'-maleimidylstilbene-2,2'-disulfonic acid (AMS) and methoxypolyethylene glycol maleimide (PEG-maleimide) are widely used for redox western blotting, with AMS shift mobility being typically 0.5-1 kDa and PEG-maleimide adding sizes up to 40 kDa to proteins. PEG-maleimide modifications result in very high gel shifts that often exceed the actual reagent mass, due to interactions of the PEG side chain with sodium dodecyl sulfate (SDS) during electrophoresis (Schumacher *et al.*, 2011, Ying *et al.*, 2007, Zheng *et al.*, 2007). PEG is also known to generally bind two to three water molecules for every ethylene oxide group present. This hydration, in addition to the flexible nature of the backbone of PEG, causes PEG-alkylated proteins to appear to be five to ten times as large as their actual size (Roberts *et al.*, 2002). Maleimides are also not highly specific and may participate in side reactions with amines at high pH values, making quantification sometimes challenging (Winther and Thorpe, 2014, Ying *et al.*, 2007).

The western blotting method is an important assay for differentiating target proteins from other cell constituents. Different aspects of the western blotting technique involving antibody choice, normalization and quantification will be discussed below. Obtaining commercial antibodies may sometimes be difficult for proteins of interest that are not widely studied, and producing native antibodies that work well may not be a viable option. Epitope tagging is a technique that involves genetically encoding a known short amino acid sequence that attaches to a protein of interest (Jarvik and Telmer, 1998). This allows one to easily obtain a commercially available antibody that is immunoreactive to the epitope tag. Epitope tagging proteins of interest is thus, a very useful tool in western blotting as it allows for specific detection of a protein of interest, and it allows for the detection of closely related proteins that would be difficult to detect with conventional antibodies (Brizzard, 2008). Additionally, it saves time and money compared to having to generate specific antibodies. FLAG is a popular epitope tag and comprises an eight amino acid sequence being Asp Tyr Lys Asp Asp Asp Asp Lys and this type of tagging has been successfully used in *Schizosaccharomyces pombe* (Hopp *et al.*, 1988, Noguchi *et al.*, 2008).

In western blotting, a normalization control is needed to determine the relative target protein amount to minimize errors that may arise during processing (Taylor and Posch, 2014). One such control is total protein staining with Ponceau S stain. Total protein staining is more reliable than using housekeeping proteins because the signal intensities of housekeeping genes often exceed the linear dynamic range on western blots where low concentration proteins are being detected. Housekeeping gene expression can also fluctuate during growth and different environmental conditions which is unreliable and stripping and re-probing antibodies could cause protein loss (Sander *et al.*, 2019). Advantages of total protein staining with Ponceau S include being an indicator of total protein on the detection membrane after transfer which enhances accuracy and total protein is generally consistent under experimental conditions (Sander *et al.*, 2019). Densitometric quantification is the last step in western blotting that involves quantification of the target protein's signal intensity and must be carefully executed to account for artefacts commonly associated with western blots (Gassmann *et al.*, 2009).

Many aspects need to be considered when carrying out redox western blotting experiments as discussed above, and require careful optimization of the whole assay to ensure reliable results (Gorr and Vogel, 2015). In this chapter, the thioredoxin redox charge quantification using the redox western blotting assay was optimized to detect *Schizosaccharomyces pombe* thioredoxin 1.

2.2 Materials

S. pombe His-tagged thioredoxin 1 (*Trx1*) clones in pET28 α vector were purchased from GenScript Ltd (Hong Kong). The FLAG-tagged *Trx1 S. pombe* strain JB35 (h⁻ade6-M216 his7-366 leu1-32 ura4-D18 *trx1::kan^{mx4}* Flag-*trx1::ura4⁺*) was kindly donated by Dr Elizabeth Veal (Newcastle University, United Kingdom). Nickel-charged nitriloacetic acid (Ni-NTA) agarose was obtained from Whitehead Scientific (Pty) Ltd (Cape Town, South Africa). SnakeSkin™ Dialysis Tubing (Molecular weight cut-off (MWCO) - 3.5 kDa), GeneJET Plasmid Miniprep Kit, PageRuler™ Unstained Protein Ladder, PageRuler™ Plus Prestained Protein Ladder and the Pierce™ Bicinchoninic Acid (BCA) Protein Assay Kit were obtained from ThermoFisher Scientific (Johannesburg, South Africa). Kanamycin sulfate, dithiothreitol (DTT) and isopropyl β -D-1-thiogalactopyranoside (IPTG) were obtained from Sigma-Aldrich (Johannesburg, South Africa). Ammonium persulfate (APS), Clarity™ Western ECL Substrate, nitrocellulose membrane (0.45 μ m), Precision Plus Protein™ WesternC™ Blotting Standards and N, N, N', N'-Tetramethylethylenediamine (TEMED) were obtained from BIO-RAD Laboratories (Pty) Ltd (Johannesburg, South Africa). Iodoacetamide (IAM), N-Ethylmaleimide (NEM) and PEG-maleimide were obtained from Sigma-Aldrich (Johannesburg, South Africa). 4-acetamido-4'-maleimidylstilbene-2,2'-disulfonic acid (AMS) and 4-acetamido-4'-((iodoacetyl)amino)stilbene-2,2'-disulfonic acid (AIS) were obtained from ThermoFisher Scientific (Johannesburg, South Africa). Monoclonal mouse ANTI-FLAG® M2 (primary) antibody produced in mouse (Product number: F3165 (Sigma), Lot #SLBQ7119V) and anti-mouse IgG horseradish peroxidase conjugate (secondary) antibody produced in rabbit (Product number: A9044 (Sigma), Lot #106M4870V) were purchased from Sigma-Aldrich (Johannesburg, South Africa). Bovine serum albumin (BSA) was purchased from Celtic Molecular Diagnostics (Cape Town, South Africa). All other general laboratory chemicals were of the highest purity available and were obtained from Merck/Saarchem (Johannesburg, South Africa).

2.2.1 Culture media and stock reagent preparation

2.2.1.1 Luria-Bertani (LB) broth and agar

Tryptone [1% (w/v)], yeast extract [0.5% (w/v)] and sodium chloride (NaCl) [1% (w/v)] were dissolved in distilled water (dH₂O) and made up to the desired volume. Bacteriological agar [1.5% (w/v)] was added when preparing agar, otherwise it was omitted when preparing broth. The solution was autoclaved for approximately 15 minutes at 121°C and

left to cool at room temperature. Once cooled, kanamycin (30 µg/ml) was added to the medium which was gently agitated (John, 2017).

2.2.1.2 Edinburgh Minimal Medium (EMM) broth

First, three stock solutions were prepared: salts (50×), mineral (10000×) and vitamin (1000×) stock solutions. The salts stock was prepared by dissolving 0.26 M magnesium chloride hexahydrate ($\text{MgCl}_2 \cdot 6\text{H}_2\text{O}$), 5 mM calcium chloride dihydrate ($\text{CaCl}_2 \cdot 2\text{H}_2\text{O}$), 0.67 M potassium chloride (KCl) and 14 mM sodium sulfate (Na_2SO_4) in dH_2O and was autoclaved for 15 minutes at 121°C. After cooling, the solution was stored at 4°C. The mineral stock was prepared by dissolving 80 mM orthoboric acid (H_3BO_3), 23.7 mM manganous sulfate monohydrate ($\text{MnSO}_4 \cdot \text{H}_2\text{O}$), 13.9 mM zinc sulfate heptahydrate ($\text{ZnSO}_4 \cdot 7\text{H}_2\text{O}$), 7.4 mM ferric chloride hexahydrate ($\text{FeCl}_3 \cdot 6\text{H}_2\text{O}$), 8.89 mM molybdc acid dihydrate ($\text{MoO}_4 \cdot 2\text{H}_2\text{O}$), 6.02 mM potassium iodide (KI), 1.60 mM cupric sulfate pentahydrate ($\text{CuSO}_4 \cdot 5\text{H}_2\text{O}$) and 47.59 mM citric acid monohydrate ($\text{C}_6\text{H}_8\text{O}_7 \cdot \text{H}_2\text{O}$) in dH_2O and was autoclaved for 15 minutes at 121°C. After cooling, the solution was stored at 4°C. The vitamin stock solution was prepared by dissolving 81.23 mM nicotinic acid, 55.51 mM myo-inositol, 0.41 mM biotin and 4.56 mM D-pantothenic acid in dH_2O and was autoclaved for 15 minutes at 121°C. The solution was stored at room temperature (Lind, 2019, Tomalin, 2015).

The following three solutions were freshly prepared as required, autoclaved separately, and combined once cooled. The EMM salts base was prepared by dissolving 15 mM potassium hydrogen phthalate ($\text{C}_8\text{H}_5\text{KO}_4$), 15.5 mM disodium hydrogenphosphate dihydrate ($\text{Na}_2\text{HPO}_4 \cdot 2\text{H}_2\text{O}$) and 93 mM ammonium chloride (NH_4Cl) in dH_2O and was autoclaved for 15 minutes at 121°C. 2% (w/v) glucose was prepared in dH_2O and was autoclaved for 10 minutes at 121°C. An amino acids solution was prepared by dissolving 225 mg/l adenine, 225 mg/l histidine, 225 mg/l uracil, 225 mg/l lysine and 250 mg/l leucine in dH_2O and was autoclaved for 15 minutes at 121°C. Finally, EMM broth medium was prepared by combining the EMM salts base, glucose solution, amino acids solution and by adding the salts stock, mineral stock and vitamin stock to a final dilution of (1×) in the total broth volume (Lind, 2019, Tomalin, 2015). It should be noted that the above freshly prepared solutions were calculated and measured considering the entire volume of broth once combined. The solutions were made up and autoclaved separately to prevent the Maillard reaction (Nakashima *et al.*, 2012).

2.2.1.3 Yeast extract with 5 amino acid supplements (YE5S) agar

YE5S agar was prepared by dissolving 3% (w/v) glucose, 0.5% (w/v) yeast extract, 2% (w/v) agar, 225 mg/l adenine, 225 mg/l histidine, 225 mg/l uracil, 225 mg/l lysine and 250 mg/l leucine in dH₂O and was autoclaved for 15 minutes at 121°C. Once cool to touch, agar was poured into plates which were stored inverted at 4°C (Lind, 2019, Tomalin, 2015).

2.2.1.4 Kanamycin stock

30 µg/ml kanamycin sulfate was dissolved in dH₂O. This solution was filter sterilized (0.2 µm filter) and stored at -20°C in 2 ml aliquots.

2.2.1.5 Isopropyl β-D-1-thiogalactopyranoside (IPTG) stock

100 mM IPTG was dissolved in dH₂O. This solution was filter sterilized (0.2 µm filter) and stored at -20°C in 2 ml aliquots.

2.2.1.6 Dithiothreitol (DTT) stock

1 M DTT was dissolved in dH₂O. This solution was stored at -20°C in 2 ml aliquots.

2.2.1.7 Ammonium persulfate (APS) solution

This solution was prepared fresh when needed by dissolving 10% (w/v) APS powder in dH₂O.

2.2.1.8 SDS-PAGE loading buffer (4×)

200 mM Tris-HCl (pH 6.8), 8% (w/v) sodium dodecyl sulfate (SDS), 0.4% (w/v) bromophenol blue, 400 mM DTT (only added if preparing reducing buffer) and 32% (v/v) glycerol were added and made up to the desired volume with dH₂O and stored at room temperature.

2.2.1.9 (1×) Laemmli SDS-PAGE tank buffer

25 mM Tris, 190 mM glycine and 0.1% (w/v) SDS were dissolved in dH₂O (pH was checked and was 8) and made up to the desired volume.

2.2.1.10 Laemmli SDS-PAGE - Tris lower gel buffer

1.5 M Tris and 0.8% (w/v) SDS were dissolved in dH₂O, pH was adjusted to 8.8 and made up to volume with dH₂O.

2.2.1.11 Laemmli SDS-PAGE - Tris upper gel buffer

0.5 M Tris and 0.4% (w/v) SDS were dissolved in dH₂O, pH was adjusted to 6.8 and made up to volume with dH₂O.

2.2.1.12 Coomassie blue stain

0.125% (w/v) Coomassie brilliant blue R-250, 10% (v/v) acetic acid and 50% (v/v) methanol were added and made to a final volume with dH₂O.

2.2.1.13 Destaining solution one

10% (v/v) acetic acid and 50% (v/v) methanol were measured and made up to a final volume with dH₂O.

2.2.1.14 Destaining solution two

7% (v/v) acetic acid and 5% (v/v) methanol were measured and made up to a final volume with dH₂O.

2.2.1.15 Lysis buffer

500 mM sodium chloride (NaCl), 10 mM disodium hydrogen phosphate (Na₂HPO₄), 1.8 mM monopotassium phosphate (KH₂PO₄), 2.7 mM potassium chloride (KCl), 20 mM imidazole and 20% (v/v) glycerol were measured and made up with dH₂O to volume with a confirmed pH of 7.4. The solution was autoclaved for 15 minutes at 121°C. Once cooled, 10 mM β-mercaptoethanol was added and the solution was stored at room temperature (John, 2017).

2.2.1.16 Equilibration buffer

500 mM sodium chloride (NaCl), 10 mM disodium hydrogen phosphate (Na₂HPO₄), 1.8 mM monopotassium phosphate (KH₂PO₄), 2.7 mM potassium chloride (KCl), 30 mM imidazole and 10 mM β-mercaptoethanol were measured and made up with dH₂O to volume with a confirmed pH of 7.4 (John, 2017).

2.2.1.17 Wash buffer

500 mM sodium chloride (NaCl), 10 mM disodium hydrogen phosphate (Na₂HPO₄), 1.8 mM monopotassium phosphate (KH₂PO₄), 2.7 mM potassium chloride (KCl), 20 mM

imidazole and 10 mM β -mercaptoethanol were measured and made up with dH₂O to volume with a confirmed pH of 7.4 (John, 2017).

2.2.1.18 Dialysis buffer

137 mM sodium chloride (NaCl), 10 mM disodium hydrogen phosphate (Na₂HPO₄), 1.8 mM monopotassium phosphate (KH₂PO₄), 2.7 mM potassium chloride (KCl) and 0.05% (w/v) sodium azide were measured and made up with sterile dH₂O to volume with a confirmed pH of 7.4 and stored at 4°C (John, 2017).

2.2.1.19 IAM alkylation buffer

100 mM Tris-HCl (pH 8), 1% (w/v) SDS and 75 mM IAM were dissolved and made up to volume in sterile dH₂O (Brown *et al.*, 2013).

2.2.1.20 NEM alkylation buffer

100 mM Tris-HCl (pH 8), 1% (w/v) SDS, 1 mM ethylenediaminetetraacetic acid (EDTA) (pH 8) and 25 mM NEM were dissolved and made up to volume in sterile dH₂O (Rogers *et al.*, 2006, Tomalin, 2015).

2.2.1.21 PEG-maleimide alkylation buffer

50 mM Tris-HCl (pH 7.5), 0.1% (w/v) SDS, 10 mM EDTA (pH 8) and 3 mM PEG-maleimide were dissolved and made up to volume in sterile dH₂O (Padayachee and Pillay, 2016).

2.2.1.22 AMS alkylation buffer

50 mM Tris-HCl (pH 8.5), 0.5% (w/v) SDS and 15 mM AMS were dissolved and made up to volume in sterile dH₂O (Ritz *et al.*, 2000).

2.2.1.23 AIS alkylation buffer

200 mM Tris-HCl (pH 8), 1% (w/v) SDS, 1 mM EDTA (pH 8) and 25 mM AIS were dissolved and made up to volume in sterile dH₂O (Tomalin, 2015).

2.2.1.24 (1×) Tris-Tricine SDS-PAGE anode tank buffer

100 mM Tris and 22.5 mM HCl were dissolved and made up to volume in dH₂O (pH 8.9) (Schägger, 2006).

2.2.1.25 (1×) Tris-Tricine SDS-PAGE cathode tank buffer

100 mM Tris, 100 mM tricine and 0.1% (w/v) SDS were dissolved and made up to volume in dH₂O (pH 8.25) (Schägger, 2006).

2.2.1.26 Tris-Tricine SDS-PAGE gel buffer

3 M Tris, 1 M HCl and 0.3% (w/v) SDS were dissolved and made up to volume in dH₂O (pH 8.45) (Schägger, 2006).

2.2.1.27 Acrylamide stock solutions

For 30% (v/v) acrylamide stock, acrylamide (29 g) and N,N'-Methylenebisacrylamide (bisacrylamide) (1 g) were dissolved in 100 ml of dH₂O and the solution was filtered through filter paper (0.5 mm) and stored at 4°C in an amber bottle. For 49.5% (v/v) acrylamide stock, acrylamide (23.25 g) and bisacrylamide (1.5 g) were dissolved in 50 ml of dH₂O and the solution was filtered through filter paper (0.5 mm) and stored at 4°C in an amber bottle.

2.2.1.28 (1×) Transfer buffer

50 mM Tris (pH 8.0), 200 mM glycine, 20% (v/v) methanol and 0.01% (w/v) SDS were measured and dissolved in dH₂O and made up to volume.

2.2.1.29 Ponceau S stain

1.5 mM Ponceau S tetrasodium salt and 1% (v/v) glacial acetic acid were mixed and made up to volume in dH₂O (Sander *et al.*, 2019).

2.2.1.30 Tris-buffered saline with TWEEN 20 (TBST)

20 mM Tris (pH 8.0), 380 mM NaCl₂ and 0.1% Tween 20 were mixed and made up to volume in dH₂O.

2.2.1.31 BSA stock solution

10% (w/v) BSA was prepared by dissolving 5g of BSA powder in 50 ml of TBST and was stored at 4°C.

2.2.1.32 Primary antibody dilution (0.5 µg/ml)

0.363 µl of monoclonal mouse ANTI-FLAG® M2 antibody was diluted in 1.5 ml TBST and 1.5 ml 10% (w/v) BSA to give a final concentration of 0.5 µg/ml.

2.2.1.33 Secondary antibody dilution (1:20 000)

0.25 µl of anti-mouse IgG horseradish peroxidase conjugate antibody produced in rabbit was diluted in 2.5 ml TBST and 2.5 ml 10% (w/v) BSA to give a final dilution of 1:20 000.

2.3 Methods

2.3.1 Induction and production of recombinant *S. pombe* Trx1

Plasmid DNA containing His-tagged *S. pombe* thioredoxin 1 (*Trx1*) was isolated from *E. coli* BL21 using the GeneJET Plasmid Miniprep Kit. The plasmid vector was sequenced (Central Analytical Facilities, Stellenbosch University) in the forward and reverse orientations and the sequence traces were manually analyzed and evaluated. The nucleic acid sequence was translated using EMBOSS Transeq (https://www.ebi.ac.uk/Tools/st/emboss_transeq/) and was aligned to the *S. pombe* Trx1 protein sequence from UniProt (<https://www.uniprot.org>) using local alignment tool EMBOSS Water (https://www.ebi.ac.uk/Tools/psa/emboss_water/).

Once the sequence was confirmed, Trx1 production from the pET28α clones was carried out. An LB agar plate was spread-plated with 150 µl of the frozen recombinant *E. coli* BL21 glycerol stock and incubated (24 hours, 37°C, inverted). A three-way streak was carried out on a fresh LB agar plate from the growth to isolate single colonies and was further incubated (24-48 hours, 37°C, inverted). A single colony was isolated and was inoculated into 25 ml of LB broth, which was incubated in a shaking water bath (200 revolutions per minute (RPM), 37°C) for approximately 16 hours (overnight). The overnight culture (5 ml) was inoculated into fresh LB broth to a final volume of 50 ml and was left to grow for two hours or until an OD₆₀₀ of 0.3-0.4 was reached (Lin *et al.*, 2010). Trx1 was induced by adding 0.5 mM IPTG to the culture. To determine the induction time that resulted in the best protein yield, samples (1 ml) from the induced culture were taken hourly for six hours, together with an overnight induction time-point (23 hours). The samples were centrifuged (9,299×g, 10 min, 4°C) and cells were pelleted. The supernatant liquid was discarded and the pellets were placed in the -20°C freezer for further processing. To ensure that a consistent protein concentration was compared over the entire time course, the pellets were thawed and resuspended in the appropriate volume of dH₂O until a final OD₆₀₀ of 10 was reached. Thereafter, 4 µl of (4×) reducing loading buffer (containing 400 mM DTT) was added to 12 µl of the resuspended samples. The samples were boiled for 10 minutes and analyzed by Laemmli SDS-PAGE on a 23% (w/v) acrylamide gel. 7 µl of the boiled samples were run on the gel at 200V for approximately 70 minutes with

Laemmli SDS-PAGE tank buffer, until the tracking dye migrated to the bottom of the gel. The gel was stained overnight (room temperature, 50 RPM) with Coomassie blue stain and destained with Destaining solution one for 30-60 minutes (room temperature, 50 RPM). The Destaining one solution was replaced with Destaining two solution and the gel was visualized under white light.

For batch induction of Trx1, after the addition of 0.5 mM IPTG, cultures were grown for 5 hours and the entire culture (50 ml) was centrifuged (9,299×g, 10 min, 4°C), supernatant discarded and the pellet was frozen and stored at -20°C until sonication (John, 2017).

2.3.2 Sonication

Frozen *E. coli* pellets from Trx1 induction were thawed on ice and 10 ml of lysis buffer was added. The samples were vortexed to resuspend the pellet and were sonicated to break open cells at 30% amplitude (7×30 second pulses; with 30-second intervals on ice) using a VirSonic 60 Ultrasonic Cell Disrupter (8W). Samples were thereafter centrifuged (9,299×g, 10 min, 4°C) and the supernatant containing Trx1 was placed on ice or stored at -20°C until Ni-NTA column purification (John, 2017).

2.3.3 Ni-NTA affinity purification

The crude protein samples from sonication containing Trx1 were purified using nickel-charged affinity resin columns (Ni-NTA). To generate a fresh column, 2 ml of nickel agarose was added to the column and the storage ethanol was allowed to elute. Thereafter, one column volume of equilibration buffer was allowed to flow through to equilibrate the column. The crude protein sample was loaded into the column, leaving a pocket of air in the column for rotation to ensure efficient protein binding. The column was rotated for 4 hours at 4°C using a Labnet Revolver™ Adjustable 360° Rotator, to allow for the His-tagged Trx1 to bind to the nickel agarose. Once complete, the crude sample from the column was eluted and the column was washed twice with wash buffer and after that imidazole gradient wash steps were performed by adding a column of wash buffer with a specific concentration of imidazole (20-250 mM imidazole). Once all washes were carried out the column was incubated with NaOH (0.5 M) for 30 minutes and was allowed to flow through, the column was stored in 2 ml of 30% (v/v) ethanol at 4°C. Samples were collected from all the wash and elution steps and were analyzed by Laemmli SDS-PAGE (John, 2017).

2.3.4 Dialysis

Imidazole wash samples containing the eluted Trx1 fraction were pooled into a single dialysis bag (MWCO - 3.5 kDa) with a dialysis buffer volume that was 100× the volume of the protein sample. The sample was revolved in dialysis buffer for 4 hours at 4°C and the dialysis buffer was replaced with fresh buffer and was revolved overnight (approx. 16 hours). The buffer was once again replaced and revolved for another 4 hours (4°C). The dialysis bag containing Trx1 was placed on a bed of polyethylene glycol 20 000 to concentrate the protein sample. The concentrated protein sample was stored at -20°C for alkylation experiments. The Pierce™ BCA Protein Assay Kit was used to determine the concentration of Trx1 (John, 2017).

2.3.5 Alkylation of purified, recombinant *S. pombe* Trx1

Purified Trx1 (1.5 μM) was reduced by adding DTT (1 mM) and incubating for one hour at 37°C. Trichloroacetic acid (TCA) [10% (w/v), 500 μl] was added to samples which were mixed and centrifuged (16,200×g, 40 minutes, 4°C) to pellet the protein. The supernatant was discarded and pellets were washed with acetone [100% (v/v), 200 μl] and centrifuged again (11,700×g, 10 minutes, 4°C) (Padayachee, 2017). The pellets were dried at 37°C for approximately 10 minutes and alkylated with a 30 μl volume of either iodoacetamide (IAM) (75 mM) alkylation buffer (Brown *et al.*, 2013), N-Ethylmaleimide (NEM) (25 mM) alkylation buffer (Rogers *et al.*, 2006, Tomalin, 2015), PEG-maleimide (PEG-mal) (3 mM) alkylation buffer (Padayachee and Pillay, 2016), 4-acetamido-4'-maleimidylstilbene-2,2'-disulfonic acid (AMS) (15 mM) alkylation buffer (Ritz *et al.*, 2000) or 4-acetamido-4'-[(iodoacetyl)amino]stilbene-2,2'-disulfonic acid (AIS) (25 mM) alkylation buffer (Tomalin, 2015). For alkylation with IAM and NEM, samples were incubated at room temperature for approximately 30 minutes, while PEG-maleimide alkylation required an incubation time of 40 minutes at 45°C and AMS and AIS alkylation required incubation times of two hours at 37°C. The samples were analyzed by Laemmli and Tris-Tricine SDS-PAGE. For Tris-Tricine SDS-PAGE (Tables 2.1 and 2.2), gels were run (100 V, 80 minutes) and then Coomassie stained as previously described (Section 2.3.1).

Table 2.1 Preparation of 23% (w/v) Laemmli SDS-PAGE acrylamide gel

	Separating 23% (w/v) (Total volume - 15.13 ml)	Stacking 6% (w/v) (Total volume - 5.01 ml)
Acrylamide (30 %) [29% (w/v) acrylamide, 1% (w/v) bisacrylamide]	11.25 ml	0.65 ml
Tris lower [1.5 M Tris-HCl, 0.8% (w/v) SDS, pH 8.8]	3.75 ml	-
Tris upper [0.5 M Tris-HCl, 0.4% (w/v) SDS, pH 6.8]	-	1.25 ml
Water	-	3.05 ml
APS (10% w/v)	0.1 ml	0.05 ml
TEMED	0.03 ml	0.01 ml

Table 2.2 Preparation of 25% (w/v) Tris-Tricine SDS-PAGE acrylamide gel

	Separating 25% (w/v) (Total volume - 18.07 ml)	Stacking 4% (w/v) (Total volume - 6.04 ml)
Acrylamide (49.5%) [46.5% (w/v) acrylamide, 3% (w/v) bisacrylamide]	9 ml	0.5 ml
Gel Buffer [3 M Tris, 1 M HCl, 0.3% (w/v) SDS, pH 8.45]	6 ml	1.5 ml
Water	3 ml	4 ml
APS (10% w/v)	0.06 ml	0.03 ml
TEMED	6 μ l	12 μ l

2.3.6 Harvesting concentrated *S. pombe* protein

A YE5S agar plate was spread-plated with 100 μ l of the frozen *S. pombe* JB35 (FLAG-tagged *Trx1*) glycerol stock and incubated (2-3 days, 30°C, inverted). A three-way streak was carried out on a fresh YE5S agar plate from the growth to isolate single colonies and was further incubated (2-3 days, 30°C, inverted). Single colonies were isolated and each colony was inoculated into a volume of EMM broth medium (15 ml), which was incubated in an orbital air-shaker (180 RPM, 30°C, overnight). The OD₅₉₅ was measured the next morning and the appropriate volume of overnight culture was inoculated into fresh EMM broth (final culture volume of 50 ml) until an OD₅₉₅ of 0.15 was reached. The cultures were left to grow until the OD₅₉₅ increased to 0.4-0.5 (3-5 hours, 180 RPM, 30°C) (Brown *et al.*, 2013, Olivares-Marin *et*

al., 2018, Tomalin, 2015). Once the exponential phase of growth (OD₅₉₅ of 0.4-0.5) was reached, the entire culture volume (50 ml) was centrifuged to pellet the cells (3,300×g, 10 min, 4°C). The supernatant was discarded and the pellet was frozen at -80°C for protein extraction.

2.3.7 Protein extraction from *S. pombe*

All steps during protein extraction were carried out on ice. TCA [10% (w/v), 200 µl] was added to the frozen cell pellets which were allowed to thaw on ice. Once thawed, the samples were vortexed and transferred to 1.5 ml screw-cap tubes and 0.5 mm glass beads were added to the tubes until the 1 ml mark on the tube (approximately 750 µl glass bead volume). The cells were then broken open in a Bioprep-24 Homogenizer (Hangzhou Allsheng Instruments Co., Ltd) for two runs (15 seconds at 7 m/s for each run), with a one-minute incubation on ice between the runs. TCA [10% (w/v), 500 µl] was added to the samples and the samples were vortexed. The bottom of the screw-cap tube was pierced with a hot needle and the tube was securely placed within a fresh 1.5 ml centrifuge tube. Both tubes were then placed within a 50 ml centrifuge tube for centrifugation (1,000×g, 1 min, 4°C) to remove the cell lysate into the clean tube without the glass beads. For the 2 mM diamide (oxidized) Trx1 control, diamide stock was mixed into samples until a final concentration of 2 mM and incubated for 15 minutes at 37°C. The cell lysate was pelleted (11,700×g, 12 min, 4°C) and the supernatant was removed. Acetone [100% (v/v), 200 µl] was added and gently mixed with the pellet and the pellet was centrifuged again (11,700×g, 3 min, 4°C) and the acetone was removed. These acetone washes were done three times. The pellets were air-dried in a 37°C incubator until all the acetone was evaporated. For the 1 mM DTT (reduced) Trx1 control, DTT (1 mM, 10 µl) was mixed with the dry pellet and left to incubate at room temperature for 20 minutes. PEG-maleimide alkylation buffer (3 mM, 30 µl) was mixed vigorously with the pellets to resuspend them and the resuspended pellets were left to alkylate at 45°C for 40 minutes. The samples were centrifuged (11,400×g, 3 min, 4°C) after incubation and the supernatant was removed and stored in a sterile tube at -20°C for further protein concentration quantification using the Pierce™ BCA Protein Assay Kit as per the kit instructions. The Pierce™ BCA Protein Assay was carried out in a 96 multi-well plate in triplicate and absorbance was quantified using a Versamax™ ELISA Microplate Reader (OD₅₆₂) (Brown *et al.*, 2013, Lind, 2019, Tomalin, 2015).

2.3.8 Western blotting of *S. pombe Trx1*

The protein extract samples were prepared for gel electrophoresis by adding non-reducing (4×) SDS-PAGE loading buffer (10 µl) and boiling for five minutes at 90-100°C. The absorbance values obtained from protein quantification using the Pierce™ BCA Protein Assay Kit were used to determine the volume of the prepared sample to load onto the gel to get an OD₅₆₂ (as per kit instructions) reading of 0.15 across all samples to standardize all samples to a set concentration value. All the gels used for western blotting were 22% (w/v) Urea Tris-Tricine gels (Table 2.3) which were run for approximately 40-50 minutes at 150 V with Tris-Tricine anode and cathode tank buffers in the correct chambers.

Table 2.3 Preparation of 22% (w/v) Urea Tris-Tricine SDS-PAGE acrylamide gel

	Separating 22% (w/v) (Total volume - 20 ml)	Stacking 10% (w/v) (Total volume - 10 ml)
Acrylamide (49.5%) [46.5% (w/v) acrylamide, 3% (w/v) bisacrylamide]	9.17 ml	2 ml
Gel buffer [3 M Tris, 1 M HCl, 0.3% (w/v) SDS, pH 8.45]	6.67 ml	3.33 ml
Urea	7.2 g	-
Water	3.43 ml	4.12 ml
APS (10% w/v)	66.7 µl	50 µl
TEMED	6.67 µl	5 µl

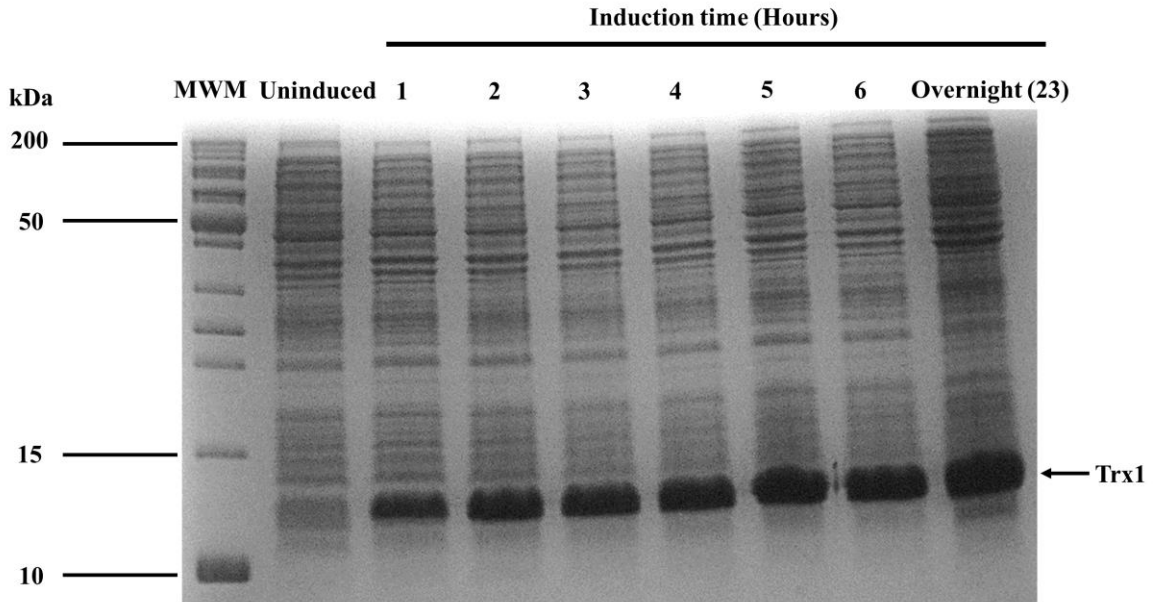
After the gel had run, the gel was carefully placed within a western blot sandwich for the transfer of proteins to a nitrocellulose membrane. First, three sheets of thin blotting paper were placed on the transfer sponge, followed by the gel, a sheet of nitrocellulose membrane (0.45 µm), three sheets of thin blotting paper and the top transfer sponge. All steps in the construction of the western blot sandwich were carried out submerged in transfer buffer. The sandwich was pressed with a roller to remove air bubbles and was securely inserted for protein transfer into the transfer cell for two hours at 400 mA constant. The ice pack was replaced with a new frozen one to keep the transfer buffer cool after one hour and the transfer resumed. After the transfer was complete the gel was Coomassie stained overnight and destained as stated in Section 2.3.1 to ensure optimal protein transfer had occurred. The nitrocellulose membrane was thereafter Ponceau S stained (1.5 mM, 3-4 ml) for 30 seconds to determine total protein transfer. The blot was imaged and dH₂O was promptly added to submerge the blot, Ponceau S was destained by adding a few drops of NaOH (0.5 M) to the dH₂O with gentle agitation. The

membrane was incubated in BSA blocking solution [10% (w/v), 3 ml] and agitated (30 min, 150 RPM, room temperature). BSA solution was removed and primary antibody (0.5 µg/ml, 3 ml) (monoclonal mouse ANTI-FLAG® M2) was added and incubated overnight with agitation (150 RPM, 4°C). After incubation, the primary antibody was removed and the membrane was washed with enough TBST to submerge the blot (5 min, 150 RPM, room temperature). The washing was done four times and after removing the last TBST wash, the secondary antibody (1:20 000 dilution, 5 ml) (anti-mouse IgG horseradish peroxidase conjugate antibody produced in rabbit) was added and incubated with agitation (1 hour, 150 RPM, room temperature). After incubation, the secondary antibody was discarded and the four TBST washes were carried out again. The membrane was thereafter partially dried and developed with Clarity™ Western ECL Substrate as per the instructions and visualized using the G-BOX Chemi-XR5 GeneSys imaging system with a range of 0-30 second exposure times. Images were obtained and adjusted such that a white background was obtained with a dark banding pattern for easy signal quantification from bands visualized. The oxidized and reduced Trx1 band intensities from the western blots were analyzed and quantified using the gel analysis function, measured in pixel density from ImageJ software (Lind, 2019, Tomalin, 2015).

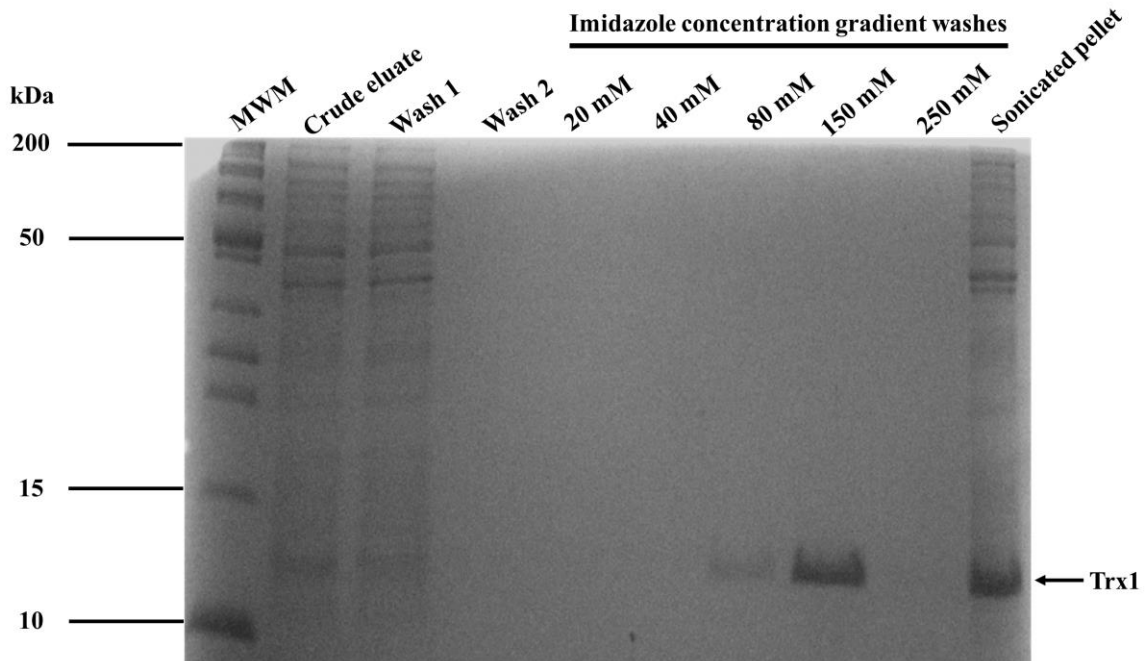
To determine the optimal combination of primary antibody concentration and secondary antibody dilution, using dot blot analysis, *S. pombe* JB35 was grown as described in Section 2.3.6 and protein was extracted as described in Section 2.3.7. This very concentrated protein extract was quantified using the Pierce™ BCA Protein Assay and was subsequently diluted with dH₂O into a set of increasing protein concentrations. Volumes of 6 µl of the increasing concentrations of protein extract were then carefully dotted onto thin strips of nitrocellulose membrane (0.45 µm) and dried. After drying, the membrane strips were blocked with BSA [10% (w/v)] and the same antibody incubation protocol was followed as described in Section 2.3.8, although differing combinations of primary and secondary antibody concentrations were tested during optimization to determine the best combination to use to ensure the most suitable signal quantification without saturation (Kurien and Scofield, 2006, Lind, 2019).

harvest time following induction by 0.5 mM IPTG was 5 hours because the Trx1 band was the thickest at this time point (Figure 2.4A).

A



B



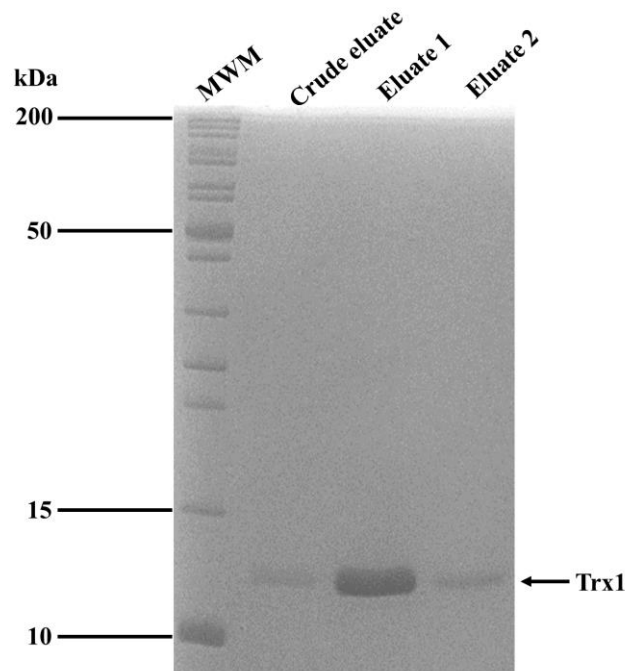
C

Figure 2.4 Successful production and purification of His-tagged, recombinant *S. pombe* Trx1. (A) *Trx1* was induced with 0.5 mM IPTG in pET28 α expression vector within *E. coli* BL21. (B) Nickel-charged affinity resin (Ni-NTA) purification of *Trx1*. Imidazole concentration gradient washes were used to determine the optimal *Trx1* elution concentration (20-250 mM). (C) Batch Ni-NTA purification of *Trx1*. All gels were 23% (w/v) Laemmli SDS-PAGE and the molecular weight marker (MWM) used in all gels was PageRuler™ Unstained Protein Ladder (10 to 200 kDa).

Optimally produced *S. pombe* Trx1 was purified using nickel-charged affinity resin columns (Ni-NTA). Imidazole step gradient washes were carried out to determine the imidazole concentration (20-250 mM) that suitably eluted Trx1 and it was determined that 150 mM imidazole eluted Trx1 (Figure 2.4B). A crude eluate sample of the flow-through after the incubation for Trx1 binding, was run on the gel to determine if Trx1 binding to the column was sufficient. A very faint Trx1 protein band was detected in the crude eluate showing successful binding of Trx1 to the column. However, Trx1 was detected in the sonicated pellet, showing a slight loss of protein during harvesting, potentially attributed to protein aggregation or incomplete cell lysis during sonication (Figure 2.4B).

Batch production and purification of Trx1 was carried out and Trx1 was eluted at 150 mM imidazole (Figure 2.4C). Trx1 samples from the first batch purification were found to contain non-specific, co-eluted bands (Supplementary material-Figure S3). Thus, a second purification of the same protein eluate from the initial purification was carried out and this

resulted in a purer protein isolate (Figure 2.4C). The pure Trx1 protein was dialyzed to remove salts and was concentrated on a bed of polyethylene glycol 20 000 and the concentration of the pure Trx1 was determined to be 180 µg/ml using the Pierce™ BCA Protein Assay Kit. Thus, the purified protein yield per litre of bacterial culture was 9 mg/l.

2.4.2 Alkylation optimization of recombinant *S. pombe* Trx1

After successfully producing and purifying recombinant *S. pombe* Trx1, alkylation experiments were carried out to determine the most suitable alkylating agent that would separate oxidized and reduced Trx1. Five different alkylating agents were tested on oxidized thioredoxin, reduced thioredoxin (sample pre-treated with DTT) and a sample which contained both oxidized and reduced thioredoxin (Figure 2.5). To determine whether the band sizes obtained were due to the alkylation treatment experiments, “no alkylation controls” were included in all analyses (Figure 2.5).

The only alkylating agent to considerably separate oxidized and reduced Trx1 was PEG-maleimide (Figure 2.5A). PEG-maleimide increased the size of reduced Trx1 to approximately 60-70 kDa, whilst the size of oxidized Trx1 (12 kDa) remained the same as expected (Figure 2.5A). The other alkylating agents caused a small, detectable shift in mobility between the Trx1 isoforms when oxidized and reduced samples were in separate gel lanes, however when combined in the same lane, the bands were indistinguishable (Figure 2.5A and B). The “no alkylation controls” resulted in insignificant migration between oxidized and reduced Trx1 bands. Thus, the reason for the separation of oxidized and reduced Trx1 bands post alkylation, was due to alkylation and there were no confounding factors (Figure 2.5). As a positive control experiment to confirm the separation of protein redox isoforms attributed to PEG-maleimide alkylation, purified fission yeast glyceraldehyde 3-phosphate dehydrogenase (GAPDH) and catalase could have been used (van Leeuwen *et al.*, 2017), although these proteins were unavailable to us.

Figure 2.5 Testing different alkylating agents to determine the most suitable alkylating agent to separate oxidized and reduced, *S. pombe* thioredoxin 1. (A) Alkylation of Trx1 with 75 mM iodoacetamide (IAM), 25 mM N-Ethylmaleimide (NEM) and 3 mM PEG-maleimide (PEG-mal), resolved on a 25% (w/v) Tris-Tricine SDS-PAGE gel. (B) Alkylation of Trx1 with 15 mM 4-acetamido-4'-maleimidylstilbene-2,2'-disulfonic acid (AMS) and 25 mM 4-acetamido-4'-[(iodoacetyl)amino]stilbene-2,2'-disulfonic acid (AIS). (C) Alkylation of Trx1 with 3 mM PEG-maleimide. Both (B) and (C) gels were 22% (w/v) Urea Tris-Tricine SDS-PAGE gels. For (A), (B) and (C), (+) represents reduced Trx1 from DTT treatment, (-) represents oxidized Trx1 without DTT treatment and both (+) and (-) for the same gel lane represents both DTT-reduced Trx1 and oxidized Trx1 samples loaded in the same gel lane. Non-specific bands are identified (*) and Trx1 protein bands are sectioned in red to allow for quick identification.

It was decided to use PEG-maleimide alkylation to separate Trx1 isoforms and alkylation experiments were then carried out in duplicates (Supplementary material-Figure S6) to confirm the band shift (Figure 2.5C). Oxidized Trx1 remained 12 kDa as expected, because it was not alkylated (Figure 2.5C). Reduced Trx1 appeared as a couplet at 70 and 95 kDa respectively (Figure 2.5C), which presumably results from a single or double alkylation of the active site cysteines in Trx1. The two reduced bands obtained can be explained by the two thiol groups present within the active site of reduced thioredoxin, resulting in partially (band 1) or fully (band 2) alkylated isoforms (Requejo *et al.*, 2010). PEG-maleimide was expected to add 5 kDa per thiol, but it also binds to amino acids like lysine and PEG-maleimide hydration causes the shift in mobility in SDS-PAGE to be much greater than anticipated (Lee and Chang, 2019, Nanda and Lorsch, 2014, Veronese, 2001). Thus, the band sizes obtained, 70 and 95 kDa, were much higher than the expected sizes of 17 and 22 kDa for partially and fully alkylated, reduced thioredoxin isoforms (Figure 2.5C). This uncertainty in the PEG-maleimide alkylated protein size is presumably why many experiments involving redox assays do not always include molecular weight markers for size comparison (Burgoyne *et al.*, 2013).

Urea was added to the Tris-Tricine SDS-PAGE gel system for gels in (B) and (C) to improve the band separation, which is why the partially and fully reduced Trx1 bands could be seen in (C), but not in (A) for PEG-maleimide alkylation (Figure 2.5). Additionally, there were consistently sized contaminating protein bands that were detected in all the alkylation experiments, even though the Trx1 protein sample was purified twice to remove contaminating bands. The Trx1 protein sample was concentrated after it had been purified and dialyzed. It

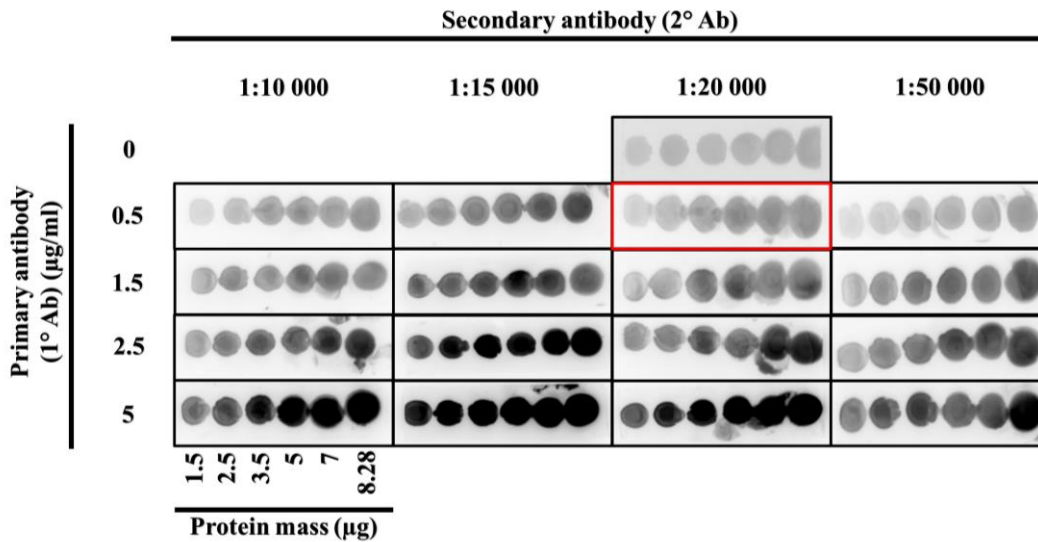
appears that this concentration step allowed for the contaminating proteins to also become concentrated and prominent, which is why the bands appear in the alkylation experiments (Figure 2.5), but not in the purification gels (Figure 2.4). Full gel images for the alkylation experiments can be found in the Supplementary material (Figures S5 and S6).

2.4.3 Optimization of the redox western blotting assay for *S. pombe* Trx1 for *in vivo* stressor experiments

We next moved on to optimizing the *in vivo* *S. pombe* stressor experiments and subsequent redox western blotting assay. First, *S. pombe* JB35 cultures were grown (Section 2.3.6), and concentrated protein was extracted (Section 2.3.7) and quantified for use in dot blot analysis. The dot blot analysis is a quicker, simplified method adapted from western blotting that involves dotting a protein sample directly onto the detection membrane and developing the blot without running gels or transferring the protein to the detection membrane (Tian *et al.*, 2017). However, this assay cannot distinguish between protein size as the sample is not separated on a gel. Still, this assay is very useful when optimizing aspects of western blotting.

Dot blot analysis was used to quantitatively compare and determine which primary antibody concentration and secondary antibody dilution combination would allow sufficient signal intensity without signal saturation. We simultaneously also tested the concentration of protein that would be required for optimal signal detection. A range of increasing protein concentrations, primary antibody concentrations and secondary antibody dilutions were tested to determine the dynamic range of Trx1 detection (Figure 2.6). The most suitable primary antibody and secondary antibody combination was 0.5 $\mu\text{g/ml}$ primary antibody and 1:20 000 secondary antibody (Figure 2.6A), which displayed an increase in signal without saturation. A control that omitted primary antibody confirmed that the signal detected was only due to the interaction between primary and secondary antibodies (Figure 2.6A). The protein concentration range, 417-583 $\mu\text{g/ml}$ (2.5-3.5 μg mass from dot blots), gave a linear increase in signal intensity (Figure 2.6B). All further western blotting assays described used a protein concentration of 400 $\mu\text{g/ml}$, which corresponded to an absorbance of 0.15 using the Pierce™ BCA Protein Assay.

A



B

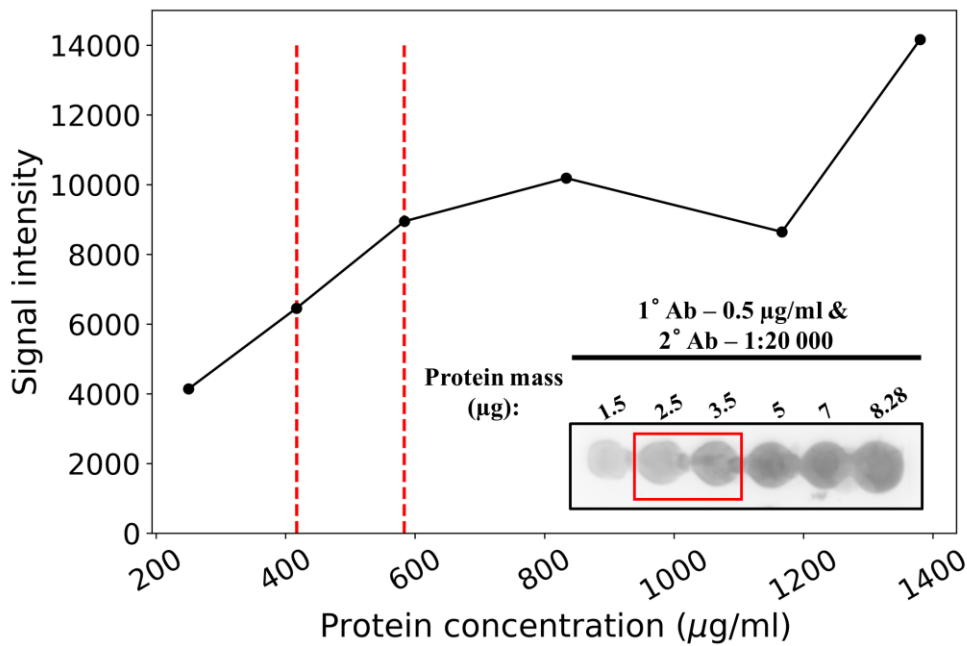
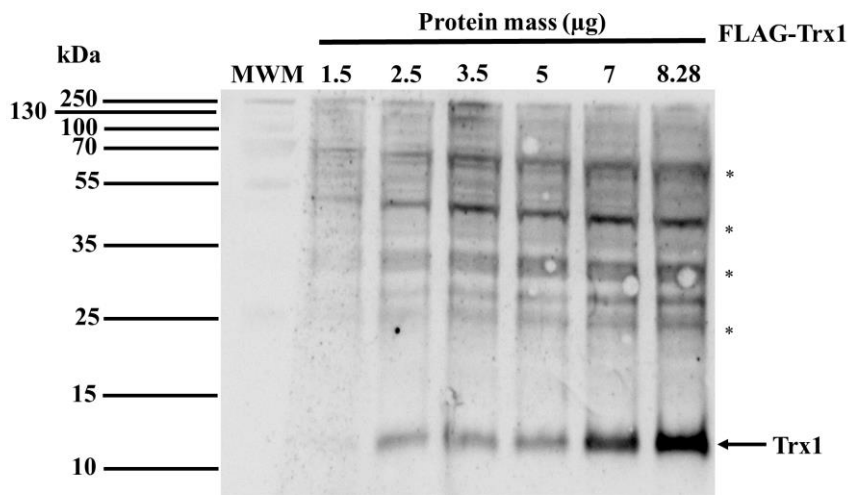


Figure 2.6 Investigating the optimal combination of primary antibody concentrations and secondary antibody dilutions for linear signal detection of *S. pombe* JB35 Trx1, to be used in the redox western blotting assay. (A) Dot blot analysis with increasing *S. pombe* JB35 protein concentrations developed with different concentrations of primary antibody and dilutions of secondary antibody. The following masses of protein were dotted; 1.5-8.28 µg. Different combinations of a primary antibody (1° Ab) concentration range (0.5-5 µg/ml) and a secondary antibody (2° Ab) dilution range (1:10 000-1:50 000) were tested and the combination selected is sectioned in red. An antibody control was carried out with 1:20 000

secondary antibody, in which primary antibody was omitted. *S. pombe* JB35 protein extracted was quantified using the Pierce™ BCA Protein Assay as per the instructions and was compared to the bovine serum albumin (BSA) standard from the assay kit. (B) Quantification of signal intensity of increasing *S. pombe* JB35 protein concentrations from dot blot analysis using ImageJ software, developed with a 0.5 µg/ml primary antibody and 1:20 000 secondary antibody combination. The red dashed area indicates the concentration range that resulted in a linear increase in signal intensity.

Western blotting was used to confirm the dot blot analyses. We found that Trx1 was detected at 12 kDa (Figure 2.7A). Non-specific bands were detected on the western blot, although these bands were detected in every protein sample and could have been an artefact in the samples formed during sample preparation (Figure 2.7A). A control experiment of the western blotting assay was carried out that confirmed the specificity of the primary antibody to the FLAG-tagged Trx1 in *S. pombe* JB35, by comparing the signal detected to a non-tagged Trx1 *S. pombe* strain, SB3 (h- ade6-M216 pap1+ (3Pk)::ura4 484 his7-366 leu1-32 ura4-D18). The Trx1 band detected in *S. pombe* JB35 was clearly visible as compared to the non-tagged strain, verifying the specificity of the primary antibody to the FLAG-tag on Trx1 in *S. pombe* JB35 (Figure 2.7B).

A



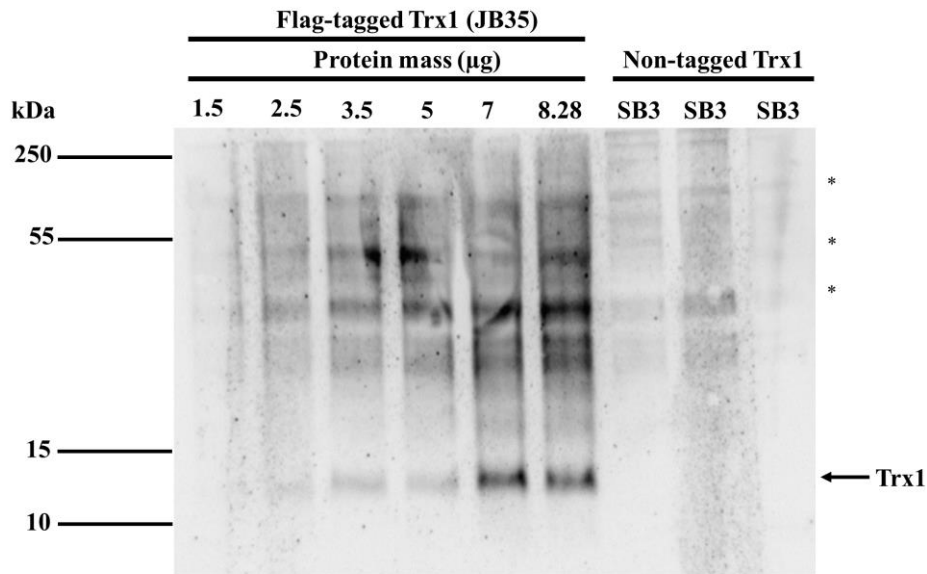
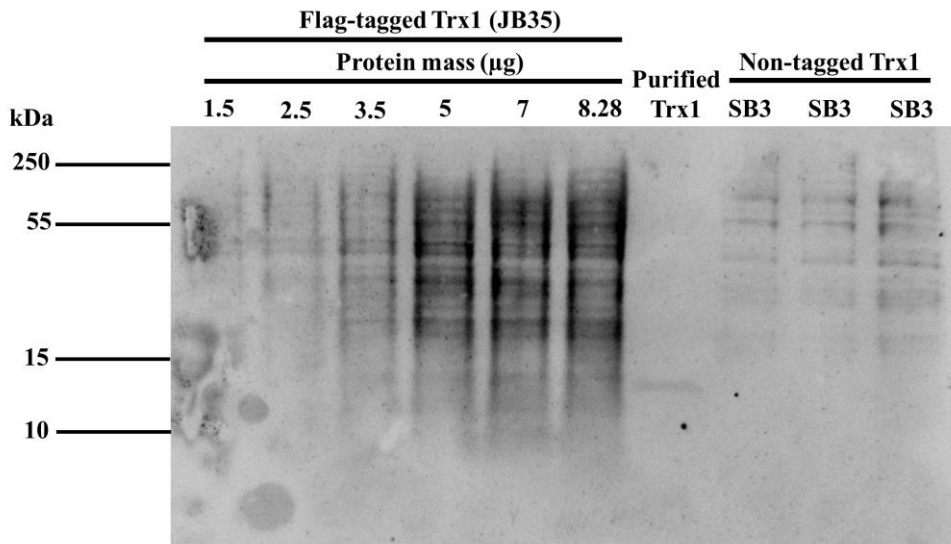
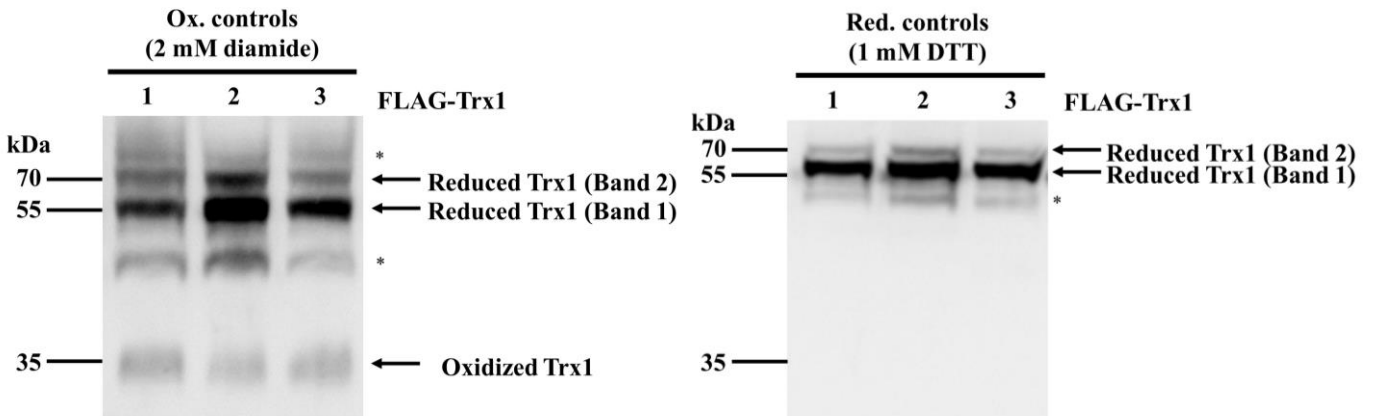
B**C****D**

Figure 2.7 Control experiments for the redox western blotting assay to detect *S. pombe* JB35 Trx1. (A) Increasing *S. pombe* JB35 protein mass (μg) analyzed by the western blotting assay to detect and size Trx1. (B) Increasing protein mass (μg) analyzed by western blotting to confirm the specificity of the primary antibody to the FLAG-tag on *S. pombe* JB35 Trx1, compared to a non-tagged Trx1 *S. pombe* strain (SB3). (C) Increasing protein mass (μg) analyzed by western blotting to test the non-specificity of secondary antibody, on *S. pombe* JB35 protein, purified recombinant Trx1 and *S. pombe* SB3 (non-tagged Trx1). The western blot was developed with no primary antibody and 1:20 000 dilution of the secondary antibody. (D) *S. pombe* JB35 protein treated with (2 mM) diamide to chemically oxidize Trx1 (Ox. controls) and (1 mM) DTT to chemically reduce Trx1 (Red. controls). The protein samples were alkylated with 3 mM PEG-maleimide to visualize Trx1 redox state separation and the analysis was done by redox western blotting. Labels 1, 2 and 3 refer to triplicate experiments with the same chemical treatment. (A), (B) and (D) western blots were developed with 0.5 $\mu\text{g}/\text{ml}$ primary antibody and 1:20 000 secondary antibody. Non-specific bands are identified (*) for all western blots.

An additional western blotting control experiment was run to confirm the specificity between the primary and secondary antibody, and to test how much signal detected was attributed to the non-specificity of secondary antibody with other protein constituents. Primary antibody was omitted in the development of the blot. There was no detection of Trx1 in *S. pombe* JB35 or *S. pombe* SB3, but faint signal can be detected from purified recombinant Trx1 (Figure 2.7C). A non-specific signal was obtained as the total protein concentration increased, showing that the non-specificity was most likely due to non-specific interactions at high protein concentrations attributed to the secondary antibody (Figure 2.7C).

Finally, the optimization and verification of the separation of oxidized and reduced Trx1 *in vivo* using the redox western blotting assay was determined, with PEG-maleimide as the alkylating agent (Figure 2.7D). Diamide was used to chemically treat the protein extract to oxidize Trx1 and DTT was used to reduce Trx1 (Gilge *et al.*, 2008). Oxidized and reduced Trx1 could be separated from one another *in vivo*, as the two reduced Trx1 bands and the oxidized Trx1 band were detected (Figure 2.7D), which was also found in the alkylation experiments on purified recombinant Trx1 (Figure 2.5). In the diamide-treated Trx1 samples, not all Trx1 was oxidized, as the two reduced Trx1 fraction bands can still be seen (Figure 2.7D) because the diamide may not have reacted with the entire fraction of Trx1 present in the sample, leaving some Trx1 still reduced. In a cell lysate, diamide also interacts with other

thiol-containing compounds e.g. glutathione which is present in mM concentrations, which is likely the reason for a fraction of Trx1 still being reduced (Ulrich and Jakob, 2019). Diamide induces disulfide bond formation by reacting with a first thiol group to form sulfenylhydrazine. The newly formed sulfenylhydrazine then reacts with a second thiol to finally form hydrazine and a disulfide (Leichert *et al.*, 2003). In the DTT-treated samples, all Trx1 was reduced as the two fractionally reduced Trx1 bands were present and no oxidized band was detected (Figure 2.7D).

2.5 Discussion

This chapter aimed to optimize and evaluate the redox western blotting assay for suitable quantification of the thioredoxin redox charge to be used in stressor experiments. To investigate which alkylating agent allowed for a clear separation of oxidized and reduced thioredoxin 1, recombinant *S. pombe* thioredoxin 1 was produced and purified. PEG-maleimide was the most suitable alkylating agent for separating oxidized and reduced thioredoxin 1 (Figure 2.5A). While other alkylating agents such as N-ethylmaleimide separated oxidized and reduced thioredoxin separately, these bands were indistinguishable when combined (Figure 2.5A and B). Other studies have successfully resolved the oxidized and reduced forms of thioredoxin 1 using 4-acetamido-4'-[(iodoacetyl)amino]stilbene-2,2'-disulfonic acid (AIS) and 4-acetamido-4'-maleimidylstilbene-2,2'-disulfonic acid (AMS) as alkylating agents, but these studies used larger gel systems and were run for a longer duration (Brown *et al.*, 2013, Debarbieux and Beckwith, 1998, Tomalin, 2015). Although PEG-maleimide alkylation resulted in unexpected band shifts for reduced thioredoxin likely due to interactions between SDS and PEG (Zheng *et al.*, 2007), PEG-maleimide alkylation was able to clearly separate oxidized and reduced thioredoxin 1, making quantification possible. Other alkylating agents could still be used and investigated, however they are often costly for routine use and they add a very small size to thiol groups. PEG-maleimide is a more cost-effective chemical that can be routinely used and does not require special gel equipment because the size it adds to protein isoforms is large enough to detect on commonly used mid-sized gel equipment.

Once PEG-maleimide was determined to be the most suitable alkylating agent for separating oxidized and reduced thioredoxin 1 *in vitro*, optimization of the redox western blotting assay for *in vivo* analysis was done using *S. pombe* JB35 protein extracts. The best combination of primary and secondary antibodies that resulted in an increase in signal intensity with increasing protein concentrations without saturation of the signal, was tested and

confirmed. The specificity of the antibodies was tested and validated and lastly controls for oxidized and reduced thioredoxin were carried out to confirm the identification of oxidized and reduced thioredoxin 1 *in vivo* from *S. pombe* JB35 cells. Although controls were undertaken to ensure antibody specificity and proper signal detection, the non-specific detection of bands was still observed to a degree in the current study, which is a common caveat of redox western blotting (Brown *et al.*, 2013, Tomalin *et al.*, 2016). Potential reasons responsible for the non-specific detection may be issues with the commercially purchased antibody, protein degradation or aggregation during processing or issues with signal detection (Mahmood and Yang, 2012). These issues will be considered in future investigations.

Other methods of measuring the redox status of proteins using enzymatic microplate and fluorescent plate assays have been recently developed which allow for faster quantification, but are often expensive and require specialized equipment and sometimes lack the specificity associated with redox western blotting (Noble *et al.*, 2021, Tuncay *et al.*, 2022). The optimization steps that ensure specificity with redox western blotting involve aspects regarding experimental design like equal protein loading between each sample lane, target protein identification and sizing and antibody specificity optimization. The production of antibodies is an expensive process and the optimization of antibodies to target proteins in a western blot or in the newer microplate assays is a lengthy process and specificity may not always be guaranteed (Pillai-Kastoori *et al.*, 2020). A promising approach that could be considered, is to use aptamers as a replacement for antibodies. Aptamers or chemical antibodies are synthesized single-stranded DNA or RNA produced to bind a variety of molecules (Toh *et al.*, 2015). The Systematic Evolution of Ligands (SELEX) methodology is commonly used to generate aptamers through selective rounds of binding of a random oligonucleotide library with the target molecule, to produce an enriched pool that specifically binds to the target (Wu and Kwon, 2016). The nucleic acids with a high binding affinity are then cloned and sequenced. Aptamers may be a better alternative to antibodies because they are cheaper to produce, they can be easily generated to bind to a range of targets, they are smaller in size and they can be easily manipulated and modified (Zhang *et al.*, 2019b).

Future work to modify the redox western blotting assay may be to investigate the use of aptamers and additionally transform the redox western blotting assay to be used in a higher throughput microplate format by adapting ELISA and incorporating streptavidin-biotin binding, while still maintaining the specificity associated with redox western blotting (Mishra *et al.*, 2019). In conclusion, the redox western blotting assay was successfully optimized and

tested to detect thioredoxin 1 in *S. pombe* JB35 cells, to be used in stressor experiments that aim to monitor the thioredoxin redox charge.

Chapter 3: Conservation of the thioredoxin redox charge in *Schizosaccharomyces pombe*

3.1 Introduction

In the fission yeast *S. pombe*, thiol-based redox systems viz. the glutathione/glutaredoxin and the thioredoxin systems are important in essential cell functions such as repairing proteins that have been oxidatively damaged, synthesis of deoxyribonucleotides, sulfur metabolism and in protein folding (Grant, 2001). Evidence of the essential role of these systems have been demonstrated through gene knockout studies. *S. pombe* with the thioredoxin 1 gene deleted was unable to grow on minimal medium and was only able to grow on rich, undefined medium under aerobic and anaerobic conditions (Pluskal *et al.*, 2016). Similarly, *S. pombe* that had the thioredoxin reductase gene deleted could grow on rich medium in aerobic conditions, but was sensitive to the addition of extracellular peroxides (Paulo *et al.*, 2014). Mutants that had genes deleted that were responsible for the glutathione synthesis pathway were also unable to grow on minimal medium, but these phenotypes were rescued by the addition of glutathione to the culture medium (Pluskal *et al.*, 2016). Glutaredoxin 1 and glutaredoxin 2 mutants grown on rich medium were sensitive to hydrogen peroxide and paraquat respectively (Chung *et al.*, 2004). Collectively, these mutations show that in minimal medium, *S. pombe* struggles to grow if these redoxin systems are disrupted.

The role of the glutathione/glutaredoxin system in stress responses has been widely studied. This system participates in oxidative stress induced by hydrogen peroxide by reducing hydroperoxides (Collinson *et al.*, 2002), in heat stress by secreting glutathione (Laman Trip and Youk, 2020), in heavy metal stress by glutathione activity (Gharieb and Gadd, 2004, Wysocki and Tamás, 2010) and glutathione peroxidase 2 was shown to preserve the functioning of the electron transport chain (ETC) and aid in decreasing production of reactive oxygen species in the mitochondria (Canizal-García *et al.*, 2021) (Figure 3.1A). However, it is not clear whether the thioredoxin system contributes to or is affected by the response of *S. pombe* to heat stress, heavy metal stress and an ETC stress (Figure 3.1A and B). The thioredoxin redox charge offers an experimentally tractable method to elucidate the role of the thioredoxin system in these stress responses (Figure 3.1B).

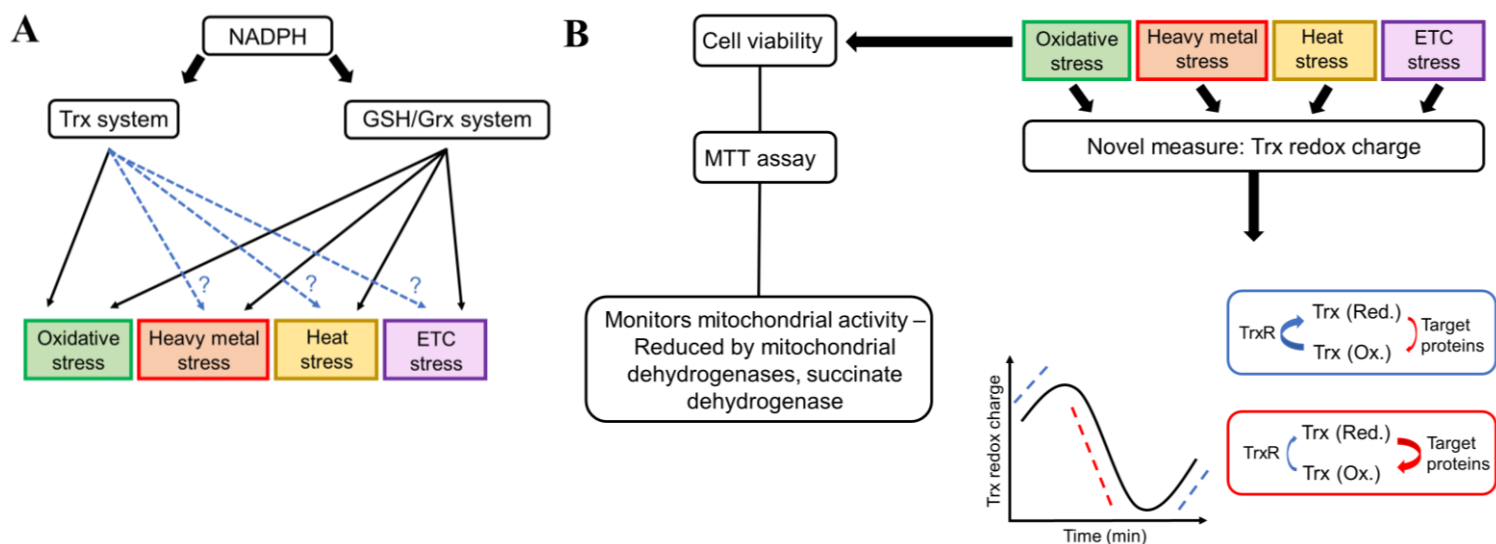


Figure 3.1 Experimental approach used to investigate the role of the thioredoxin system in response to stressors in *S. pombe* and its relation to cell viability. (A) Reducing equivalents from NADPH are transferred to both the glutathione/glutaredoxin (Grx/GSH) and the thioredoxin (Trx) systems. The glutathione/glutaredoxin system plays a role in protecting the cell from oxidative stress, heavy metal stress, heat stress and in electron transport chain (ETC) stress (details in text). The thioredoxin system plays a role in the oxidative stress response, but its role in responding to other stressor types is less clear. (B) The thioredoxin redox charge was measured in stressed *S. pombe* and related to cell viability that was inferred by using the 3-(4,5-dimethylthiazol-2-yl)-2,5-diphenyltetrazolium bromide (MTT) assay, which monitors mitochondrial activity. Increases in the thioredoxin redox charge profile (blue) are attributed to thioredoxin reductase (TrxR) converting oxidized thioredoxin [Trx (Ox.)] to reduced thioredoxin [Trx (Red.)] at a faster rate than Trx (Red.) is oxidized by target proteins (depicted by the broader blue arrow). Decreases in the thioredoxin redox charge profile (red) are attributed to target proteins oxidizing Trx (Red.) to Trx (Ox.) at a faster rate than TrxR converts Trx (Ox.) to Trx (Red.) (depicted by the broader red arrow).

To monitor the cell viability of *S. pombe*, the 3-(4,5-dimethylthiazol-2-yl)-2,5-diphenyltetrazolium bromide (MTT) assay was used. The MTT assay is based on the reduction of MTT by mitochondrial dehydrogenase enzymes such as succinate dehydrogenase, to a spectrophotometrically detectable (wavelength between 550 and 600 nm) violet/blue colored molecule called formazan (Rai *et al.*, 2018). It is inferred that the higher the production of formazan from mitochondrial activity, the higher the number of viable cells (Ghasemi *et al.*, 2021) (Figure 3.1B).

Four stressor types were chosen to stress *S. pombe* and these will be discussed briefly. Hydrogen peroxide was used as an oxidative stressor as the response of *S. pombe* to hydrogen peroxide-induced oxidative stress has been extensively described in the literature. The thioredoxin system enables detoxification of hydrogen peroxide through the cycling of reducing equivalents to target proteins such as peroxiredoxins, and activates different detoxification and signaling pathways (Jara *et al.*, 2007). *S. pombe* responds to hydrogen peroxide induced oxidative stress by detoxifying hydrogen peroxide with the peroxiredoxin, Tpx1 and induction of two pathways, the Pap1 and Sty1 mitogen-activated protein kinase (MAPK) pathways (Toone *et al.*, 1998). Pap1 is a transcription factor that induces an antioxidant gene response upon activation by the upstream activator, Tpx1. Under low hydrogen peroxide concentrations (0.2 mM) Pap1 is activated, however at higher concentrations (1 mM), Tpx1 is reversibly inactivated through hyperoxidation which postpones Pap1 activation. The breakdown of hydrogen peroxide by Tpx1 involves the “peroxidatic” and the “resolving” cysteines in Tpx1 (Bozonet *et al.*, 2005). First, the peroxidatic cysteine becomes oxidized to a sulfenic acid by hydrogen peroxide, this sulfenic form can either be reduced back by thioredoxin at its resolving cysteine or it becomes further oxidized to an inactive sulfinic or sulfonic form resulting in hyperoxidation (Troussicot *et al.*, 2021). After initial detoxification at high peroxide concentrations, Tpx1 becomes hyperoxidized and stops drawing reducing equivalents from the thioredoxin system. Reversal of hyperoxidized Tpx1 in the sulfinic form only (not in the sulfonic form), can occur through reduction by sulfiredoxin (Srx1). The expression of Srx1 is dependent on the Sty1 and Atf1 MAPK pathway (Domènech *et al.*, 2018, Vivancos *et al.*, 2005). Tpx1 hyperoxidation is important because it preserves the pool of reduced thioredoxin in cells, and allows for thioredoxin to participate in other essential cellular repair processes, aiding in survival (Brown *et al.*, 2013). Therefore the response to hydrogen peroxide in *S. pombe*, involves the Pap1 pathway being primarily responsible for the adaptive response to hydrogen peroxide, while the Sty1 MAPK pathway aids in cell survival post high hydrogen peroxide exposure (Quinn *et al.*, 2002).

Cadmium sulfate was used as a toxic, heavy metal pollutant stressor in our experiments and is known to cause damage to various organs in mammals through cell degeneration and through indirect oxidative damage to DNA (Rani *et al.*, 2014). This pollutant enters cells through transporters that are generally responsible for the uptake of essential cations like zinc, iron, and calcium (Mikolić *et al.*, 2016). Cadmium’s ability to displace these essential metals and its reactivity with thiol groups during protein folding in baker’s yeast, causes elevated

oxidative stress and eventual cell death (Bjørklund *et al.*, 2019, Jacobson *et al.*, 2017). Heat was used as a general environmental stress. The heat shock response mechanism is highly conserved and allows eukaryotic cells to adapt to a constantly fluctuating natural environment (Gallo *et al.*, 1993). Small heat shock proteins are a class of heat shock related-chaperone proteins, that are responsible for thermotolerance in cells and prevent thermal aggregation of proteins (Hirose *et al.*, 2005). As with high oxidative stress loads in *S. pombe*, the Sty1 MAPK pathway is also activated in response to heat shock (Shiozaki *et al.*, 1998, Toone *et al.*, 1998). To disrupt global redox poise within fission yeast, potassium ferricyanide was used as an electron transport chain (ETC) stress as it oxidizes cytochrome *c*, thus disrupting oxidative phosphorylation and the use of oxygen by the cell during cellular respiration (Hampton *et al.*, 1998, Medentsev *et al.*, 2002).

This chapter aimed to investigate the response of *S. pombe* through the thioredoxin redox charge, to different types of stress and to also investigate whether changes in the thioredoxin redox charge could be associated with cell viability.

3.2 Materials

The same materials were used as stated in Section 2.2 and the same culture medium and stock reagent preparation were carried out as stated in Section 2.2.1. Additionally, hydrogen peroxide (30% v/v) was obtained from Laboratory & Analytical Supplies (Pty) Ltd (Durban, South Africa) and was used within one month after opening. The Cell Proliferation Kit I (MTT) (Lot #42575000) by Roche was purchased from Sigma-Aldrich (Johannesburg, South Africa). All other general laboratory chemicals were of the highest purity available and were obtained from Merck/Saarchem (Johannesburg, South Africa).

3.3 Methods

3.3.1 *S. pombe* in vivo stress test experiments

A YE5S agar plate was spread-plated with 100 µl of the frozen *S. pombe* JB35 (FLAG-tagged *Trx1*) glycerol stock and incubated (2-3 days, 30°C, inverted). A three-way streak was then carried out on a fresh YE5S agar plate from the growth to isolate single colonies and was further incubated (2-3 days, 30°C, inverted). Single colonies were isolated and each colony was inoculated into a volume of EMM broth medium (15 ml), which was incubated in an orbital air-shaker (180 RPM, 30°C, overnight). The OD₅₉₅ was measured the next morning and the

appropriate volume of overnight culture was inoculated into fresh EMM broth (final culture volume of 50 ml) until an OD₅₉₅ of 0.15 was reached. The cultures were left to grow until the OD₅₉₅ increased to 0.4-0.5 (3-5 hours, 180 RPM, 30°C). Once the exponential phase of growth (OD₅₉₅ of 0.4-0.5) was reached, the cells were stressed by adding a specific stressor to the flask, namely hydrogen peroxide (H₂O₂) (100-1250 µM) (Brown *et al.*, 2013); heat stress (50°C) (Bonnet *et al.*, 2000, Lackner *et al.*, 2012); cadmium sulfate (CdSO₄) (8 mM) (Chen *et al.*, 2003) or potassium ferricyanide [K₃Fe(CN)₆] (30 mM) (Liu *et al.*, 2009, Zhao *et al.*, 2007). All chemical stressors were freshly prepared in dH₂O. For the 50°C heat stress, once the exponential phase of growth was reached the cultures were incubated in a 50°C water bath for the duration of the stress test (180 RPM, 50°C), while the other stressor tests were conducted in an air-shaker (180 RPM, 30°C). The cultures were incubated and 2 ml samples were removed at set time-point intervals and were added to ice-cold TCA [20% (w/v), 2 ml], within 15 ml centrifuge tubes. The samples were centrifuged (3,300×g, 10 min, 4°C) to pellet the cells. The supernatant was discarded and the pellets were frozen at -80°C for protein extraction (Day *et al.*, 2012, Tomalin, 2015).

3.3.2 Protein extraction and redox western blotting of *S. pombe* JB35 *Trx1*

Protein extraction was carried out as described in Section 2.3.7 and the redox western blotting assay was carried out as described in Section 2.3.8.

3.3.3 Measuring *S. pombe* cell viability using the 3-(4,5-dimethylthiazol-2-yl)-2,5-diphenyltetrazolium bromide (MTT) reduction assay

A YE5S agar plate was spread-plated with 100 µl of the frozen *S. pombe* JB35 (FLAG-tagged *Trx1*) glycerol stock and incubated (2-3 days, 30°C, inverted). A three-way streak was then carried out on a fresh YE5S agar plate from the growth to isolate single colonies and was further incubated (2-3 days, 30°C, inverted). Single colonies were isolated and each colony was inoculated into EMM broth medium (15 ml), which was incubated in an orbital air-shaker overnight (180 RPM, 30°C). The OD₅₉₅ was measured the next morning and the appropriate volume of overnight culture was inoculated into fresh EMM broth (final culture volume of 50 ml) until an OD₅₉₅ of 0.15 was reached. The cultures were left to grow until the OD₅₉₅ increased to 0.4-0.5 (3-5 hours, 180 RPM, 30°C). Once the exponential phase of growth (OD₅₉₅ of 0.4-0.5) was reached, the culture was removed from the air-shaker and 100 µl of culture was seeded into a 96 multi-well plate in triplicate for all the specified stressor tests as stated in

Section 3.3.1 (Day *et al.*, 2012, Tomalin, 2015). The specific concentration of stressor was added to the wells, mixed and incubated (30°C) for the set time-point intervals as in Section 3.3.1. The Cell Proliferation Kit I (MTT) was used to measure cell viability and was followed as per the kit instructions. Once the time point was reached, 10 µl of the labelling reagent (Solution A – MTT solution) from the Cell Proliferation Kit I (MTT) was added to the specific wells, mixed with agitation with a pipette and incubated (4 hours, 37°C). After incubation, 100 µl of solubilizing solution (Solution B) was mixed into the wells and was left to stand overnight at 37°C. The next day the absorbance was measured using a Versamax™ ELISA Microplate Reader (OD₅₆₂) and results were computed.

3.3.4 Computational analyses of data

Data obtained from all stressor experiments were processed and analyzed in the Jupyter notebook (<https://jupyter.org/>) using Python (Supplementary material-Appendix 1). All stressor tests and cell viability experiments were carried out in triplicate independent experiments and analysed for statistical significance (Supplementary material-Appendix 1). Four correlation coefficients were calculated to evaluate potential correlations that may exist between the thioredoxin redox charge and cell viability. The Pearson correlation test measures the extent of the relationship between linearly related variables (continuous and normally distributed variables are assumed); the Spearman rank correlation is a non-parametric test that measures the extent of association between ordinal variables (ordinal and monotonic variables are assumed); the Kendall rank correlation is a non-parametric test that aims to measure how strong the dependence between two variables are (continuous or ordinal and monotonic variables are assumed) and the distance correlation measures the dependence between a pair of arbitrary vectors and can detect linear and non-linear associations (de Siqueira Santos *et al.*, 2013, Hauke and Kossowski, 2011, Székely *et al.*, 2007, Székely and Rizzo, 2013). Regression analysis was also done to determine how well the data fit a linear model. The correlation coefficients do not imply causation between variables, although the linear regression analysis aims to predict the variation in the proposed dependent variable by analyzing the independent variable (Osborne and Waters, 2002). Correlation coefficient values calculated from the Pearson, Spearman and Kendall tests that are closer to +1 or -1 represent stronger positively correlated and negatively correlated relationships respectively, as opposed to weaker relationships with values closer to zero. For the distance correlation measure, values are limited

to between zero and one, with values closer to one indicating a stronger association between variables.

3.4 Results

3.4.1 Evidence of potential correlation from the literature between the thioredoxin redox charge and cell viability

We aimed to investigate whether a correlation exists between the thioredoxin redox charge and cell viability, and to determine whether this measure could be useful in thioredoxin inhibition studies. A published study investigated the effect of using silver and ebselen, a thioredoxin reductase inhibitor, to treat multidrug-resistant, Gram-negative bacterial infections in mice (Zou *et al.*, 2017). This study used *E. coli* DHB4 cells which were treated with 5 mM silver nitrate and a range of ebselen concentrations (0-80 μ M). *E. coli* cell viability was measured by propidium iodide staining (bacterial cells with compromised membranes or dead cells were stained) and the redox state of thioredoxin 1 (Trx1) was determined by western blotting (Zou *et al.*, 2017).

Data were extrapolated from this paper (Figures 2D and 3C) using the WebPlotDigitizer application (<https://apps.automeris.io/wpd/>) and reanalyzed to determine whether there was a correlation between the redox charge and cell viability (Zou *et al.*, 2017). A strong negative correlation was obtained between the thioredoxin redox charge and *E. coli* cell death (Table 3.1, Figure 3.2). The results also fitted the predicted linear model well and the dependent variable (cell death) could be predicted from the independent variable (the thioredoxin redox charge) as indicated from the strong R-squared value from the linear regression analysis (0.879) (Table 3.1). Collectively, these results support a correlation between the thioredoxin redox charge and cell viability and suggested that combination therapies like silver and ebselen, as in this paper, have higher antimicrobial efficiency compared to single-drug treatments (May *et al.*, 2018).

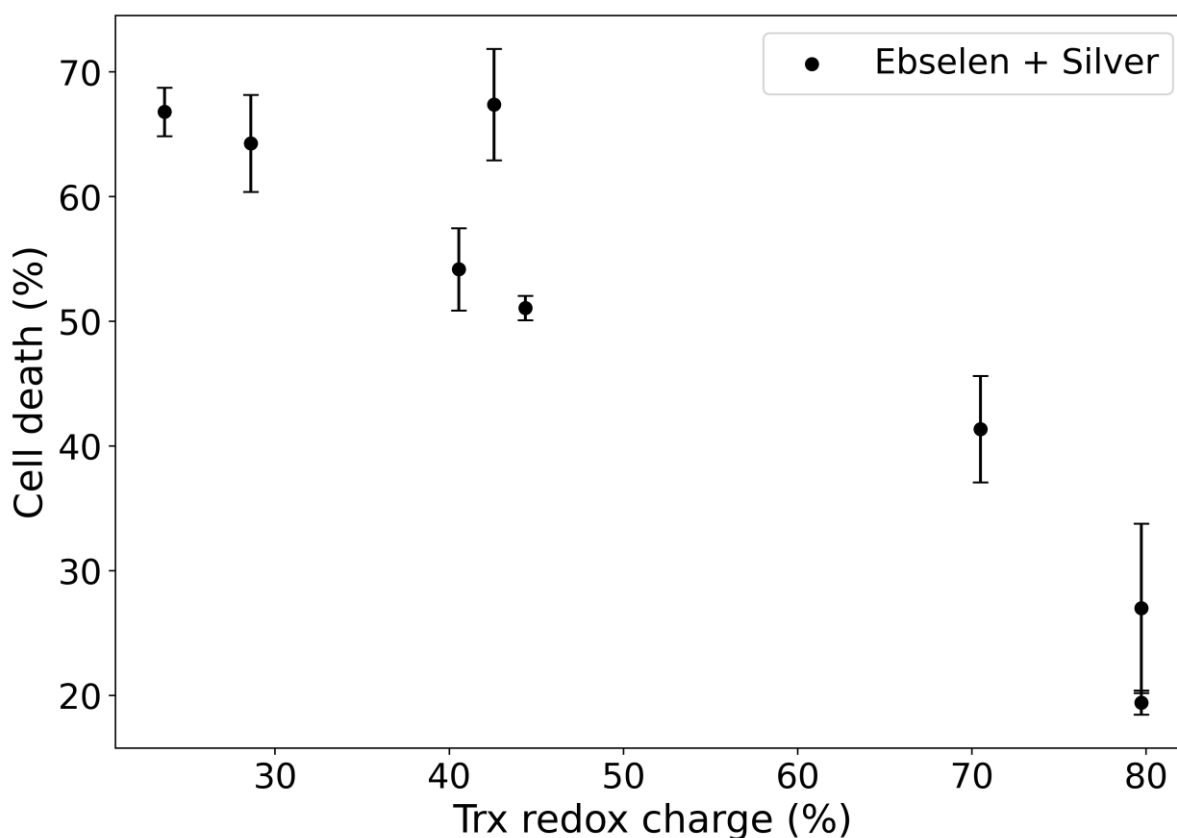


Figure 3.2 Evidence of a correlation between the thioredoxin (Trx) redox charge and cell death from data extrapolated from the literature. *The Trx redox charge and cell death were measured in *E. coli* DHB4 treated with various ebselen and silver combinations. Propidium iodide staining that indicated cell death (%) was carried out in triplicate and standard deviations are shown. [Data extrapolated from Zou et al., (2017)].*

Table 3.1 Correlation analyses and their coefficients calculated between the thioredoxin redox charge and cell death for ebselen and silver treated *E. coli* DHB4 (Zou et al., 2017)

Type of stressor	Correlation analyses				
	Pearson's r	Spearman's rho	Kendall's tau	R-squared value	Distance correlation
Ebselen and silver (Data extrapolated)	-0.937***	-0.850**	-0.764**	0.879***	0.944**

*Correlation coefficients and an R-squared value from a linear regression were calculated with statistical significance. Significance is represented as * = $p < 0.05$, ** = $p < 0.01$, *** = $p < 0.001$, **** = $p < 0.0001$ and ns = non-significant.*

3.4.2 Cell viability and the thioredoxin redox charge quantified in unstressed *S. pombe* JB35

To determine a eukaryotic cell's response to stressors in terms of the thioredoxin redox charge and to relate changes in the thioredoxin redox charge to cell viability, stressor time course experiments were carried out on *S. pombe* JB35 (Section 3.3.1). The thioredoxin redox charge was measured using the optimized redox western blotting assay and cell viability was quantified using the MTT reduction assay (Sections 3.3.2 and 3.3.3 respectively). The concentrations of the stressors were determined from the literature and were in the mid to high toxicity concentration range (Table 3.2), with all experiments carried out in triplicate.

Table 3.2 Stressors and concentrations used in the *S. pombe* stressor experiments

Stressor:	Concentration:	References:
Hydrogen peroxide (H ₂ O ₂)	100-1250 μM	(Brown <i>et al.</i> , 2013, Vivancos <i>et al.</i> , 2006)
Heat	50°C	(Bonnet <i>et al.</i> , 2000, Lackner <i>et al.</i> , 2012, Péter <i>et al.</i> , 2017)
Cadmium sulfate (CdSO ₄)	8 mM	(Chen <i>et al.</i> , 2003, Kennedy <i>et al.</i> , 2008)
Potassium ferricyanide [K ₃ Fe(CN) ₆]	30 mM	(Liu <i>et al.</i> , 2009, Zhao <i>et al.</i> , 2007).

Before the stressor tests were carried out, “No stress control” experiments were first undertaken to measure the baseline thioredoxin redox charge and cell viability. Ponceau S stains were carried out on every blot as an additional loading control to the Pierce™ BCA Protein Assay (Section 2.4.3), to confirm equal total protein loading across all lanes (Supplementary material-Section S6) (Romero-Calvo *et al.*, 2010, Sander *et al.*, 2019).

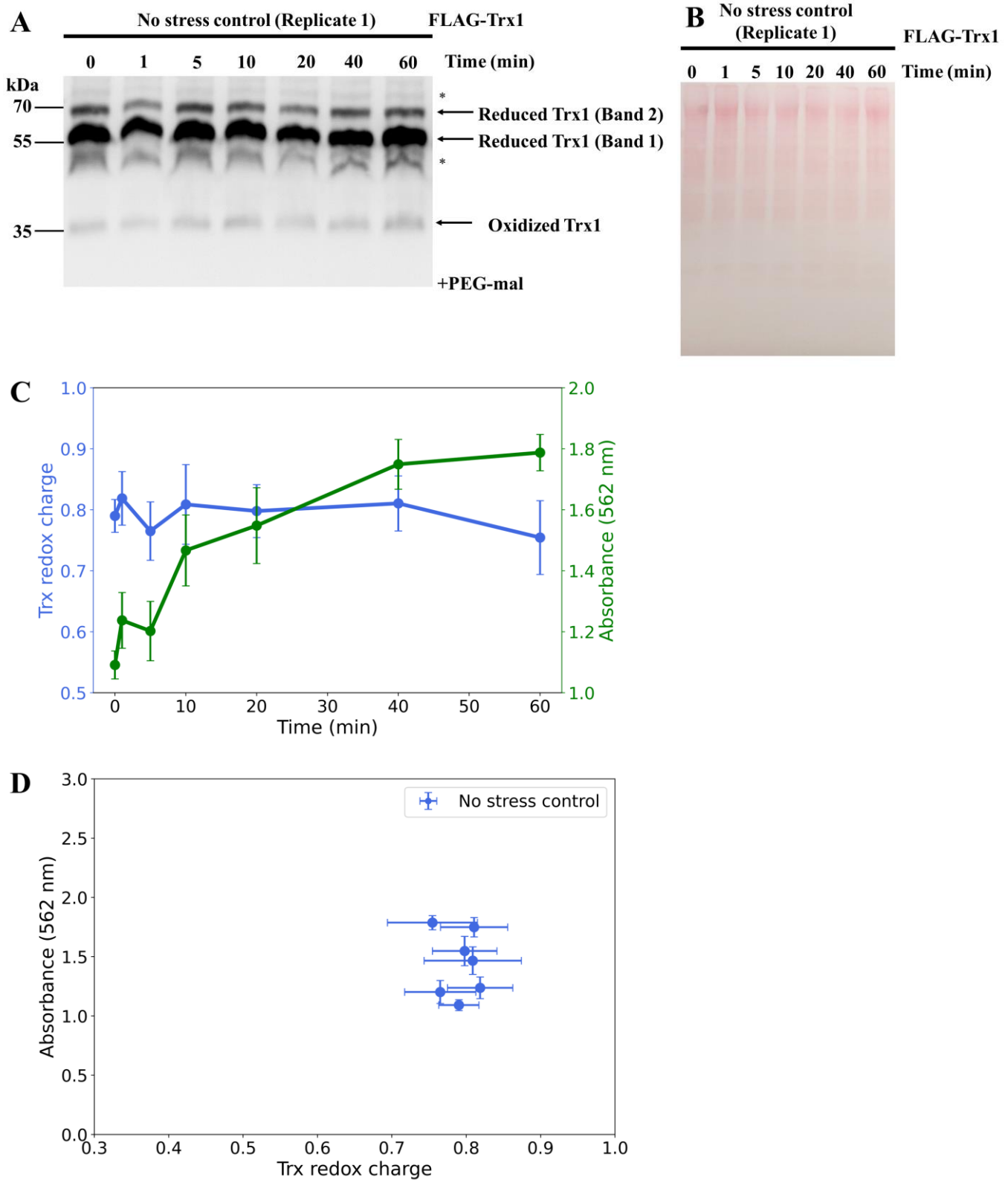


Figure 3.3 Quantification of the thioredoxin (Trx) redox charge and cell viability (562 nm) of unstressed *S. pombe* JB35 over a 60-minute time course. (A) Representative redox western blot detecting thioredoxin 1 (Trx1). Non-specific bands are identified (*). (B) Representative Ponceau S stain. (C) Trx redox charge (blue) and cell viability (measured at an

absorbance of 562 nm) (green) profiles plotted over time (minutes). (D) Trx redox charge and cell viability (measured at an absorbance of 562 nm) phase plot. All experiments were carried out in triplicate ($n = 3$) and the mean and standard errors were plotted.

The results from the no stress control experiments were analyzed which involved calculating the thioredoxin redox charge from stressed *S. pombe* JB35 over the 60-minute time course. Two reduced thioredoxin bands were identified as previously determined (Figure 2.7), at 70 (band 2) and 55 kDa (band 1) (Figure 3.3A). These two reduced thioredoxin bands were predicted to be the partially (band 1) and fully (band 2) alkylated thioredoxin isoforms. The oxidized thioredoxin band was at 35 kDa (Figure 3.3A). Interestingly, there was evidence of baseline thioredoxin oxidation over the entire time course (Figure 3.3A). This level of oxidation was expected, even in the absence of an external stressor as the thioredoxin system participates in functions such as DNA replication, thiol metabolism and defense against oxidative stress generated from metabolic processes (Herrero *et al.*, 2008). Consistent protein loading was confirmed from the Ponceau S stained image (Figure 3.3B).

A dynamic profile plot was generated for the thioredoxin redox charge (reduced thioredoxin/total thioredoxin) and cell viability time courses (Figure 3.3C). For the no stress control experiments, the cell viability profile (green) increased steadily over the time course as opposed to the thioredoxin redox charge profile (blue) which remained relatively consistent with very little change (Figure 3.3C).

Table 3.3 Correlation analyses and their coefficients calculated between the thioredoxin redox charge and cell viability for unstressed *S. pombe* JB35

Correlation analyses					
Type of stressor	Pearson's r	Spearman's rho	Kendall's tau	R-squared value	Distance correlation
No stress control	-0.115 ^{ns}	-0.036 ^{ns}	-0.048 ^{ns}	0.013 ^{ns}	0.423 ^{ns}

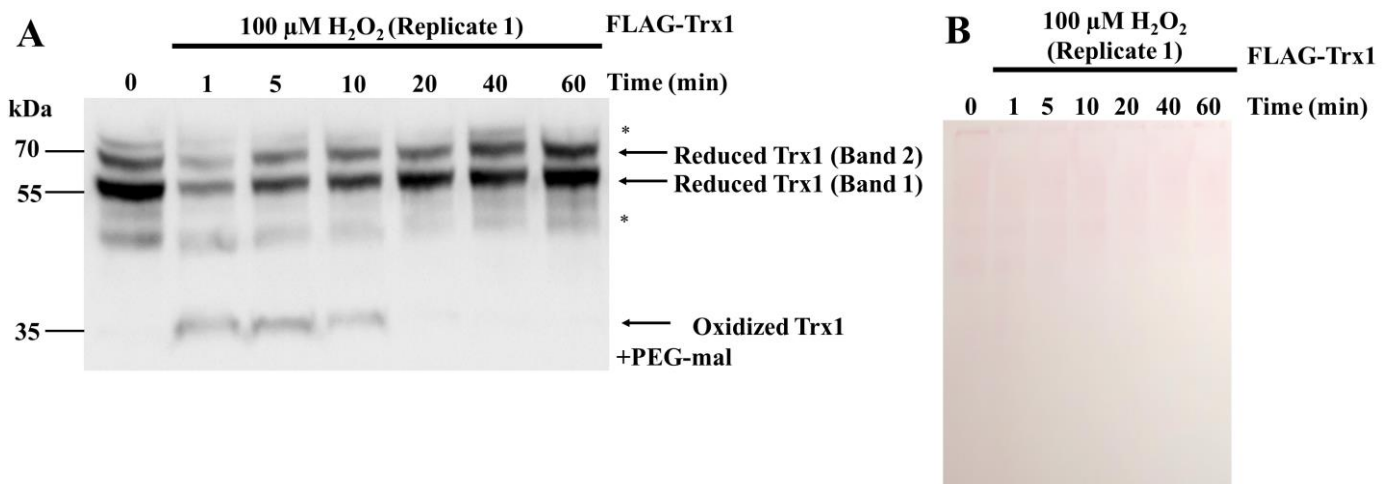
Correlation coefficients and an R-squared value from a linear regression were calculated with statistical significance. Significance is represented as ns = non-significant.

A phase plot of the thioredoxin redox charge and cell viability was generated for the no stress control results by plotting the thioredoxin charge values against the cell viability absorbance values over the same time points (Figure 3.3D). The data points clustered at high thioredoxin redox charge values with high absorbance values for cell viability (Figure 3.3D).

Correlation coefficients were calculated to give statistical values to correlations between the thioredoxin redox charge and cell viability. A very weak, almost negligible negative correlation was obtained between the thioredoxin redox charge and cell viability (Table 3.3). We next investigated the effect of different stressors on cell viability and the thioredoxin redox charge.

3.4.3 Cell viability and the thioredoxin redox charge quantified in *S. pombe* JB35 stressed with hydrogen peroxide (H_2O_2)

For the next set of experiments, the cells were exposed to a range of hydrogen peroxide concentrations (100-1250 μ M). Representative western blot (Figure 3.4A, C, E and G) and Ponceau S stained images are shown (Figure 3.4B, D, F and H) for each concentration of hydrogen peroxide (all western blot and Ponceau S stained images for all experiments can be found in the Supplementary material-Sections S4 and S6 respectively). The thioredoxin oxidation profiles observed from the western blots changed with different concentrations of hydrogen peroxide (Figure 3.4A, C, E and G). At 100 μ M hydrogen peroxide, a single peak in thioredoxin oxidation was observed between 1-10 minutes (Figure 3.4A). On the other hand, at 300 μ M hydrogen peroxide two thioredoxin oxidation peaks were obtained at one and 40 minutes (Figure 3.4C). At 500 μ M hydrogen peroxide, thioredoxin oxidation started at one minute and gradually increased over time (Figure 3.4E). The same gradual increase in thioredoxin oxidation was also obtained at 1250 μ M hydrogen peroxide (Figure 3.4G).



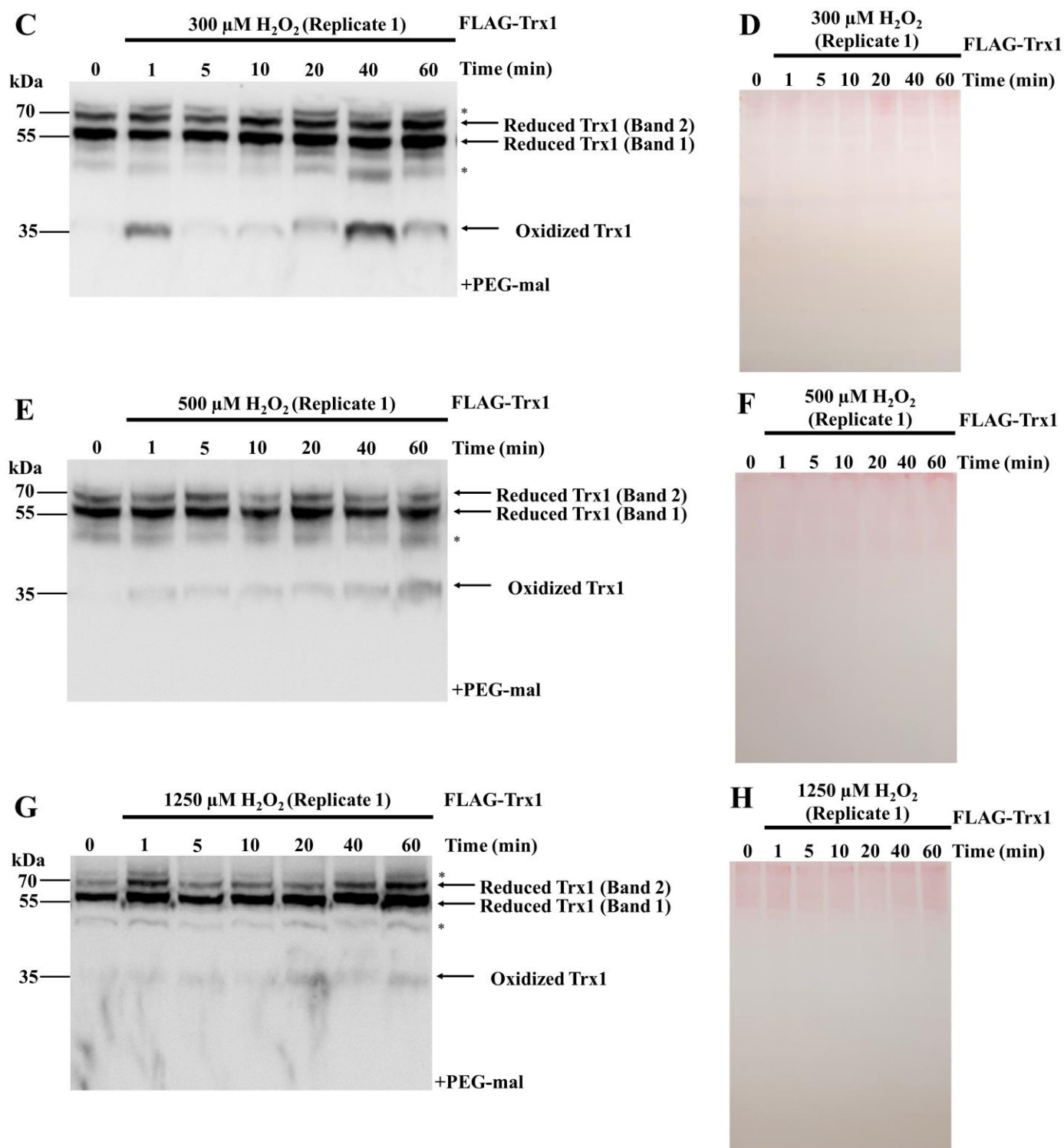
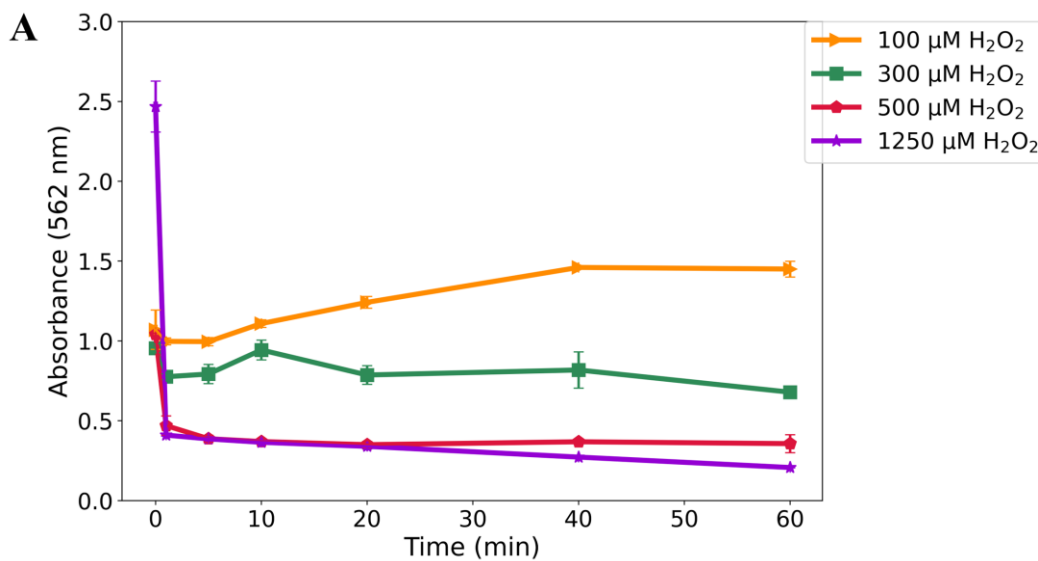


Figure 3.4 Quantification of the thioredoxin (Trx) redox charge of *S. pombe* JB35 stressed with 100, 300, 500 and 1250 μM hydrogen peroxide (H_2O_2), over 60-minute time courses. Representative redox western blots detecting thioredoxin 1 (Trx1) for (A) 100 μM H_2O_2 , (C) 300 μM H_2O_2 , (E) 500 μM H_2O_2 and (G) 1250 μM H_2O_2 stressor time courses. Non-specific bands are identified (*). Representative Ponceau S stains for (B) 100 μM H_2O_2 , (D) 300 μM

H_2O_2 , (F) 500 $\mu M H_2O_2$ and (H) 1250 $\mu M H_2O_2$ stressor time courses. All experiments were carried out in triplicate ($n = 3$).

The dynamic cell viability profiles displayed variability in response to treatment with different concentrations of hydrogen peroxide. At 100 and 300 μM hydrogen peroxide, no major changes in cell viability were detected, with viability even slightly increasing from five minutes for 100 μM hydrogen peroxide (Figure 3.5A). In contrast, at both 500 and 1250 μM hydrogen peroxide, an appreciable decline in cell viability was observed (Figure 3.5A). These results suggest that the threshold limit that *S. pombe* JB35 can survive externally introduced hydrogen peroxide, is approximately 300 μM and beyond this, cells rapidly enter a stressed, survival state (Figure 3.5A). These results were consistent with literature, showing that hydrogen peroxide concentrations above 300 μM cause cell damage and likely lead to death (Day *et al.*, 2012, Pekmez *et al.*, 2008).



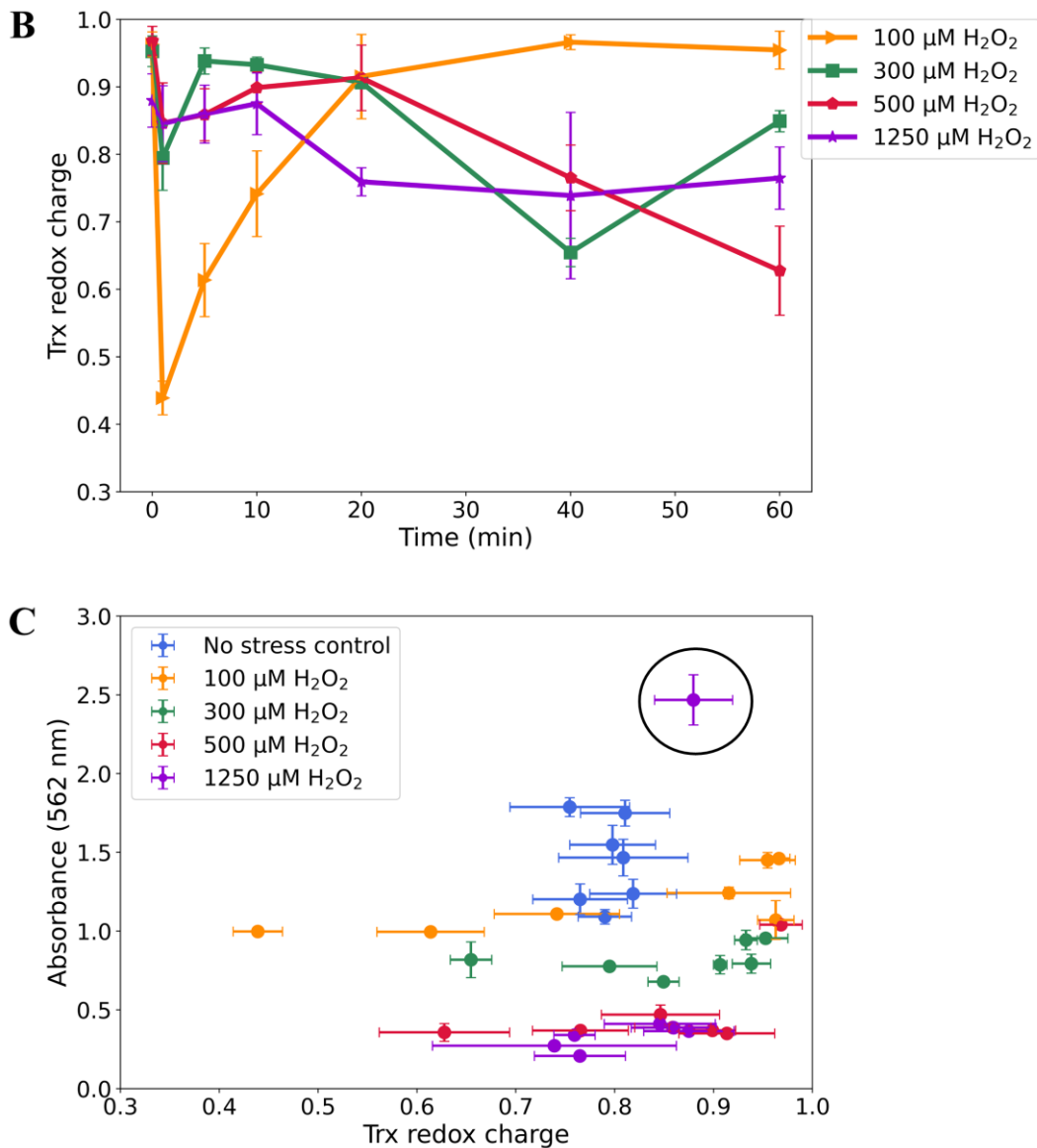


Figure 3.5 Quantification of the thioredoxin (Trx) redox charge and cell viability (562 nm) of *S. pombe* JB35 stressed with a range of hydrogen peroxide (H_2O_2) concentrations, over 60-minute time courses. (A) Cell viability (measured at an absorbance of 562 nm) plotted over time (minutes), after 100 μM H_2O_2 , 300 μM H_2O_2 , 500 μM H_2O_2 and 1250 μM H_2O_2 stress. (B) Trx redox charge plotted over time (minutes), after 100 μM H_2O_2 , 300 μM H_2O_2 , 500 μM H_2O_2 and 1250 μM H_2O_2 stress. (C) Trx redox charge and cell viability (measured at an absorbance of 562 nm) phase plot, of 100 μM H_2O_2 , 300 μM H_2O_2 , 500 μM H_2O_2 and 1250 μM H_2O_2 stressor concentrations, including the no stress control. The time zero outlier is circled. All experiments were carried out in triplicate ($n = 3$) and the mean and standard errors were plotted.

Treatment of cells with 100 μM hydrogen peroxide resulted in the thioredoxin redox charge profile decreasing considerably at one minute and promptly recovering to a thioredoxin redox charge value of almost one (Figure 3.5B). In contrast, for the 300 μM hydrogen peroxide treatment, two local decreases in the thioredoxin redox charge were observed at one and 40 minutes. Similarly, when the hydrogen peroxide treatment was increased to a concentration of 500 μM hydrogen peroxide, two local decreases in the thioredoxin redox charge were observed at one and 60 minutes. Interestingly, at an even higher hydrogen peroxide treatment of 1250 μM , minimal changes in the thioredoxin redox charge were observed, with a slight decrease in the charge at one minute and recovery at 10 minutes (Figure 3.5B).

A study investigated the differences between bacterial (OxyR) and eukaryotic (Pap1-Tpx1) redox relays that sense and signal hydrogen peroxide. A section of their experiments involved measuring the reduced thioredoxin protein percentage, following the addition of 100 and 500 μM hydrogen peroxide to *S. pombe*. Their results showed at 100 μM , a major decrease in reduced thioredoxin and a prompt recovery, while at 500 μM , two local minima were observed during the time course (Domènech *et al.*, 2018). Similar oxidation profiles were obtained in our experiments. For the 500 μM hydrogen peroxide perturbation that was tested in our experiments, the second decrease in charge was also delayed, with it starting at 20 minutes and continuing after 60 minutes (Figure 3.5B), this trend was also observed in the abovementioned study (Domènech *et al.*, 2018).

The two decreases in the thioredoxin redox charge can be explained by the temporary inactivation of Tpx1 through hyperoxidation (Bozonet *et al.*, 2005, Vivancos *et al.*, 2005). Srx1 expression occurs at 20 minutes which reactivates Tpx1, leading to a new round of thioredoxin oxidation that can be detected from the second decrease in the thioredoxin redox charge (Figure 3.5B), which was also observed in unpublished data (Tomalin, 2015). At a very high hydrogen peroxide concentration (1-6 mM), extensive hyperoxidation of Tpx1 in *S. pombe* occurs (Day *et al.*, 2012). Thus, the thioredoxin redox charge remained relatively stable considering the high hydrogen peroxide concentration that was introduced (Figure 3.5B).

An interesting observation from the phase plot was that most of the data points clustered in the bottom, right quadrant of the plot, which represented a low cell viability and a high thioredoxin redox charge (Figure 3.5C). The outlier near the top right quadrant (circled), can be attributed to the time zero point, before the addition of hydrogen peroxide. The time zero points for the cell viability analysis were obtained within an absorbance range because the exponential phase until which the cells were grown, was also within a spectrophotometrically detectable range (OD₅₉₅ of 0.4-0.5) (Section 3.3.3). Thus, the outliers seen at the top of the

phase plots can be attributed to the time zero points for cell viability being at the higher end of the absorbance range. In contrast to the hydrogen peroxide results, the no stress control data points clustered higher, but still toward the right quadrant of the plot, which represented a high cell viability and a high thioredoxin redox charge (Figure 3.5C). Thus, it appears that the thioredoxin redox charge was preserved even in the face of high levels of hydrogen peroxide (Figure 3.5C). Given this result, weak to mid-strength positive correlations were detected for the hydrogen peroxide treatments (Table 3.4).

Table 3.4 Correlation analyses and their coefficients calculated between the thioredoxin redox charge and cell viability for *S. pombe* JB35 stressed with hydrogen peroxide (H₂O₂)

Type of stressor	Correlation analyses				
	Pearson's r	Spearman's rho	Kendall's tau	R-squared value	Distance correlation
100 μM H ₂ O ₂	0.730 ^{ns}	0.750 ^{ns}	0.619 ^{ns}	0.533 ^{ns}	0.755 ^{ns}
300 μM H ₂ O ₂	0.360 ^{ns}	0.536 ^{ns}	0.429 ^{ns}	0.130 ^{ns}	0.592 ^{ns}
500 μM H ₂ O ₂	0.520 ^{ns}	0.321 ^{ns}	0.238 ^{ns}	0.271 ^{ns}	0.594 ^{ns}
1250 μM H ₂ O ₂	0.508 ^{ns}	0.750 ^{ns}	0.524 ^{ns}	0.258 ^{ns}	0.532 ^{ns}

Correlation coefficients and an R-squared value from a linear regression were calculated with statistical significance. Significance is represented as ns = non-significant.

3.4.4 Cell viability and the thioredoxin redox charge quantified in *S. pombe* JB35 stressed with heat, cadmium sulfate (CdSO₄) and potassium ferricyanide [K₃Fe(CN)₆]

Could other stressors affect the thioredoxin redox charge? Given the surprising discovery that the thioredoxin redox charge was conserved in response to hydrogen peroxide treatment, other types of stressors were tested including heat, cadmium sulfate and potassium ferricyanide. Representative western blot (Figure 3.6A, C and E) and Ponceau S stained images (Figure 3.6B, D and F) are shown for each type of stressor. In response to heat stress, thioredoxin oxidation was detected at 20 minutes and increased over time (Figure 3.6A). Similarly, in response to cadmium sulfate, thioredoxin oxidation started at five minutes and gradually increased (Figure 3.6C). Potassium ferricyanide treatment also resulted in thioredoxin oxidation increasing from one minute (Figure 3.6E).

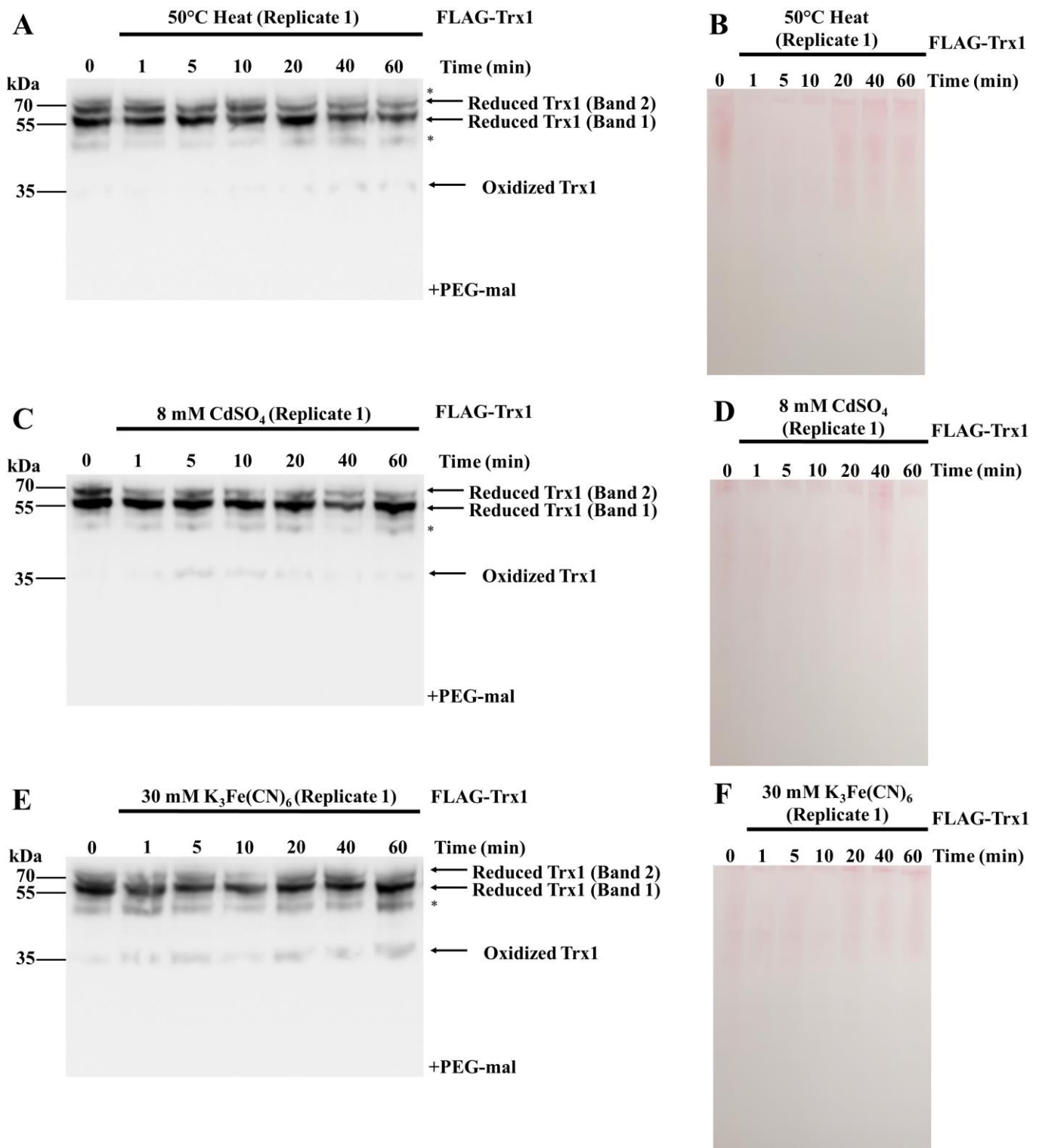
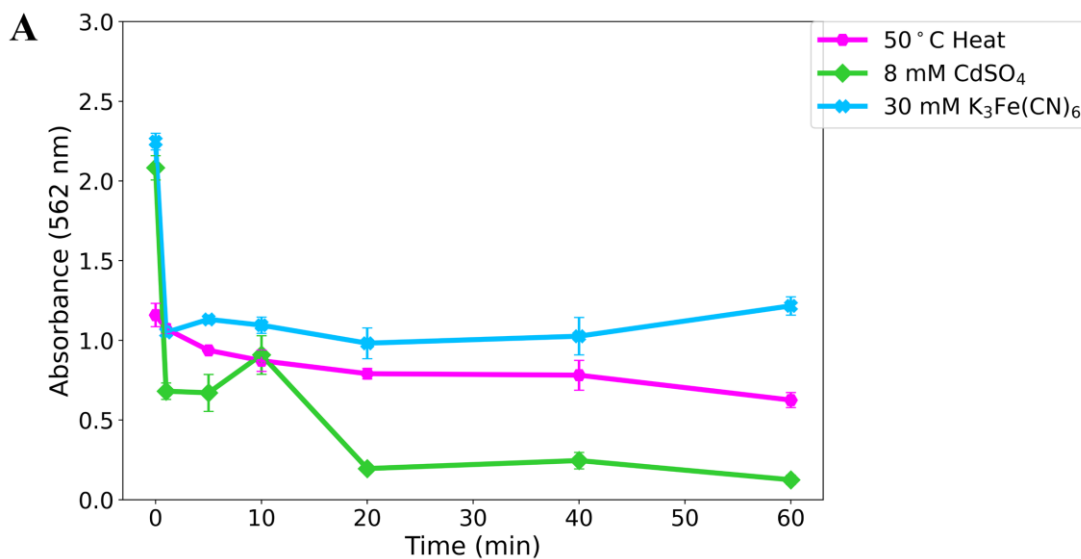


Figure 3.6 Quantification of the thioredoxin (Trx) redox charge of *S. pombe* JB35 stressed with heat, cadmium sulfate (CdSO₄) and potassium ferricyanide [K₃Fe(CN)₆] over 60-minute time courses. Representative redox western blots detecting thioredoxin 1 (Trx1) for (A) heat (50°C), (C) 8 mM CdSO₄ and (E) 30 mM K₃Fe(CN)₆ stressor time courses. Non-specific bands are identified (*). Representative Ponceau S stains for (B) heat (50°C), (D)

8 mM CdSO₄ and (F) 30 mM K₃Fe(CN)₆ stressor time courses. All experiments were carried out in triplicate (n = 3).

Heat treatment resulted in a gradual decrease in cell viability for the duration of the time course (Figure 3.7A). In contrast, cadmium sulfate treatment resulted in a unique cell viability profile which appreciably declined after the addition of the stressor, with recovery occurring at 10 minutes (Figure 3.7A). A sharp decline in cell viability post potassium ferricyanide treatment was observed and remained low (Figure 3.7A).

The dynamic profile plots of the thioredoxin redox charge for heat treatment showed a surprising increase in the thioredoxin redox charge at five minutes, and thereafter a decrease was observed (Figure 3.7B). On the other hand, cadmium sulfate treatment resulted in a significant decrease in the thioredoxin redox charge from 1-5 minutes with a recovery of the charge from 5-10 minutes (Figure 3.7B). In a similar manner, the thioredoxin redox charge profile for the potassium ferricyanide treatment resulted in a decrease in the thioredoxin redox charge from 1-5 minutes and recovery occurred from 5-20 minutes. Thereafter another slight decrease in the charge occurred (Figure 3.7B).



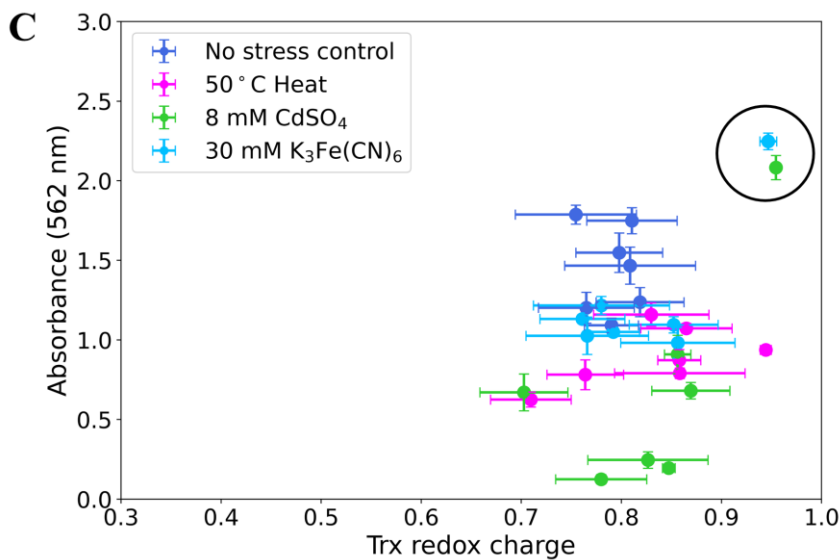
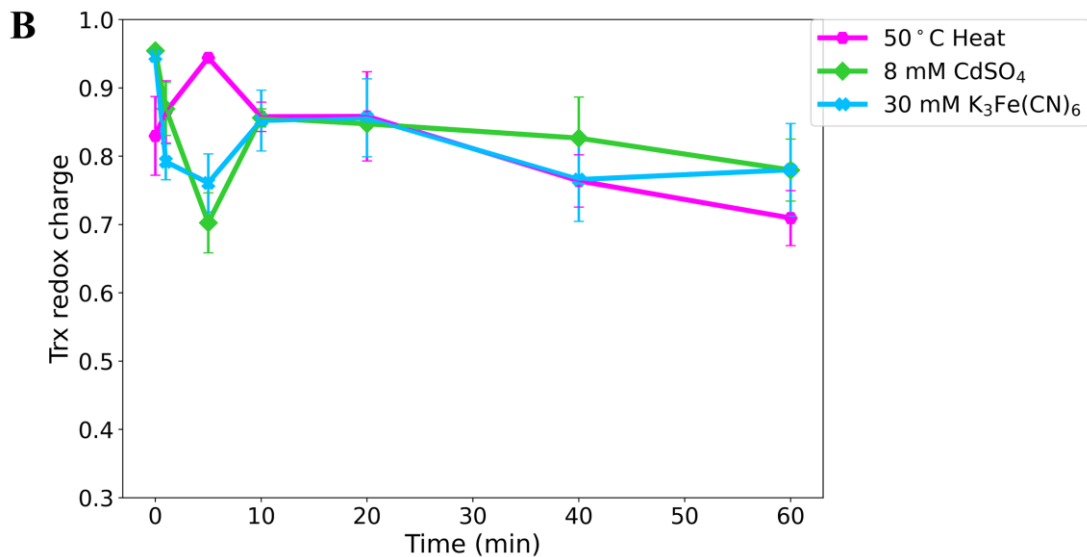


Figure 3.7 Quantification of the thioredoxin (Trx) redox charge and cell viability (562 nm) of *S. pombe* JB35 stressed with heat, cadmium sulfate (CdSO₄) and potassium ferricyanide [K₃Fe(CN)₆], over 60-minute time courses. (A) Cell viability (measured at an absorbance of 562 nm) plotted over time (minutes), after heat (50°C), 8 mM CdSO₄ and 30 mM K₃Fe(CN)₆ stress. (B) Trx redox charge plotted over time (minutes), after heat (50°C), 8 mM CdSO₄ and 30 mM K₃Fe(CN)₆ stress. (C) Trx redox charge and cell viability (measured at an absorbance of 562 nm) phase plot, of heat (50°C), 8 mM CdSO₄ and 30 mM K₃Fe(CN)₆ stressors, including the no stress control. The time zero outliers are circled. All experiments were carried out in triplicate ($n = 3$) and the mean and standard errors were plotted.

The dynamic thioredoxin redox charge profile for the heat stress was unusual as there was an increase in the thioredoxin redox charge after heat stress was introduced until five minutes, after which the charge decreased (Figure 3.7B). A functional switch from peroxidase activity to chaperone activity in yeast has been reported in response to reactive oxygen species that are generated within the cell due to heat stress (Jang *et al.*, 2004, Lim *et al.*, 2008, Troussicot *et al.*, 2021). Although, protein denaturation itself attributed to high heat may be a more significant cause of damage to the cell. The initial increase in the thioredoxin redox charge (Figure 3.7B) could presumably be attributed to increased chaperone activity of Tpx1, which decreases the rate of thioredoxin oxidation, although this would require further investigation into Tpx1 activity (Kim *et al.*, 2010).

The upregulation of thioredoxin system components and heat shock proteins in response to cadmium stress in *S. pombe* has been reported (Bae and Chen, 2004). This upregulation may be the result of cadmium sulfate inducing secondary reactive oxygen species within the cell (Bae and Chen, 2004). Potassium ferricyanide oxidizes cytochrome *c*, resulting in mitochondrial stress and cytochrome *c* associated mitochondrial mutants in *S. pombe*, produced higher levels of intrinsic oxidative stress (Zuin *et al.*, 2008). Collectively, these studies reported that the induction of oxidative stress in yeast occurred in response to heat, cadmium sulfate and potassium ferricyanide stress.

We observed from the thioredoxin redox charge and cell viability phase plot for the heat, cadmium sulfate and potassium ferricyanide treatments, that the data points also clustered in the bottom, right quadrant of the plot, as observed in the hydrogen peroxide plot (Figure 3.7C). The outliers near the top right quadrant (circled), are due to the time zero data points, before the addition of the stressors (Figure 3.7C). The statistical correlation coefficient results between the thioredoxin redox charge and cell viability for the different stressor types showed mid-strength, positive correlations (Table 3.5).

Table 3.5 Correlation analyses and their coefficients calculated between the thioredoxin redox charge and cell viability for *S. pombe* JB35 stressed with heat, cadmium sulfate (CdSO₄) and potassium ferricyanide [K₃Fe(CN)₆]

Type of stressor	Correlation analyses				
	Pearson's r	Spearman's rho	Kendall's tau	R-squared value	Distance correlation
50°C heat	0.570 ^{ns}	0.571 ^{ns}	0.429 ^{ns}	0.325 ^{ns}	0.714 ^{ns}
8 mM CdSO ₄	0.637 ^{ns}	0.714 ^{ns}	0.524 ^{ns}	0.406 ^{ns}	0.755 ^{ns}
30 mM K ₃ Fe(CN) ₆	0.764*	0.071 ^{ns}	0.048 ^{ns}	0.583*	0.796 ^{ns}

*Correlation coefficients and an R-squared value from a linear regression were calculated with statistical significance. Significance is represented as * = p < 0.05, ** = p < 0.01, *** = p < 0.001, **** = p < 0.0001 and ns = non-significant.*

A summary phase plot consisting of the thioredoxin redox charge and cell viability data for all stressors tested showed that all stressor data points, except for the time zero outliers (circled), clustered in the bottom, right quadrant which represents a high thioredoxin redox charge and a low cell viability (Figure 3.8). This result showed that the thioredoxin redox charge was preserved, despite the exposure to a number of stressors (Figure 3.8).

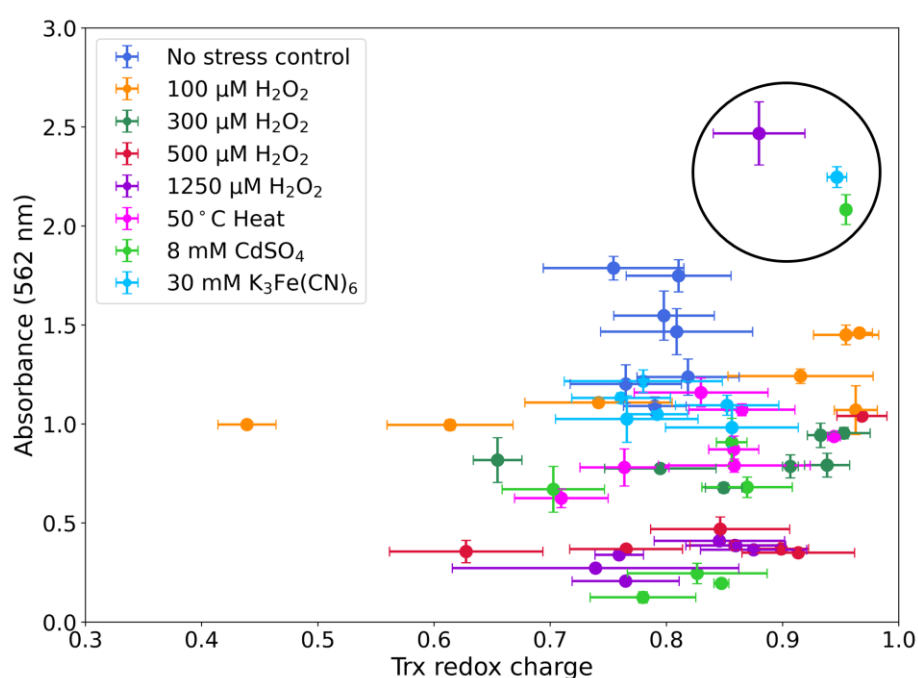


Figure 3.8 Summary phase plot of thioredoxin (Trx) redox charge and cell viability (measured at an absorbance of 562 nm) for all stressors tested. The time zero outliers are circled. All experiments were carried out in triplicate ($n = 3$) and the mean and standard errors were plotted.

3.5 Discussion

This chapter aimed to investigate the thioredoxin redox charge and whether it could be used as a general measure of the cellular redox state in *S. pombe* and to also assess the relationship between the thioredoxin redox charge and cell viability. We hoped the thioredoxin redox charge could lend itself as a tool to evaluate the efficacy of novel drugs targeting the thioredoxin system.

First, data were reanalyzed from a published study that investigated the effect of using silver and ebselen (a thioredoxin reductase inhibitor) to treat multidrug-resistant, Gram-negative bacterial infections in mice, to determine whether it was possible to relate the thioredoxin redox charge to cell viability (Zou *et al.*, 2017). A strong negative correlation between the thioredoxin redox charge and cell death was obtained: as the thioredoxin redox charge decreased in these treated cells, the cell viability decreased. Ebselen is a thioredoxin reductase inhibitor in bacterial cells and this treatment prevented thioredoxin from being reduced, which likely resulted in elevated reactive oxygen species and a loss in essential cellular functions like DNA replication, and the glutathione/glutaredoxin system was unable to compensate for these effects (Ren *et al.*, 2018, Zeller and Klug, 2006). The negative correlation between the thioredoxin redox charge and cell death supported the idea that quantifying the thioredoxin redox charge and its association with cell viability was possible and also supported the utility of the thioredoxin redox charge in thioredoxin system inhibition studies. To extend this result we aimed to quantify the thioredoxin redox charge and cell viability in *S. pombe* treated with various stressors. The stressor experiments showed weak positive correlations between the thioredoxin redox charge and cell viability for all stressors tested, and the *p*-values for most correlation analyses were non-significant.

Interestingly, a trend was observed from the phase plots of the thioredoxin redox charge and cell viability. These plots of the thioredoxin redox charge and cell viability could be divided into four quadrants (Figure 3.9A). We observed that the no stress control results clustered within quadrant two as the cells exhibited high cell viability and high thioredoxin redox charge values, which was expected as there was no added external stress perturbation (Figure 3.9A).

For the stressor experiments, we had expected our results to cluster within quadrant three, which represents low cell viability and low thioredoxin redox charge values. We assumed that the stressed cells would have a correspondingly low thioredoxin redox charge because of the thioredoxin system's involvement in reactive oxygen species detoxification. Yet, the results for these stressors appeared to cluster in quadrant four of the plot, which represents high thioredoxin redox charge values and a low cell viability (Figure 3.9A). These results showed that even though the cells were experiencing significant stress as evidenced from the corresponding low cell viability results, fluctuations in the thioredoxin redox charge were subtle and not extensive. We observed that the thioredoxin redox charge did not decrease below 0.45 and was generally maintained between 0.6 and 1 (Figure 3.8). In contrast to our initial hypothesis, this result shows that the thioredoxin redox charge may fluctuate in response to the external stressors we tested, but generally recovers and is resistant to a total collapse in the redox charge. Thus, a type of kinetic buffering of the thioredoxin redox charge may be occurring.

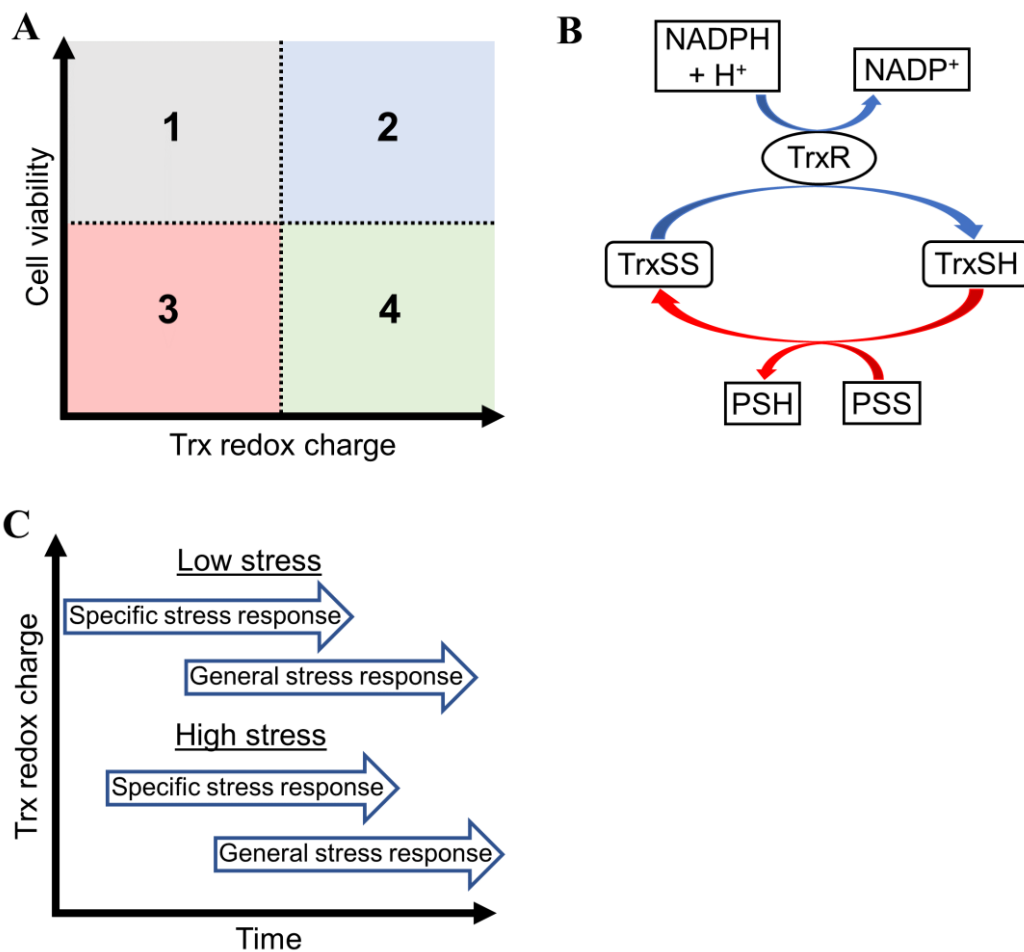


Figure 3.9 Analysis of trends in the phase plot results of the thioredoxin redox charge and cell viability in *S. pombe* JB35 for potential correlations, in response to stress. (A) The thioredoxin redox charge and cell viability correlation phase plots could be divided into four quadrants to characterize the experimental stressor results. (B) Supply (blue) and demand (red) of reducing equivalents in the thioredoxin system, details in text [Adapted (B) from Padayachee *et al.*, 2020]. (C) Potential future investigation of the underlying cellular mechanisms responsible for the thioredoxin redox charge profiles, for low and high stress, involving different specific and general stress response trends.

Within the thioredoxin system, reducing equivalents supplied from NADPH are transferred via thioredoxin reductase (TrxR) to thioredoxin which becomes reduced thioredoxin (TrxSH) (Figure 3.9B). Reduced thioredoxin then passes on the reducing equivalents to other target protein disulfides (PSS) which then form thiol groups (PSH) (Figure 3.9B). Oxidized thioredoxin (TrxSS) is again reduced by thioredoxin reductase and this cycle continues (Figure 3.9B). From this cycle, the relative amount of reduced and oxidized thioredoxin will depend on supply (blue) and demand (red) (Figure 3.9B). Our thioredoxin redox charge results appear to demonstrate that when an external stress is introduced to *S. pombe* cells, increased demand creates more TrxSS, which then increases the activity of TrxR, making more TrxSH available. In effect, the supply increases to match the demand, if NADPH is not limiting (Figure 3.9B).

This buffering ability of the thioredoxin system could also result from a decreased demand in the thioredoxin system because of hyperoxidation of Tpx1 which in turn stops drawing reducing equivalents from the thioredoxin system (reduced demand) or increased supply of reducing equivalents to thioredoxin from another system e.g. the glutathione/glutaredoxin system (increased supply) (Bozonet *et al.*, 2005, García-Santamarina *et al.*, 2013, Tan *et al.*, 2010, Vivancos *et al.*, 2005). This supply and demand of the thioredoxin system is not completely clear and would be the next step in future investigations involving the thioredoxin redox charge. It appears the only way to inflict a collapse in the thioredoxin redox charge, would be to directly inhibit thioredoxin reductase using a potent chemical inhibitor, as seen from the published data that was analyzed (Figure 3.2). To investigate this hypothesis in preparation for publication, experiments are being done to disrupt the supply of reducing equivalents to the thioredoxin system in fission yeast by treatment with auranofin. Auranofin is a robust thioredoxin reductase inhibitor that was found to exhibit potent activity against *Mycobacterium tuberculosis*, *Trypanosoma* species and *Plasmodium falciparum* that causes

malaria (da Silva *et al.*, 2016, Harbut *et al.*, 2015, Sannella *et al.*, 2008). The buffering quality of the thioredoxin system to external stressors, suggests that this system is vital to support essential functions in *S. pombe*, and studies involving thioredoxin 1 and thioredoxin reductase deletion mutants confirm this (Paulo *et al.*, 2014, Pluskal *et al.*, 2016).

The stability of the thioredoxin redox charge was also reaffirmed using a validated computational model of hydrogen peroxide metabolism in *S. pombe* (Computational model script S1) (Padayachee *et al.*, 2020, Tomalin *et al.*, 2016). The concentrations of hydrogen peroxide used in the current study (100-1250 μ M) were used in the computational model to determine what effect these perturbations had on the thioredoxin redox charge (Supplementary material-Section S8). For all hydrogen peroxide concentrations, the thioredoxin redox charge appeared to recover from 0.992 to almost 1 (Supplementary material-Section S8). This computational model also showed that the recovery of the charge occurred more rapidly than the *in vivo* results from our study (Supplementary material-Section S8). This difference could be attributed to the computational model only including hydrogen peroxide metabolism and Tpx1 hyperoxidation, but not other thioredoxin-dependant functions such as DNA synthesis and methionine sulfoxide reduction, contributing to differences between the *in silico* and *in vivo* results. Nonetheless, conservation of the thioredoxin redox charge was still detected in this model, confirming our experimental results.

It is clear the thioredoxin redox charge did not correlate well with cell viability and the charge was conserved, but the thioredoxin redox charge profiles themselves were interesting to examine and underlying cellular mechanisms could be inferred from them (Figure 3.9C). We suspect from the thioredoxin redox charge results in response to hydrogen peroxide, that there are differences in the activation of the specific (transcription factor, Pap1 and the peroxiredoxin, Tpx1) and the general stress responses (Sty1 MAPK pathway) when detoxifying low and high concentrations of hydrogen peroxide. We aim to investigate these differences in the future by assessing suitable transcriptomic datasets from the literature.

Unlike hydrogen peroxide stress, the exact stress response systems that are involved in the heat, cadmium sulfate and potassium ferricyanide stressors have not been completely described or elucidated in *S. pombe*. A study investigated the global transcriptional response of *S. pombe* to environmental stress and showed that the stressors that induced the most similar stress-specific genes were hydrogen peroxide and heat stress, having an overlap of 200 genes. The other stressors that shared a considerable overlap were hydrogen peroxide and cadmium stress, in addition to heat and cadmium stress (Chen *et al.*, 2003). Heat stress, as well as other diverse forms of stress, have been shown to activate the Sty1 MAPK pathway (Degols *et al.*,

1996). Another study investigated mutants of *S. pombe* to identify genes that were responsible for cadmium tolerance. They found a number of genes that conferred tolerance to be associated with various cell pathways including sulfate assimilation, ubiquinone (Coenzyme Q10) biosynthesis, phytochelatin synthesis and transport, cell wall biosynthesis and cell morphology and stress signaling among other pathways (Kennedy *et al.*, 2008). *S. pombe* that had the gene for thioredoxin 1 deleted showed decreased population growth at high temperatures and was unable to grow in the presence of hydrogen peroxide (Song and Roe, 2008), and also displayed sensitivity towards the addition of cadmium sulfate to the growth medium (Pluskal *et al.*, 2016), showing the importance of the thioredoxin system in the tolerance and response to these stressors.

Cross-stress protection is an interesting idea that suggests different stressors may activate similar defense pathways and mechanisms or a generic stress response can allow for a basic protection to a variety of stressors (Chen *et al.*, 2003). This type of generic protection may be an evolutionary result of yeast having to adapt to a changing environment and thus evolving defense mechanisms that can react to a range of stressors (Dhar *et al.*, 2012, Święciło, 2016). Cross-stress protection may be a reason why a large number of overlapping genes are transcribed in response to hydrogen peroxide, cadmium and heat stress. The thioredoxin system as measured by the thioredoxin redox charge, could be involved in the cross-stress protection and that may explain the reason we saw dynamic changes to the thioredoxin redox charge upon exposure to the different stressors (Figures 3.7 and 3.5). However, the thioredoxin redox charge appeared to recover even when cell viability decreased.

Future work could include testing thioredoxin system inhibitors specifically, such as auranofin in *S. pombe*, and to assess both the thioredoxin and glutathione/glutaredoxin systems, given their overlapping roles (Trotter and Grant, 2003). It would also be useful to further evaluate various aspects of the redox western blotting assay and its controls to ensure accurate quantification of the thioredoxin redox charge i.e. investigating how Ponceau S stain concentration and reusing the stain effects total protein staining on the detection membrane. To conclude, we demonstrated that the thioredoxin redox charge dynamics could be used to quantify the thioredoxin system in response to external stress perturbations in *S. pombe*, and it appeared to be buffered within particular boundaries.

Chapter 4: General discussion and conclusion

The aim of this study was to evaluate whether the thioredoxin redox charge could be used as a general measure of the cellular redox state in *S. pombe*. In Chapter 2, components of the redox western blotting assay used to quantify the thioredoxin redox charge were tested, optimized and confirmed. It would be useful to adapt the redox western blotting assay to detect the thioredoxin redox charge in a more convenient, higher throughput and cheaper format (microplate format), whilst still maintaining the specificity associated with redox western blotting. Developing a novel, high throughput thioredoxin redox charge assay is a complex undertaking, but would still be a worthwhile and attractive venture in future studies.

In Chapter 3, the thioredoxin redox charge and cell viability were measured in *S. pombe* in response to various stressors. Weak, positive correlations between the thioredoxin redox charge and cell viability were obtained. An interesting finding from the thioredoxin redox charge and cell viability phase plots was the thioredoxin redox charge appeared to be buffered in response to external stress and did not decrease below 0.45, even though cell viability was low. The thioredoxin redox charge may only be a suitable indicator of cell viability in cells that lack the glutathione/glutaredoxin system and in cells that are treated with a direct thioredoxin reductase inhibitor (Watson *et al.*, 2003). Future work could include determining the thioredoxin redox charge in cells exposed to thioredoxin reductase inhibitors such as auranofin, in addition to investigating the glutathione/glutaredoxin system to determine how both the systems fluctuate in comparison to each other. This way, we would expound how the inhibitor influences both the thiol systems. More so, for these inhibition studies, both the thioredoxin and the glutathione/glutaredoxin systems could be targeted, compounding the antimicrobial effect. A study that used this type of experimental approach where both thiol systems were measured, analyzed both thioredoxin and glutathione/glutaredoxin system components using a genetically encoded fluorescent biosensor in HEK293T mammalian cells in response to hydrogen peroxide, auranofin and arsenic trioxide in addition to other compounds. The response of both systems to hydrogen peroxide seemed to follow each other in that oxidation in both systems increased, whereas the exposure to auranofin and arsenic trioxide increased thioredoxin oxidation, but kept glutaredoxin oxidation stable (Fan *et al.*, 2017).

In conclusion, this work serves as potential evidence for the use of a novel measure, the thioredoxin redox charge, as a single, whole-system measure to determine the redox poise of the entire thioredoxin system. Further, this work shows that the thioredoxin system is important in *S. pombe* to support essential functions, because it is buffered to external stressors.

Reference List

- Alcock, L. J., Perkins, M. V. & Chalker, J. M. 2018. Chemical methods for mapping cysteine oxidation. *Chemical Society Reviews*, 47, 231-268.
- Andrade, R. M. & Reed, S. L. 2015. New drug target in protozoan parasites: the role of thioredoxin reductase. *Frontiers in Microbiology*, 6, 1-7.
- Arnér, E. S. & Holmgren, A. 2000. Physiological functions of thioredoxin and thioredoxin reductase. *European Journal of Biochemistry*, 267, 6102-6109.
- Arnér, E. S. & Holmgren, A. 2006. The thioredoxin system in cancer. *Seminars in Cancer Biology*, 16, 420-426.
- Arnér, E. S., Nordberg, J. & Holmgren, A. 1996. Efficient reduction of lipoamide and lipoic acid by mammalian thioredoxin reductase. *Biochemical and Biophysical Research Communications*, 225, 268-274.
- Åslund, F., Berndt, K. D. & Holmgren, A. 1997. Redox potentials of glutaredoxins and other thiol-disulfide oxidoreductases of the thioredoxin superfamily determined by direct protein-protein redox equilibria. *Journal of Biological Chemistry*, 272, 30780-30786.
- Azad, G. K. & Tomar, R. S. 2014. Ebselen, a promising antioxidant drug: mechanisms of action and targets of biological pathways. *Molecular Biology Reports*, 41, 4865-4879.
- Bae, W. & Chen, X. 2004. Proteomic study for the cellular responses to Cd²⁺ in *Schizosaccharomyces pombe* through amino acid-coded mass tagging and liquid chromatography tandem mass spectrometry*. *Molecular & Cellular Proteomics*, 3, 596-607.
- Bailey, D. M. 2019. Oxygen, evolution and redox signalling in the human brain; quantum in the quotidian. *The Journal of Physiology*, 597, 15-28.
- Balsera, M. & Buchanan, B. B. 2019. Evolution of the thioredoxin system as a step enabling adaptation to oxidative stress. *Free Radical Biology and Medicine*, <https://doi.org/10.1016/j.freeradbiomed.2019.03.003>.
- Banerjee, R., Becker, D., Dickman, M., Gladyshev, V. & Ragsdale, S. 2008. *Redox Biochemistry*, Wiley Online Library.
- Bao, R., Zhang, Y., Lou, X., Zhou, C. Z. & Chen, Y. 2009. Structural and kinetic analysis of *Saccharomyces cerevisiae* thioredoxin Trx1: implications for the catalytic mechanism of GSSG reduced by the thioredoxin system. *Biochimica et Biophysica Acta*, 1794, 1218-1223.

- Becker, K., Gromer, S., Schirmer, R. H. & Müller, S. 2000. Thioredoxin reductase as a pathophysiological factor and drug target. *European Journal of Biochemistry*, 267, 6118-6125.
- Bedford, E., Tabor, S. & Richardson, C. C. 1997. The thioredoxin binding domain of bacteriophage T7 DNA polymerase confers processivity on *Escherichia coli* DNA polymerase I. *Proceedings of the National Academy of Sciences*, 94, 479-484.
- Berndt, C., Christ, L., Rouhier, N. & Mühlhoff, U. 2021. Glutaredoxins with iron-sulphur clusters in eukaryotes - Structure, function and impact on disease. *Biochimica et Biophysica Acta (BBA) - Bioenergetics*, 1862, 148317.
- Berndt, C., Lillig, C. H. & Holmgren, A. 2008. Thioredoxins and glutaredoxins as facilitators of protein folding. *Biochimica et Biophysica Acta (BBA) - Molecular Cell Research*, 1783, 641-650.
- Bhatia, M., McGrath, K. L., Di Trapani, G., Charoentong, P., Shah, F., King, M. M., Clarke, F. M. & Tonissen, K. F. 2016. The thioredoxin system in breast cancer cell invasion and migration. *Redox Biology*, 8, 68-78.
- Bick, J. A., Dennis, J. J., Zylstra, G. J., Nowack, J. & Leustek, T. 2000. Identification of a new class of 5'-adenylylsulfate (APS) reductases from sulfate-assimilating bacteria. *Journal of Bacteriology*, 182, 135-142.
- Bilan, D. S., Lukyanov, S. A. & Belousov, V. V. 2015. Genetically encoded fluorescent sensors for redox processes. *Russian Journal of Bioorganic Chemistry*, 41, 231-244.
- Billack, B., Pietka-Ottlik, M., Santoro, M., Nicholson, S., Mlochowski, J. & Lau-Cam, C. 2010. Evaluation of the antifungal and plasma membrane H⁺-ATPase inhibitory action of ebselen and two ebselen analogs in *S. cerevisiae* cultures. *Journal of Enzyme Inhibition and Medicinal Chemistry*, 25, 312-317.
- Bjørklund, G., Crisponi, G., Nurchi, V. M., Cappai, R., Buha Djordjevic, A. & Aaseth, J. 2019. A review on coordination properties of thiol-containing chelating agents towards mercury, cadmium, and lead. *Molecules*, 24, 3247.
- Björnstedt, M., Hamberg, M., Kumar, S., Xue, J. & Holmgren, A. 1995. Human thioredoxin reductase directly reduces lipid hydroperoxides by NADPH and selenocystine strongly stimulates the reaction via catalytically generated selenols. *Journal of Biological Chemistry*, 270, 11761-11764.
- Bonilla, M., Denicola, A., Novoselov, S. V., Turanov, A. A., Protasio, A., Izmendi, D., Gladyshev, V. N. & Salinas, G. 2008. Platyhelminth mitochondrial and cytosolic redox

- homeostasis is controlled by a single thioredoxin glutathione reductase and dependent on selenium and glutathione. *Journal of Biological Chemistry*, 283, 17898-17907.
- Bonnet, C., Perret, E., Dumont, X., Picard, A., Caput, D. & Lenaers, G. 2000. Identification and transcription control of fission yeast genes repressed by an ammonium starvation growth arrest. *Yeast*, 16, 23-33.
- Bozonet, S. M., Findlay, V. J., Day, A. M., Cameron, J., Veal, E. A. & Morgan, B. A. 2005. Oxidation of a eukaryotic 2-Cys peroxiredoxin is a molecular switch controlling the transcriptional response to increasing levels of hydrogen peroxide. *Journal of Biological Chemistry*, 280, 23319-23327.
- Branco, V. & Carvalho, C. 2019. The thioredoxin system as a target for mercury compounds. *BBA-General Subjects*, 1863, 129255.
- Briehl, M. M. 2015. Oxygen in human health from life to death--An approach to teaching redox biology and signaling to graduate and medical students. *Redox Biology*, 5, 124-139.
- Brizzard, B. 2008. Epitope tagging. *BioTechniques*, 44, 693-695.
- Brown, J. D., Day, A. M., Taylor, S. R., Tomalin, L. E., Morgan, B. A. & Veal, E. A. 2013. A peroxiredoxin promotes H₂O₂ signaling and oxidative stress resistance by oxidizing a thioredoxin family protein. *Cell Reports*, 5, 1425-1435.
- Brzywczy, J., Sieńko, M., Kucharska, A. & Paszewski, A. 2002. Sulphur amino acid synthesis in *Schizosaccharomyces pombe* represents a specific variant of sulphur metabolism in fungi. *Yeast*, 19, 29-35.
- Burgoyne, J. R., Oviusu, O. & Eaton, P. 2013. The PEG-switch assay: A fast semi-quantitative method to determine protein reversible cysteine oxidation. *Journal of Pharmacological and Toxicological Methods*, 68, 297-301.
- Camier, S., Ma, E., Leroy, C., Pruvost, A., Toledano, M. & Marsolier-Kergoat, M.-C. 2007. Visualization of ribonucleotide reductase catalytic oxidation establishes thioredoxins as its major reductants in yeast. *Free Radical Biology and Medicine*, 42, 1008-1016.
- Canizal-García, M., Olmos-Orizaba, B. E., Moreno-Jiménez, M., Calderón-Cortés, E., Saavedra-Molina, A. & Cortés-Rojo, C. 2021. Glutathione peroxidase 2 (Gpx2) preserves mitochondrial function and decreases ROS levels in chronologically aged yeast. *Free Radical Research*, 55, 165-175.
- Carmel-Harel, O. & Storz, G. 2000. Roles of the glutathione-and thioredoxin-dependent reduction systems in the *Escherichia coli* and *Saccharomyces cerevisiae* responses to oxidative stress. *Annual Reviews in Microbiology*, 54, 439-461.

- Cassetta, M. I., Marzo, T., Fallani, S., Novelli, A. & Messori, L. 2014. Drug repositioning: auranofin as a prospective antimicrobial agent for the treatment of severe staphylococcal infections. *BioMetals*, 27, 787-791.
- Cencioni, C., Spallotta, F., Martelli, F., Valente, S., Mai, A., Zeiher, A. & Gaetano, C. 2013. Oxidative stress and epigenetic regulation in ageing and age-related diseases. *International Journal of Molecular Sciences*, 14, 17643-17663.
- Chae, H. Z., Chung, S. J. & Rhee, S. G. 1994. Thioredoxin-dependent peroxide reductase from yeast. *Journal of Biological Chemistry*, 269, 27670-27678.
- Chae, H. Z., Kim, I. H., Kim, K. & Rhee, S. G. 1993. Cloning, sequencing, and mutation of thiol-specific antioxidant gene of *Saccharomyces cerevisiae*. *Journal of Biological Chemistry*, 268, 16815-16821.
- Chen, D., Toone, W. M., Mata, J., Lyne, R., Burns, G., Kivinen, K., Brazma, A., Jones, N. & Bähler, J. 2003. Global transcriptional responses of fission yeast to environmental stress. *Molecular Biology of the Cell*, 14, 214-229.
- Cheng, Z., Arscott, L. D., Ballou, D. P. & Williams, C. H. 2007. The relationship of the redox potentials of thioredoxin and thioredoxin reductase from *Drosophila melanogaster* to the enzymatic mechanism: Reduced thioredoxin is the reductant of glutathione in *Drosophila*. *Biochemistry*, 46, 7875-7885.
- Chong, C.-R., Chan, W. P. A., Nguyen, T. H., Liu, S., Procter, N. E. K., Ngo, D. T., Sverdlov, A. L., Chirkov, Y. Y. & Horowitz, J. D. 2014. Thioredoxin-interacting protein: Pathophysiology and emerging pharmacotherapeutics in cardiovascular disease and diabetes. *Cardiovascular Drugs and Therapy*, 28, 347-360.
- Chrestensen, C. A., Starke, D. W. & Mieyal, J. J. 2000. Acute cadmium exposure inactivates thioltransferase (Glutaredoxin), inhibits intracellular reduction of protein-glutathionyl-mixed disulfides, and initiates apoptosis. *Journal of Biological Chemistry*, 275, 26556-26565.
- Chung, W. H., Kim, K. D., Cho, Y. J. & Roe, J. H. 2004. Differential expression and role of two dithiol glutaredoxins Grx1 and Grx2 in *Schizosaccharomyces pombe*. *Biochemical and Biophysical Research Communications*, 321, 922-929.
- Cody, G. D. 2004. Transition metal sulfides and the origins of metabolism. *Annual Review of Earth and Planetary Sciences*, 32, 569-599.
- Collet, J.-F. & Messens, J. 2010. Structure, function, and mechanism of thioredoxin proteins. *Antioxidants & Redox Signaling*, 13, 1205-1216.

- Collinson, E. J., Wheeler, G. L., Garrido, E. O., Avery, A. M., Avery, S. V. & Grant, C. M. 2002. The yeast glutaredoxins are active as glutathione peroxidases. *Journal of Biological Chemistry*, 277, 16712-16717.
- Collinson, L. P. & Dawes, I. W. 1995. Isolation, characterization and overexpression of the yeast gene, GLR1, encoding glutathione reductase. *Gene*, 156, 123-127.
- Cunniff, B., Snider, G. W., Fredette, N., Hondal, R. J. & Heintz, N. H. 2013. A direct and continuous assay for the determination of thioredoxin reductase activity in cell lysates. *Analytical Biochemistry*, 443, 34-40.
- Cunniff, B., Snider, G. W., Fredette, N., Stumpff, J., Hondal, R. J. & Heintz, N. H. 2014. Resolution of oxidative stress by thioredoxin reductase: Cysteine versus selenocysteine. *Redox Biology*, 2, 475-484.
- da Silva, M. T. A., Silva-Jardim, I., Portapilla, G. B., de Lima, G. M. A., Costa, F. C., Anibal, F. d. F. & Thiemann, O. H. 2016. *In vivo* and *in vitro* auranofin activity against *Trypanosoma cruzi*: Possible new uses for an old drug. *Experimental Parasitology*, 166, 189-193.
- Davies, M. J. 2005. The oxidative environment and protein damage. *BBA-Proteins and Proteomics*, 1703, 93-109.
- Day, Alison M., Brown, Jonathon D., Taylor, Sarah R., Rand, Jonathan D., Morgan, Brian A. & Veal, Elizabeth A. 2012. Inactivation of a peroxiredoxin by hydrogen peroxide is critical for thioredoxin-mediated repair of oxidized proteins and cell survival. *Molecular Cell*, 45, 398-408.
- de Siqueira Santos, S., Takahashi, D. Y., Nakata, A. & Fujita, A. 2013. A comparative study of statistical methods used to identify dependencies between gene expression signals. *Briefings in Bioinformatics*, 15, 906-918.
- Debarbieux, L. & Beckwith, J. 1998. The reductive enzyme thioredoxin 1 acts as an oxidant when it is exported to the *Escherichia coli* periplasm. *Proceedings of the National Academy of Sciences of the United States of America*, 95, 10751-10756.
- Debnath, A., Parsonage, D., Andrade, R. M., He, C., Cobo, E. R., Hirata, K., Chen, S., Garcia-Rivera, G., Orozco, E., Martinez, M. B., Gunatilleke, S. S., Barrios, A. M., Arkin, M. R., Poole, L. B., McKerrow, J. H. & Reed, S. L. 2012. A high-throughput drug screen for *Entamoeba histolytica* identifies a new lead and target. *Nature Medicine*, 18, 956-960.

- Degols, G., Shiozaki, K. & Russell, P. 1996. Activation and regulation of the Spc1 stress-activated protein kinase in *Schizosaccharomyces pombe*. *Molecular and Cellular Biology*, 16, 2870-2877.
- Dhar, R., Sägesser, R., Weikert, C. & Wagner, A. 2012. Yeast adapts to a changing stressful environment by evolving cross-protection and anticipatory gene regulation. *Molecular Biology and Evolution*, 30, 573-588.
- Domènech, A., Ayté, J., Antunes, F. & Hidalgo, E. 2018. Using *in vivo* oxidation status of one- and two-component redox relays to determine H₂O₂ levels linked to signaling and toxicity. *BMC Biology*, 16, 61.
- Draculic, T., Dawes, I. W. & Grant, C. M. 2000. A single glutaredoxin or thioredoxin gene is essential for viability in the yeast *Saccharomyces cerevisiae*. *Molecular Microbiology*, 36, 1167-1174.
- Eaton, P. 2006. Protein thiol oxidation in health and disease: Techniques for measuring disulfides and related modifications in complex protein mixtures. *Free Radical Biology and Medicine*, 40, 1889-1899.
- Ejiri, S., Weissbach, H. & Brot, N. 1979. Reduction of methionine sulfoxide to methionine by *Escherichia coli*. *Journal of Bacteriology*, 139, 161-164.
- Espinosa-Diez, C., Miguel, V., Mennerich, D., Kietzmann, T., Sanchez-Perez, P., Cadenas, S. & Lamas, S. 2015. Antioxidant responses and cellular adjustments to oxidative stress. *Redox Biology*, 6, 183-197.
- Fan, C., Zheng, W., Fu, X., Li, X., Wong, Y. S. & Chen, T. 2014. Enhancement of auranofin-induced lung cancer cell apoptosis by selenocystine, a natural inhibitor of TrxR1 *in vitro* and *in vivo*. *Cell Death & Disease*, 5, e1191.
- Fan, Y., Makar, M., Wang, M. X. & Ai, H.-w. 2017. Monitoring thioredoxin redox with a genetically encoded red fluorescent biosensor. *Nature Chemical Biology*, 13, 1045-1052.
- Felix, L., Mylonakis, E. & Fuchs, B. B. 2021. Thioredoxin reductase is a valid target for antimicrobial therapeutic development against Gram-positive bacteria. *Frontiers in Microbiology*, 12, 10.3389/fmicb.2021.663481.
- Fernandes, A. P., Fladvad, M., Berndt, C., Andresen, C., Lillig, C. H., Neubauer, P., Sunnerhagen, M., Holmgren, A. & Vlamis-Gardikas, A. 2005. A novel monothiol glutaredoxin (Grx4) from *Escherichia coli* can serve as a substrate for thioredoxin reductase. *Journal of Biological Chemistry*, 280, 24544-24552.

- Fernandes, A. P. & Holmgren, A. 2004. Glutaredoxins: glutathione-dependent redox enzymes with functions far beyond a simple thioredoxin backup system. *Antioxidants & Redox Signaling*, 6, 63-74.
- Finkelstein, A., Walz, D., Batista, V., Mizraji, M., Roisman, F. & Misher, A. 1976. Auranofin. New oral gold compound for treatment of rheumatoid arthritis. *Annals of the Rheumatic Diseases*, 35, 251-257.
- Finkelstein, J. D. & Mudd, S. H. 1967. Trans-sulfuration in mammals the methionine-sparing effect of cystine. *Journal of Biological Chemistry*, 242, 873-880.
- Forman, H. J., Zhang, H. & Rinna, A. 2009. Glutathione: overview of its protective roles, measurement, and biosynthesis. *Molecular Aspects of Medicine*, 30, 1-12.
- Fra, A., Yoboue, E. D. & Sitia, R. 2017. Cysteines as redox molecular switches and targets of disease. *Frontiers in Molecular Neuroscience*, 10, 10.3389/fnmol.2017.00167.
- Franco, R. & Vargas, M. R. 2018. Redox biology in neurological function, dysfunction, and aging. *Antioxidants & Redox Signaling*, 28, 1583-1586.
- Fuchs, B. B., RajaMuthiah, R., Souza, A. C. R., Eatemadpour, S., Rossoni, R. D., Santos, D. A., Junqueira, J. C., Rice, L. B. & Mylonakis, E. 2016. Inhibition of bacterial and fungal pathogens by the orphaned drug auranofin. *Future Medicinal Chemistry*, 8, 117-132.
- Fukuse, T., Hirata, T., Yokomise, H., Hasegawa, S., Inui, K., Mitsui, A., Hirakawa, T., Hitomi, S., Yodoi, J. & Wada, H. 1995. Attenuation of ischaemia reperfusion injury by human thioredoxin. *Thorax*, 50, 387-391.
- Gallo, G. J., Prentice, H. & Kingston, R. E. 1993. Heat shock factor is required for growth at normal temperatures in the fission yeast *Schizosaccharomyces pombe*. *Molecular and Cell Biology*, 13, 749-761.
- García-Santamarina, S., Boronat, S., Calvo, I. A., Rodríguez-Gabriel, M., Ayté, J., Molina, H. & Hidalgo, E. 2013. Is oxidized thioredoxin a major trigger for cysteine oxidation? Clues from a redox proteomics approach. *Antioxidants & Redox Signaling*, 18, 1549-1556.
- Gassmann, M., Grenacher, B., Rohde, B. & Vogel, J. 2009. Quantifying western blots: Pitfalls of densitometry. *Electrophoresis*, 30, 1845-1855.
- Gharieb, M. M. & Gadd, G. M. 2004. Role of glutathione in detoxification of metal(loid)s by *Saccharomyces cerevisiae*. *Biometals*, 17, 183-188.
- Ghasemi, M., Turnbull, T., Sebastian, S. & Kempson, I. 2021. The MTT assay: Utility, limitations, pitfalls, and interpretation in bulk and single-cell analysis. *International Journal of Molecular Sciences*, 22, 12827.

- Ghosh, S., Hamdan, S. M., Cook, T. E. & Richardson, C. C. 2008. Interactions of *Escherichia coli* thioredoxin, the processivity factor, with bacteriophage T7 DNA polymerase and helicase. *The Journal of Biological Chemistry*, 283, 32077-32084.
- Gilge, J. L., Fisher, M. & Chai, Y.-C. 2008. The effect of oxidant and the non-oxidant alteration of cellular thiol concentration on the formation of protein mixed-disulfides in HEK 293 cells. *PLOS One*, 3, e4015.
- Glasauer, A. & Chandel, N. S. 2013. ROS. *Current Biology*, 23, R100-R102.
- Go, Y.-M. & Jones, D. P. 2013. Thiol/disulfide redox states in signaling and sensing. *Critical Reviews in Biochemistry and Molecular Biology*, 48, 173-181.
- Gorr, T. A. & Vogel, J. 2015. Western blotting revisited: critical perusal of underappreciated technical issues. *Proteomics—Clinical Applications*, 9, 396-405.
- Grant, C. M. 2001. Role of the glutathione/glutaredoxin and thioredoxin systems in yeast growth and response to stress conditions. *Molecular Microbiology*, 39, 533-541.
- Grant, C. M., MacIver, F. H. & Dawes, I. W. 1996. Glutathione is an essential metabolite required for resistance to oxidative stress in the yeast *Saccharomyces cerevisiae*. *Current Genetics*, 29, 511-515.
- Grimaud, R., Ezraty, B., Mitchell, J. K., Lafitte, D., Briand, C., Derrick, P. J. & Barras, F. 2001. Repair of oxidized proteins. Identification of a new methionine sulfoxide reductase. *Journal of Biological Chemistry*, 276, 48915-48920.
- Grippo, J. F., Holmgren, A. & Pratt, W. 1985. Proof that the endogenous, heat-stable glucocorticoid receptor-activating factor is thioredoxin. *Journal of Biological Chemistry*, 260, 93-97.
- Gustafsson, T. N., Osman, H., Werngren, J., Hoffner, S., Engman, L. & Holmgren, A. 2016. Ebselen and analogs as inhibitors of *Bacillus anthracis* thioredoxin reductase and bactericidal antibacterials targeting *Bacillus* species, *Staphylococcus aureus* and *Mycobacterium tuberculosis*. *Biochimica et Biophysica Acta*, 1860, 1265-1271.
- Hampton, B. M., Zhivotovsky, B., Slater, F. A., Burgess, H. D. & Orrenius, S. 1998. Importance of the redox state of cytochrome c during caspase activation in cytosolic extracts. *Biochemical Journal*, 329, 95-99.
- Hanschmann, E.-M., Godoy, J. R., Berndt, C., Hudemann, C. & Lillig, C. H. 2013. Thioredoxins, glutaredoxins, and peroxiredoxins—molecular mechanisms and health significance: from cofactors to antioxidants to redox signaling. *Antioxidants & Redox Signaling*, 19, 1539-1605.

- Harbut, M. B., Vilchèze, C., Luo, X., Hensler, M. E., Guo, H., Yang, B., Chatterjee, A. K., Nizet, V., Jacobs, W. R. & Schultz, P. G. 2015. Auranofin exerts broad-spectrum bactericidal activities by targeting thiol-redox homeostasis. *Proceedings of the National Academy of Sciences*, 112, 4453-4458.
- Hashemy, S. I., Ungerstedt, J. S., Zahedi Avval, F. & Holmgren, A. 2006. Motexafin gadolinium, a tumor-selective drug targeting thioredoxin reductase and ribonucleotide reductase. *Journal of Biological Chemistry*, 281, 10691-10697.
- Hattori, N., Hayashi, T., Nakachi, K., Ichikawa, H., Goto, C., Tokudome, Y., Kuriki, K., Hoshino, H., Shibata, K., Yamada, N., Tokudome, M., Suzuki, S., Nagaya, T., Kobayashi, M. & Tokudome, S. 2009. Changes of ROS during a two-day ultra-marathon race. *International Journal of Sports Medicine*, 30, 426-429.
- Hauke, J. & Kossowski, T. 2011. Comparison of values of Pearson's and Spearman's correlation coefficient on the same sets of data. *Quaestiones Geographicae*, 30, 88-93.
- He, L., He, T., Farrar, S., Ji, L., Liu, T. & Ma, X. 2017. Antioxidants maintain cellular redox homeostasis by elimination of reactive oxygen species. *Cellular Physiology and Biochemistry*, 44, 532-553.
- Held, J. M. 2020. Redox systems biology: Harnessing the sentinels of the cysteine redoxome. *Antioxidants & Redox Signaling*, 32, 659-676.
- Herrero, E. & de la Torre-Ruiz, M. A. 2007. Monothiol glutaredoxins: a common domain for multiple functions. *Cellular and Molecular Life Sciences*, 64, 1518.
- Herrero, E., Ros, J., Bellí, G. & Cabisco, E. 2008. Redox control and oxidative stress in yeast cells. *Biochimica et Biophysica Acta (BBA) - General Subjects*, 1780, 1217-1235.
- Hirose, M., Tohda, H., Giga-Hama, Y., Tsushima, R., Zako, T., Iizuka, R., Pack, C., Kinjo, M., Ishii, N. & Yohda, M. 2005. Interaction of a small heat shock protein of the fission yeast, *Schizosaccharomyces pombe*, with a denatured protein at elevated temperature*. *Journal of Biological Chemistry*, 280, 32586-32593.
- Hokai, Y., Jurkowicz, B., Fernandez-Gallardo, J., Zakirkhodjaev, N., Sanau, M., Muth, T. R. & Contel, M. 2014. Auranofin and related heterometallic gold(I)-thiolates as potent inhibitors of methicillin-resistant *Staphylococcus aureus* bacterial strains. *Journal of Inorganic Biochemistry*, 138, 81-88.
- Holmgren, A. 1984. Enzymatic reduction-oxidation of protein disulfides by thioredoxin. *Methods in Enzymology*. Academic Press.
- Holmgren, A. 1995. Thioredoxin structure and mechanism: conformational changes on oxidation of the active-site sulfhydryls to a disulfide. *Structure*, 3, 239-243.

- Hopp, T. P., Prickett, K. S., Price, V. L., Libby, R. T., March, C. J., Pat Cerretti, D., Urdal, D. L. & Conlon, P. 1988. A short polypeptide marker sequence useful for recombinant protein identification and purification. *Bio/technology*, 6, 1204-1210.
- Ilari, A., Baiocco, P., Messori, L., Fiorillo, A., Boffi, A., Gramiccia, M., Di Muccio, T. & Colotti, G. 2012. A gold-containing drug against parasitic polyamine metabolism: the X-ray structure of trypanothione reductase from *Leishmania infantum* in complex with auranofin reveals a dual mechanism of enzyme inhibition. *Amino Acids*, 42, 803-811.
- Ithayaraja, C. M. 2011. Mini-review: Metabolic functions and molecular structure of glutathione reductase. *International Journal of Pharmaceutical Sciences Review and Research*, 9, 104-115.
- Jacobson, T., Priya, S., Sharma, S. K., Andersson, S., Jakobsson, S., Tanghe, R., Ashouri, A., Rauch, S., Goloubinoff, P., Christen, P. & Tamás, M. J. 2017. Cadmium causes misfolding and aggregation of cytosolic proteins in yeast. *Molecular and Cellular Biology*, 37, e00490-00416.
- Jang, H. H., Lee, K. O., Chi, Y. H., Jung, B. G., Park, S. K., Park, J. H., Lee, J. R., Lee, S. S., Moon, J. C., Yun, J. W., Choi, Y. O., Kim, W. Y., Kang, J. S., Cheong, G.-W., Yun, D.-J., Rhee, S. G., Cho, M. J. & Lee, S. Y. 2004. Two enzymes in one: Two yeast peroxiredoxins display oxidative stress-dependent switching from a peroxidase to a molecular chaperone function. *Cell*, 117, 625-635.
- Jara, M., Vivancos, A. P., Calvo, I. A., Moldón, A., Sansó, M. & Hidalgo, E. 2007. The peroxiredoxin Tpx1 is essential as a H₂O₂ scavenger during aerobic growth in fission yeast. *Molecular Biology of the Cell*, 18, 2288-2295.
- Jarvik, J. W. & Telmer, C. A. 1998. Epitope tagging. *Annual Review of Genetics*, 32, 601-618.
- Jeelani, G. & Nozaki, T. 2016. Entamoeba thiol-based redox metabolism: A potential target for drug development. *Molecular and Biochemical Parasitology*, 206, 39-45.
- Jia, J.-J., Geng, W.-S., Wang, Z.-Q., Chen, L. & Zeng, X.-S. 2019. The role of thioredoxin system in cancer: Strategy for cancer therapy. *Cancer Chemotherapy and Pharmacology*, 84, 453-470.
- John, N. 2017. *Structural analysis of the Mycobacterium tuberculosis redox defence network reveals a unique bi-fan motif design associated with hydrogen peroxide reduction*. MSc, University of KwaZulu-Natal.
- Kalantari, P., Narayan, V., Natarajan, S. K., Muralidhar, K., Gandhi, U. H., Vunta, H., Henderson, A. J. & Prabhu, K. S. 2008. Thioredoxin reductase-1 negatively regulates

- HIV-1 transactivating protein Tat-dependent transcription in human macrophages. *Journal of Biological Chemistry*, 283, 33183-33190.
- Kawagishi, H. & Finkel, T. 2014. Unraveling the truth about antioxidants: ROS and disease: finding the right balance. *Nature Medicine*, 20, 711-713.
- Kawano, Y., Suzuki, K. & Ohtsu, I. 2018. Current understanding of sulfur assimilation metabolism to biosynthesize l-cysteine and recent progress of its fermentative overproduction in microorganisms. *Applied Microbiology and Biotechnology*, 102, 8203-8211.
- Kaya, A., Lee, B. C. & Gladyshev, V. N. 2015. Regulation of protein function by reversible methionine oxidation and the role of selenoprotein MsrB1. *Antioxidants & Redox Signaling*, 23, 814-822.
- Kennedy, P. J., Vashisht, A. A., Hoe, K.-L., Kim, D.-U., Park, H.-O., Hayles, J. & Russell, P. 2008. A genome-wide screen of genes involved in cadmium tolerance in *Schizosaccharomyces pombe*. *Toxicological Sciences*, 106, 124-139.
- Kim, G., Weiss, S. J. & Levine, R. L. 2014. Methionine oxidation and reduction in proteins. *Biochimica et Biophysica Acta*, 1840, 901-905.
- Kim, H.-Y. 2013. The methionine sulfoxide reduction system: selenium utilization and methionine sulfoxide reductase enzymes and their functions. *Antioxidants & Redox Signaling*, 19, 958-969.
- Kim, J.-S., Bang, M., Lee, S.-M., Chae, H.-Z. & Kim, K.-H. 2010. Distinct functional roles of peroxiredoxin isozymes and glutathione peroxidase from fission yeast, *Schizosaccharomyces pombe*. *BMB Reports*, 43, 170-175.
- Kim, K., Kim, I. H., Lee, K. Y., Rhee, S. G. & Stadtman, E. R. 1988. The isolation and purification of a specific "protector" protein which inhibits enzyme inactivation by a thiol/Fe(III)/O₂ mixed-function oxidation system. *Journal of Biological Chemistry*, 263, 4704-4711.
- Koc, A., Mathews, C. K., Wheeler, L. J., Gross, M. K. & Merrill, G. F. 2006. Thioredoxin is required for deoxyribonucleotide pool maintenance during S phase. *Journal of Biological Chemistry*, 281, 15058-15063.
- Koháryová, M. & Kolářová, M. 2008. Oxidative stress and thioredoxin system. *General Physiology and Biophysics*, 27, 71-84.
- Kopriva, S. & Koprivova, A. 2003. Sulphate assimilation: A pathway which likes to surprise. In: Abrol, Y. P. & Ahmad, A. (eds.) *Sulphur in Plants*. Dordrecht: Springer Netherlands.

- Kostyuk, A. I., Panova, A. S., Bilan, D. S. & Belousov, V. V. 2018. Redox biosensors in a context of multiparameter imaging. *Free Radical Biology and Medicine*, 128, 23-39.
- Kostyuk, A. I., Panova, A. S., Kokova, A. D., Kotova, D. A., Maltsev, D. I., Podgorny, O. V., Belousov, V. V. & Bilan, D. S. 2020. In vivo imaging with genetically encoded redox biosensors. *International Journal of Molecular Sciences*, 21, 8164.
- Kurien, B. T. & Scofield, R. H. 2006. Western blotting. *Methods*, 38, 283-293.
- Lackner, D. H., Schmidt, M. W., Wu, S., Wolf, D. A. & Bähler, J. 2012. Regulation of transcriptome, translation, and proteome in response to environmental stress in fission yeast. *Genome Biology*, 13, R25.
- Laman Trip, D. S. & Youk, H. 2020. Yeasts collectively extend the limits of habitable temperatures by secreting glutathione. *Nature Microbiology*, 5, 943-954.
- Lanier, K. & Williams, L. 2017. The Origin of Life: Models and Data. *Journal of Molecular Evolution*, 84, 85-92.
- Laurent, T. C., Moore, E. C. & Reichard, P. 1964. Enzymatic synthesis of deoxyribonucleotides. IV. Isolation and characterization of thioredoxin, the hydrogen donor from *Escherichia coli* B. *Journal of Biological Chemistry*, 239, 3436-3444.
- Lee, S., Kim, S. M. & Lee, R. T. 2013. Thioredoxin and thioredoxin target proteins: From molecular mechanisms to functional significance. *Antioxidants & Redox Signaling*, 18, 1165-1207.
- Lee, Y. J. & Chang, G. D. 2019. Quantitative display of the redox status of proteins with maleimide-polyethylene glycol tagging. *Electrophoresis*, 40, 491-498.
- Leichert, L. I., Scharf, C. & Hecker, M. 2003. Global characterization of disulfide stress in *Bacillus subtilis*. *Journal of Bacteriology*, 185, 1967-1975.
- Lennicke, C. & Cochemé, H. M. 2021. Redox metabolism: ROS as specific molecular regulators of cell signaling and function. *Molecular Cell*, 81, 3691-3707.
- Lillig, C. H. & Holmgren, A. 2007. Thioredoxin and related molecules—from biology to health and disease. *Antioxidants & Redox Signaling*, 9, 25-47.
- Lillig, C. H., Prior, A., Schwenn, J. D., Aslund, F., Ritz, D., Vlami-Gardikas, A. & Holmgren, A. 1999. New thioredoxins and glutaredoxins as electron donors of 3'-phosphoadenylylsulfate reductase. *Journal of Biological Chemistry*, 274, 7695-7698.
- Lim, J. C., Choi, H.-I., Park, Y. S., Nam, H. W., Woo, H. A., Kwon, K.-S., Kim, Y. S., Rhee, S. G., Kim, K. & Chae, H. Z. 2008. Irreversible oxidation of the active-site cysteine of peroxiredoxin to cysteine sulfonic acid for enhanced molecular chaperone activity. *Journal of Biological Chemistry*, 283, 28873-28880.

- Lim, J. M., Kim, G. & Levine, R. L. 2019. Methionine in proteins: It's not just for protein initiation anymore. *Neurochemical Research*, 44, 247-257.
- Lin, H. L., Lin, C. C., Lin, Y. J., Lin, H. C., Shih, C. M., Chen, C. R., Huang, R. N. & Kuo, T. C. 2010. Revisiting with a relative-density calibration approach the determination of growth rates of microorganisms by use of optical density data from liquid cultures. *Applied and Environmental Microbiology*, 76, 1683-1685.
- Lind, D. 2019. *Quantification of time-dependent redox signalling in the Tpx1/Pap1 pathway in Schizosaccharomyces pombe*. MSc, University of KwaZulu-Natal.
- Liu, C., Sun, T., Zhai, Y. & Dong, S. 2009. Evaluation of ferricyanide effects on microorganisms with multi-methods. *Talanta*, 78, 613-617.
- Lobanov, A. V., Gromer, S., Salinas, G. & Gladyshev, V. N. 2006. Selenium metabolism in *Trypanosoma*: characterization of selenoproteomes and identification of a Kinetoplastida-specific selenoprotein. *Nucleic Acids Research*, 34, 4012-4024.
- Loh, B., Kuhn, A. & Leptihn, S. 2019. The fascinating biology behind phage display: Filamentous phage assembly. *Molecular Microbiology*, 111, 1132-1138.
- Lourenço Dos Santos, S., Petropoulos, I. & Friguet, B. 2018. The oxidized protein repair enzymes methionine sulfoxide reductases and their roles in protecting against oxidative stress, in ageing and in regulating protein function. *Antioxidants (Basel, Switzerland)*, 7, 191.
- Lu, J., Chew, E.-H. & Holmgren, A. 2007. Targeting thioredoxin reductase is a basis for cancer therapy by arsenic trioxide. *Proceedings of the National Academy of Sciences*, 104, 12288-12293.
- Lu, J. & Holmgren, A. 2014. The thioredoxin antioxidant system. *Free Radical Biology and Medicine*, 66, 75-87.
- Lu, J., Vlamis-Gardikas, A., Kandasamy, K., Zhao, R., Gustafsson, T. N., Engstrand, L., Hoffner, S., Engman, L. & Holmgren, A. 2013. Inhibition of bacterial thioredoxin reductase: an antibiotic mechanism targeting bacteria lacking glutathione. *FASEB Journal*, 27, 1394-1403.
- Lundberg, M., Curbo, S., Reiser, K., Masterman, T., Braesch-Andersen, S., Areström, I. & Ahlborg, N. 2014. Methodological aspects of ELISA analysis of thioredoxin 1 in human plasma and cerebrospinal fluid. *PLOS One*, 9, e103554.
- Luo, S. & Levine, R. L. 2009. Methionine in proteins defends against oxidative stress. *The FASEB Journal*, 23, 464-472.

- Mahmood, T. & Yang, P.-C. 2012. Western blot: Technique, theory, and trouble shooting. *North American Journal of Medical Sciences*, 4, 429-434.
- Mark, D. F. & Richardson, C. C. 1976. Escherichia coli thioredoxin: a subunit of bacteriophage T7 DNA polymerase. *Proceedings of the National Academy of Sciences of the United States of America*, 73, 780-784.
- Marumoto, M., Suzuki, S., Hosono, A., Arakawa, K., Shibata, K., Fuku, M., Goto, C., Tokudome, Y., Hoshino, H., Imaeda, N., Kobayashi, M., Yodoi, J. & Tokudome, S. 2010. Changes in thioredoxin concentrations: an observation in an ultra-marathon race. *Environmental Health and Preventive Medicine*, 15, 129-134.
- Mashamaite, L., Rohwer, J. & Pillay, C. 2014. The glutaredoxin mono- And di-thiol mechanisms for deglutathionylation are functionally equivalent: Implications for redox systems biology. *Bioscience Reports*, 35.
- Masutani, H., Ueda, S. & Yodoi, J. 2005. The thioredoxin system in retroviral infection and apoptosis. *Cell Death & Differentiation*, 12, 991-998.
- Matsuzawa, A. 2017. Thioredoxin and redox signaling: Roles of the thioredoxin system in control of cell fate. *Archives of Biochemistry and Biophysics*, 617, 101-105.
- Maurice, M. M., Nakamura, H., Gringhuis, S., Okamoto, T., Yoshida, S., Kullmann, F., Lechner, S., van der Voort, E. A., Leow, A., Versendaal, J., Muller-Ladner, U., Yodoi, J., Tak, P. P., Breedveld, F. C. & Verweij, C. L. 1999. Expression of the thioredoxin-thioredoxin reductase system in the inflamed joints of patients with rheumatoid arthritis. *Arthritis & Rheumatology*, 42, 2430-2439.
- May, H. C., Yu, J.-J., Guentzel, M. N., Chambers, J. P., Cap, A. P. & Arulanandam, B. P. 2018. Repurposing Auranofin, Ebselen, and PX-12 as antimicrobial agents targeting the thioredoxin system. *Frontiers in Microbiology*, 9, 1-10.
- Medentsev, A. G., Arinbasarova, A. Y., Golovchenko, N. P. & Akimenko, V. K. 2002. Involvement of the alternative oxidase in respiration of *Yarrowia lipolytica* mitochondria is controlled by the activity of the cytochrome pathway. *FEMS Yeast Research*, 2, 519-524.
- Medhi, B., Kaur, H., Prakash, A. & Medhi, B. 2013. Drug therapy in stroke: From preclinical to clinical studies. *Pharmacology*, 92, 324-334.
- Mendoza-Cozatl, D., Loza-Tavera, H., Hernández-Navarro, A. & Moreno-Sánchez, R. 2005. Sulfur assimilation and glutathione metabolism under cadmium stress in yeast, protists and plants. *FEMS Microbiology Reviews*, 29, 653-671.

- Meyer, A. J. & Dick, T. P. 2010. Fluorescent protein-based redox probes. *Antioxidants & Redox Signaling*, 13, 621-650.
- Meyer, Y., Buchanan, B. B., Vignols, F. & Reichheld, J.-P. 2009. Thioredoxins and glutaredoxins: unifying elements in redox biology. *Annual Review of Genetics*, 43, 335-367.
- Mikolić, A., Schönwald, N. & Piasek, M. 2016. Cadmium, iron and zinc interaction and hematological parameters in rat dams and their offspring. *Journal of Trace Elements in Medicine and Biology*, 38, 108-116.
- Miller, C. G., Holmgren, A., Arner, E. S. J. & Schmidt, E. E. 2018. NADPH-dependent and -independent disulfide reductase systems. *Free Radical Biology and Medicine*, 127, 248-261.
- Mishra, M., Tiwari, S., Gunaseelan, A., Li, D., Hammock, B. D. & Gomes, A. V. 2019. Improving the sensitivity of traditional western blotting via streptavidin containing poly-horseradish peroxidase (PolyHRP). *Electrophoresis*, 40, 1731-1739.
- Montano, S. J., Lu, J., Gustafsson, T. N. & Holmgren, A. 2014. Activity assays of mammalian thioredoxin and thioredoxin reductase: Fluorescent disulfide substrates, mechanisms, and use with tissue samples. *Analytical Biochemistry*, 449, 139-146.
- Monteiro, H. P., Ogata, F. T. & Stern, A. 2017. Thioredoxin promotes survival signaling events under nitrosative/oxidative stress associated with cancer development. *Biomedical Journal*, 40, 189-199.
- Mulani, M. S., Kamble, E. E., Kumkar, S. N., Tawre, M. S. & Pardesi, K. R. 2019. Emerging strategies to combat ESKAPE pathogens in the era of antimicrobial resistance: A review. *Frontiers in Microbiology*, 10.
- Muller, E. 1991. Thioredoxin deficiency in yeast prolongs S phase and shortens the G1 interval of the cell cycle. *Journal of Biological Chemistry*, 266, 9194-9202.
- Muller, E. G. 1995. A redox-dependent function of thioredoxin is necessary to sustain a rapid rate of DNA synthesis in yeast. *Archives of Biochemistry and Biophysics*, 318, 356-361.
- Muller, E. G. 1996. A glutathione reductase mutant of yeast accumulates high levels of oxidized glutathione and requires thioredoxin for growth. *Molecular Biology of the Cell*, 7, 1805-1813.
- Murphy, M. P. 2009. How mitochondria produce reactive oxygen species. *The Biochemical Journal*, 417, 1-13.
- Mustacich, D. & Powis, G. 2000. Thioredoxin reductase. *Biochemical Journal*, 346, 1-8.

- Nakamura, H. 2005. Thioredoxin and its related molecules: update 2005. *Antioxidants & Redox Signaling*, 7, 823-828.
- Nakamura, H., De Rosa, S., Roederer, M., Anderson, M. T., Dubs, J. G., Yodoi, J., Holmgren, A., Herzenberg, L. A. & Herzenberg, L. A. 1996. Elevation of plasma thioredoxin levels in HIV-infected individuals. *International Immunology*, 8, 603-611.
- Nakashima, T., Ōmura, S. & Takahashi, Y. 2012. Generation of superoxide anions by a glycation reaction in conventional laboratory media. *Journal of Bioscience and Bioengineering*, 114, 275-280.
- Nanda, J. S. & Lorsch, J. R. 2014. Labeling of a protein with fluorophores using maleimide derivitization. *Methods in Enzymology*, 536, 79-86.
- Netto, L. E. S. & Antunes, F. 2016. The Roles of Peroxiredoxin and Thioredoxin in Hydrogen Peroxide Sensing and in Signal Transduction. *Molecules and Cells*, 39, 65-71.
- Ngo, H. X., Shrestha, S. K. & Garneau-Tsodikova, S. 2016. Identification of Ebsulfur analogues with broad-spectrum antifungal activity. *ChemMedChem*, 11, 1507-1516.
- Nieri, P., Carpi, S., Fogli, S., Polini, B., Breschi, M. C. & Podestà, A. 2017. Cholinesterase-like organocatalysis by imidazole and imidazole-bearing molecules. *Scientific Reports*, 7, 45760.
- Nishida, K., Watanabe, H., Miyahisa, M., Hiramoto, Y., Nosaki, H., Fujimura, R., Maeda, H., Otagiri, M. & Maruyama, T. 2020. Systemic and sustained thioredoxin analogue prevents acute kidney injury and its-associated distant organ damage in renal ischemia reperfusion injury mice. *Scientific Reports*, 10, 20635.
- Nishinaka, Y., Masutani, H., Nakamura, H. & Yodoi, J. 2001. Regulatory roles of thioredoxin in oxidative stress-induced cellular responses. *Redox Report*, 6, 289-295.
- Noble, A., Guille, M. & Cobley, J. N. 2021. ALISA: A microplate assay to measure protein thiol redox state. *Free Radical Biology and Medicine*, 174, 272-280.
- Noguchi, C., Garabedian, M. V., Malik, M. & Noguchi, E. 2008. A vector system for genomic FLAG epitope-tagging in *Schizosaccharomyces pombe*. *Biotechnology Journal*, 3, 1280-1285.
- Noh, M. R., Kim, K. Y., Han, S. J., Kim, J. I., Kim, H. Y. & Park, K. M. 2017. Methionine sulfoxide reductase A deficiency exacerbates cisplatin-induced nephrotoxicity via increased mitochondrial damage and renal cell death. *Antioxidants & Redox Signaling*, 27, 727-741.
- Nordberg, J. & Arnér, E. S. 2001. Reactive oxygen species, antioxidants, and the mammalian thioredoxin system. *Free Radical Biology and Medicine*, 31, 1287-1312.

- O'Loughlin, J., Napolitano, S., Alkhathami, F., O'Beirne, C., Marhöfer, D., O'Shaughnessy, M., Howe, O., Tacke, M. & Rubini, M. 2021. The antibacterial drug candidate SBC3 is a potent inhibitor of bacterial thioredoxin reductase. *ChemBioChem*, 22, 1093-1098.
- Oien, D. B. & Moskovitz, J. 2007. Substrates of the methionine sulfoxide reductase system and their physiological relevance. *Current Topics in Developmental Biology*. Academic Press.
- Olivares-Marin, I. K., González-Hernández, J. C., Regalado-Gonzalez, C. & Madrigal-Perez, L. A. 2018. *Saccharomyces cerevisiae* exponential growth kinetics in batch culture to analyze respiratory and fermentative metabolism. *Journal of Visualized Experiments*, 139, 58192.
- Osborne, J. W. & Waters, E. 2002. Four assumptions of multiple regression that researchers should always test. *scholarworks.umass.edu*, 8, 1-5.
- Padayachee, L. 2017. *Quantification of the thioredoxin system*. PhD, University of KwaZulu-Natal.
- Padayachee, L. & Pillay, C. S. 2016. The thioredoxin system and not the Michaelis–Menten equation should be fitted to substrate saturation datasets from the thioredoxin insulin assay. *Redox Report*, 21, 170-179.
- Padayachee, L., Rohwer, J. M. & Pillay, C. S. 2020. The thioredoxin redox potential and redox charge are surrogate measures for flux in the thioredoxin system. *Archives of Biochemistry and Biophysics*, 680, 108231.
- Pannala, V. R. & Dash, R. K. 2015. Mechanistic characterization of the thioredoxin system in the removal of hydrogen peroxide. *Free Radical Biology & Medicine*, 78, 42-55.
- Paulo, E., García-Santamarina, S., Calvo, I. A., Carmona, M., Boronat, S., Domènech, A., Ayté, J. & Hidalgo, E. 2014. A genetic approach to study H₂O₂ scavenging in fission yeast – distinct roles of peroxiredoxin and catalase. *Molecular Microbiology*, 92, 246-257.
- Pedrajas, J. R., Kosmidou, E., Miranda-Vizuete, A., Gustafsson, J.-Å., Wright, A. P. H. & Spyrou, G. 1999. Identification and Functional Characterization of a Novel Mitochondrial Thioredoxin System in *Saccharomyces cerevisiae*. *Journal of Biological Chemistry*, 274, 6366-6373.
- Pekmez, M., Arda, N., Hamad, İ., Kiğ, C. & Temizkan, G. 2008. Hydrogen peroxide-induced oxidative damages in *Schizosaccharomyces pombe*. *Biologia*, 63, 151-155.

- Péter, M., Glatz, A., Gudmann, P., Gombos, I., Török, Z., Horváth, I., Vígh, L. & Balogh, G. 2017. Metabolic crosstalk between membrane and storage lipids facilitates heat stress management in *Schizosaccharomyces pombe*. *PLOS One*, 12, e0173739.
- Pietka-Ottlik, M., Wojtowicz-Mlochowska, H., Kolodziejczyk, K., Piasecki, E. & Mlochowski, J. 2008. New organoselenium compounds active against pathogenic bacteria, fungi and viruses. *Chemical and Pharmaceutical Bulletin (Tokyo)*, 56, 1423-1427.
- Pillai-Kastoori, L., Heaton, S., Shiflett, S. D., Roberts, A. C., Solache, A. & Schutz-Geschwender, A. R. 2020. Antibody validation for Western blot: by the user, for the user. *Journal of Biological Chemistry*, 295, 926-939.
- Pillay, C. S., Hofmeyr, J.-H., Mashamaite, L. N. & Rohwer, J. M. 2013. From top-down to bottom-up: Computational modeling approaches for cellular redoxin networks. *Antioxidants & Redox Signaling*, 18, 2075-2086.
- Pillay, C. S., Hofmeyr, J. H. & Rohwer, J. M. 2011. The logic of kinetic regulation in the thioredoxin system. *BMC Systems Biology*, 5, 1-15.
- Pluskal, T., Sajiki, K., Becker, J., Takeda, K. & Yanagida, M. 2016. Diverse fission yeast genes required for responding to oxidative and metal stress: Comparative analysis of glutathione-related and other defense gene deletions. *Genes to Cells*, 21, 530-542.
- Poole, L. B. 2015. The basics of thiols and cysteines in redox biology and chemistry. *Free Radical Biology & Medicine*, 80, 148-157.
- Porqué, P. G., Baldesten, A. & Reichard, P. 1970. The involvement of the thioredoxin system in the reduction of methionine sulfoxide and sulfate. *Journal of Biological Chemistry*, 245, 2371-2374.
- Powis, G. & Montfort, W. R. 2001. Properties and biological activities of thioredoxins. *Annual Review of Biophysics and Biomolecular Structure*, 30, 421-455.
- Prieto-Álamo, M. a.-J., Jurado, J., Gallardo-Madueño, R., Monje-Casas, F., Holmgren, A. & Pueyo, C. 2000. Transcriptional regulation of glutaredoxin and thioredoxin pathways and related enzymes in response to oxidative stress. *Journal of Biological Chemistry*, 275, 13398-13405.
- Quinn, J., Findlay, V. J., Dawson, K., Millar, J. B., Jones, N., Morgan, B. A. & Toone, W. M. 2002. Distinct regulatory proteins control the graded transcriptional response to increasing H₂O₂ levels in fission yeast *Schizosaccharomyces pombe*. *Molecular Biology of the Cell*, 13, 805-816.

- Rai, Y., Pathak, R., Kumari, N., Sah, D. K., Pandey, S., Kalra, N., Soni, R., Dwarakanath, B. & Bhatt, A. N. 2018. Mitochondrial biogenesis and metabolic hyperactivation limits the application of MTT assay in the estimation of radiation induced growth inhibition. *Scientific Reports*, 8, 1-15.
- Rani, A., Kumar, A., Lal, A. & Pant, M. 2014. Cellular mechanisms of cadmium-induced toxicity: A review. *International Journal of Environmental Health Research*, 24, 378-399.
- Ren, X., Zou, L., Lu, J. & Holmgren, A. 2018. Selenocysteine in mammalian thioredoxin reductase and application of ebselen as a therapeutic. *Free Radical Biology and Medicine*, 127, 238-247.
- Ren, X., Zou, L., Zhang, X., Branco, V., Wang, J., Carvalho, C., Holmgren, A. & Lu, J. 2017. Redox signaling mediated by thioredoxin and glutathione systems in the central nervous system. *Antioxidants & Redox Signaling*, 27, 989-1010.
- Requejo, R., Chouchani, E. T., Hurd, T. R., Menger, K. E., Hampton, M. B. & Murphy, M. P. 2010. Chapter 8 - Measuring mitochondrial protein thiol redox state. In: Cadenas, E. & Packer, L. (eds.) *Methods in Enzymology*. Academic Press.
- Rhee, S. G. 2016. Overview on peroxiredoxin. *Molecules and Cells*, 39, 1-5.
- Rice, L. B. 2008. Federal funding for the study of antimicrobial resistance in nosocomial pathogens: no ESKAPE. The University of Chicago Press.
- Riddles, P. W., Blakeley, R. L. & Zerner, B. 1979. Ellman's reagent: 5, 5'-dithiobis (2-nitrobenzoic acid)—a reexamination. *Analytical Biochemistry*, 94, 75-81.
- Ritz, D., Patel, H., Doan, B., Zheng, M., Åslund, F., Storz, G. & Beckwith, J. 2000. Thioredoxin 2 is involved in the oxidative stress response in *Escherichia coli*. *Journal of Biological Chemistry*, 275, 2505-2512.
- Roberts, M. J., Bentley, M. D. & Harris, J. M. 2002. Chemistry for peptide and protein PEGylation. *Advanced Drug Delivery Reviews*, 54, 459-476.
- Roder, C. & Thomson, M. J. 2015. Auranofin: repurposing an old drug for a golden new age. *Drugs in R&D*, 15, 13-20.
- Rogers, L. K., Leinweber, B. L. & Smith, C. V. 2006. Detection of reversible protein thiol modifications in tissues. *Analytical Biochemistry*, 358, 171-184.
- Rollins, M. F., van der Heide, D. M., Weisend, C. M., Kundert, J. A., Comstock, K. M., Suvorova, E. S., Capecchi, M. R., Merrill, G. F. & Schmidt, E. E. 2010. Hepatocytes lacking thioredoxin reductase 1 have normal replicative potential during development and regeneration. *Journal of Cell Science*, 123, 2402-2412.

- Romero-Calvo, I., Ocón, B., Martínez-Moya, P., Suárez, M. D., Zarzuelo, A., Martínez-Augustin, O. & de Medina, F. S. 2010. Reversible Ponceau staining as a loading control alternative to actin in Western blots. *Analytical Biochemistry*, 401, 318-320.
- Rudyk, O. & Eaton, P. 2014. Biochemical methods for monitoring protein thiol redox states in biological systems. *Redox Biology*, 2, 803-813.
- Russel, M. 1991. Filamentous phage assembly. *Molecular Microbiology*, 5, 1607-1613.
- Russel, M. & Model, P. 1985. Thioredoxin is required for filamentous phage assembly. *Proceedings of the National Academy of Sciences*, 82, 29-33.
- Russel, M. & Model, P. 1986. The role of thioredoxin in filamentous phage assembly. Construction, isolation, and characterization of mutant thioredoxins. *Journal of Biological Chemistry*, 261, 14997-15005.
- Russel, M., Model, P. & Holmgren, A. 1990. Thioredoxin or glutaredoxin in *Escherichia coli* is essential for sulfate reduction but not for deoxyribonucleotide synthesis. *Journal of Bacteriology*, 172, 1923-1929.
- Sander, H., Wallace, S., Plouse, R., Tiwari, S. & Gomes, A. V. 2019. Ponceau S waste: Ponceau S staining for total protein normalization. *Analytical Biochemistry*, 575, 44-53.
- Sannella, A. R., Casini, A., Gabbiani, C., Messori, L., Bilia, A. R., Vincieri, F. F., Majori, G. & Severini, C. 2008. New uses for old drugs. Auranofin, a clinically established antiarthritic metallodrug, exhibits potent antimalarial effects *in vitro*: Mechanistic and pharmacological implications. *FEBS Letters*, 582, 844-847.
- Santajit, S. & Indrawattana, N. 2016. Mechanisms of antimicrobial resistance in ESKAPE pathogens. *BioMed Research International*, 2016.
- Sato, I., Shimatani, K., Fujita, K., Abe, T., Shimizu, M., Fujii, T., Hoshino, T. & Takaya, N. 2011. Glutathione reductase/glutathione is responsible for cytotoxic elemental sulfur tolerance via polysulfide shuttle in fungi. *The Journal of Biological Chemistry*, 286, 20283-20291.
- Schafer, F. Q. & Buettner, G. R. 2001. Redox environment of the cell as viewed through the redox state of the glutathione disulfide/glutathione couple. *Free Radical Biology and Medicine*, 30, 1191-1212.
- Schägger, H. 2006. Tricine-SDS-PAGE. *Nature Protocols*, 1, 16-22.
- Schallreuter, K. U., Gleason, F. K. & Wood, J. M. 1990. The mechanism of action of the nitrosourea anti-tumor drugs on thioredoxin reductase, glutathione reductase and ribonucleotide reductase. *Biochimica et Biophysica Acta*, 1054, 14-20.

- Schumacher, F. F., Nobles, M., Ryan, C. P., Smith, M. E. B., Tinker, A., Caddick, S. & Baker, J. R. 2011. In situ maleimide bridging of disulfides and a new approach to protein PEGylation. *Bioconjugate Chemistry*, 22, 132-136.
- Sengupta, R. & Holmgren, A. 2014. Thioredoxin and glutaredoxin-mediated redox regulation of ribonucleotide reductase. *World Journal of Biological Chemistry*, 5, 68-74.
- Sessions, A. L., Doughty, D. M., Welander, P. V., Summons, R. E. & Newman, D. K. 2009. The continuing puzzle of the great oxidation event. *Current Biology*, 19, R567-R574.
- Shabani, S., Nourizadeh, N. & Soltankhah, M. 2014. The over expression of thioredoxin during malignancies. *Reviews in Clinical Medicine*, 1, 218-224.
- Sharpley, A. L., Williams, C., Holder, A. A., Godlewska, B. R., Singh, N., Shanyinde, M., MacDonald, O. & Cowen, P. J. 2020. A phase 2a randomised, double-blind, placebo-controlled, parallel-group, add-on clinical trial of ebselen (SPI-1005) as a novel treatment for mania or hypomania. *Psychopharmacology (Berl)*, 237, 3773-3782.
- Shiozaki, K., Shiozaki, M. & Russell, P. 1998. Heat stress activates fission yeast Spc1/StyI MAPK by a MEKK-independent mechanism. *Molecular Biology of the Cell*, 9, 1339-1349.
- Sies, H. 2015. Oxidative stress: a concept in redox biology and medicine. *Redox Biology*, 4, 180-183.
- Sies, H., Berndt, C. & Jones, D. P. 2017. Oxidative Stress. *Annual Review of Biochemistry*, 86, 715-748.
- Sin, M. L., Mach, K. E., Wong, P. K. & Liao, J. C. 2014. Advances and challenges in biosensor-based diagnosis of infectious diseases. *Expert Review of Molecular Diagnostics*, 14, 225-244.
- Slesak, I., Slesak, H. & Kruk, J. 2012. Oxygen and hydrogen peroxide in the early evolution of life on earth: *in silico* comparative analysis of biochemical pathways. *Astrobiology*, 12, 775-784.
- Song, J.-Y., Cha, J., Lee, J. & Roe, J.-H. 2006. Glutathione reductase and a mitochondrial thioredoxin play overlapping roles in maintaining iron-sulfur enzymes in fission yeast. *Eukaryotic Cell*, 5, 1857-1865.
- Song, J. Y. & Roe, J. H. 2008. The role and regulation of Trx1, a cytosolic thioredoxin in *Schizosaccharomyces pombe*. *Journal of Microbiology*, 46, 408-414.
- Spector, D., Labarre, J. & Toledano, M. B. 2001. A genetic investigation of the essential role of glutathione: mutations in the proline biosynthesis pathway are the only suppressors of glutathione auxotrophy in yeast. *Journal of Biological Chemistry*, 276, 7011-7016.

- Su, D., Novoselov, S. V., Sun, Q.-A., Moustafa, M. E., Zhou, Y., Oko, R., Hatfield, D. L. & Gladyshev, V. N. 2005. Mammalian selenoprotein thioredoxin-glutathione reductase roles in disulfide bond formation and sperm maturation. *Journal of Biological Chemistry*, 280, 26491-26498.
- Sugama, K., Suzuki, K., Yoshitani, K., Shiraishi, K., Miura, S., Yoshioka, H., Mori, Y. & Kometani, T. 2015. Changes of thioredoxin, oxidative stress markers, inflammation and muscle/renal damage following intensive endurance exercise. *Exercise Immunology Review* 21, 130-142.
- Świącilo, A. 2016. Cross-stress resistance in *Saccharomyces cerevisiae* yeast--new insight into an old phenomenon. *Cell Stress Chaperones*, 21, 187-200.
- Székely, G. J., Rizzo, M. L. & Bakirov, N. K. 2007. Measuring and testing dependence by correlation of distances. *The Annals of Statistics*, 35, 2769-2794.
- Székely, G. J. & Rizzo, M. L. J. J. o. M. A. 2013. The distance correlation t-test of independence in high dimension. *Journal of Multivariate Analysis*, 117, 193-213.
- Takashima, Y., Hirota, K., Nakamura, H., Nakamura, T., Akiyama, K., Cheng, F. S., Maeda, M. & Yodoi, J. 1999. Differential expression of glutaredoxin and thioredoxin during monocytic differentiation. *Immunology Letters*, 68, 397-401.
- Tan, S. X., Greetham, D., Raeth, S., Grant, C. M., Dawes, I. W. & Perrone, G. G. 2010. The thioredoxin-thioredoxin reductase system can function *in vivo* as an alternative system to reduce oxidized glutathione in *Saccharomyces cerevisiae*. *Journal of Biological Chemistry*, 285, 6118-6126.
- Tartaglia, L. A., Storz, G., Brodsky, M. H., Lai, A. & Ames, B. N. 1990. Alkyl hydroperoxide reductase from *Salmonella typhimurium*. Sequence and homology to thioredoxin reductase and other flavoprotein disulfide oxidoreductases. *The Journal of Biological Chemistry*, 265, 10535-10540.
- Taverne, Y. J., Merkus, D., Bogers, A. J., Halliwell, B., Duncker, D. J. & Lyons, T. W. 2018. Reactive oxygen species: Radical factors in the evolution of animal life. *Bioessays*, 40, 1700158.
- Taylor, S. C. & Posch, A. 2014. The design of a quantitative western blot experiment. *BioMed Research International*, 2014, 361590.
- Tejman-Yarden, N., Miyamoto, Y., Leitsch, D., Santini, J., Debnath, A., Gut, J., McKerrow, J. H., Reed, S. L. & Eckmann, L. 2013. A reprofiled drug, auranofin, is effective against metronidazole-resistant *Giardia lamblia*. *Antimicrobial Agents and Chemotherapy*, 57, 2029-2035.

- Thangamani, S., Eldesouky, H. E., Mohammad, H., Pascuzzi, P. E., Avramova, L., Hazbun, T. R. & Seleem, M. N. 2017. Ebselen exerts antifungal activity by regulating glutathione (GSH) and reactive oxygen species (ROS) production in fungal cells. *Biochimica et Biophysica Acta - General Subjects*, 1861, 3002-3010.
- Thangamani, S., Mohammad, H., Abushahba, M. F., Sobreira, T. J., Hedrick, V. E., Paul, L. N. & Seleem, M. N. 2016. Antibacterial activity and mechanism of action of auranofin against multi-drug resistant bacterial pathogens. *Scientific Reports*, 6, 22571.
- Thangamani, S., Younis, W. & Seleem, M. N. 2015. Repurposing clinical molecule Ebselen to combat drug resistant pathogens. *PLOS One*, 10, e0133877.
- Thomas, D., Barbey, R. & Surdin-Kerjan, Y. 1990. Gene-enzyme relationship in the sulfate assimilation pathway of *Saccharomyces cerevisiae*. Study of the 3'-phosphoadenylylsulfate reductase structural gene. *Journal of Biological Chemistry*, 265, 15518-15524.
- Tian, G., Tang, F., Yang, C., Zhang, W., Bergquist, J., Wang, B., Mi, J. & Zhang, J. 2017. Quantitative dot blot analysis (QDB), a versatile high throughput immunoblot method. *Oncotarget*, 8, 58553.
- Toh, S. Y., Citartan, M., Gopinath, S. C. B. & Tang, T.-H. 2015. Aptamers as a replacement for antibodies in enzyme-linked immunosorbent assay. *Biosensors and Bioelectronics*, 64, 392-403.
- Toledano, M. B., Delaunay-Moisan, A., Outten, C. E. & Igarria, A. 2013. Functions and cellular compartmentation of the thioredoxin and glutathione pathways in yeast. *Antioxidants & Redox Signaling*, 18, 1699-1711.
- Toledano, M. B., Kumar, C., Le Moan, N., Spector, D. & Tacnet, F. 2007. The system biology of thiol redox system in *Escherichia coli* and yeast: Differential functions in oxidative stress, iron metabolism and DNA synthesis. *FEBS Letters*, 581, 3598-3607.
- Tomalin, L. E. 2015. *A systems biology approach to investigate the role of peroxiredoxins in responses to hydrogen peroxide*. PhD, Newcastle University.
- Tomalin, L. E., Day, A. M., Underwood, Z. E., Smith, G. R., Dalle Pezze, P., Rallis, C., Patel, W., Dickinson, B. C., Bähler, J., Brewer, T. F., Chang, C. J.-L., Shanley, D. P. & Veal, E. A. 2016. Increasing extracellular H₂O₂ produces a bi-phasic response in intracellular H₂O₂, with peroxiredoxin hyperoxidation only triggered once the cellular H₂O₂-buffering capacity is overwhelmed. *Free Radical Biology & Medicine*, 95, 333-348.
- Toone, W. M., Kuge, S., Samuels, M., Morgan, B. A., Toda, T. & Jones, N. 1998. Regulation of the fission yeast transcription factor Pap1 by oxidative stress: Requirement for the

- nuclear export factor Crm1 (Exportin) and the stress-activated MAP kinase Sty1/Spc1. *Genes & Development*, 12, 1453-1463.
- Trotter, E. W. & Grant, C. M. 2003. Non-reciprocal regulation of the redox state of the glutathione-glutaredoxin and thioredoxin systems. *EMBO Reports*, 4, 184-188.
- Troussicot, L., Burmann, B. M. & Molin, M. 2021. Structural determinants of multimerization and dissociation in 2-Cys peroxiredoxin chaperone function. *Structure*, 29, 640-654.
- Tuncay, A., Noble, A., Guille, M. & Cobley, J. N. 2022. RedoxiFluor: A microplate technique to quantify target-specific protein thiol redox state in relative percentage and molar terms. *Free Radical Biology and Medicine*, 181, 118-129.
- Ueno, M., Masutani, H., Arai, R. J., Yamauchi, A., Hirota, K., Sakai, T., Inamoto, T., Yamaoka, Y., Yodoi, J. & Nikaido, T. 1999. Thioredoxin-dependent redox regulation of p53-mediated p21 activation. *Journal of Biological Chemistry*, 274, 35809-35815.
- Ukuwela, A. A., Bush, A. I., Wedd, A. G. & Xiao, Z. 2018. Glutaredoxins employ parallel monothiol–dithiol mechanisms to catalyze thiol–disulfide exchanges with protein disulfides. *Chemical Science*, 9, 1173-1183.
- Ulrich, K. & Jakob, U. 2019. The role of thiols in antioxidant systems. *Free Radical Biology and Medicine*, 140, 14-27.
- van Leeuwen, L. A. G., Hinchy, E. C., Murphy, M. P., Robb, E. L. & Cochemé, H. M. 2017. Click-PEGylation - A mobility shift approach to assess the redox state of cysteines in candidate proteins. *Free Radical Biology and Medicine*, 108, 374-382.
- Veal, E. A., Tomalin, L. E., Morgan, B. A. & Day, A. M. 2014. The fission yeast *Schizosaccharomyces pombe* as a model to understand how peroxiredoxins influence cell responses to hydrogen peroxide. *Biochemical Society Transactions*, 42, 909-916.
- Veronese, F. M. 2001. Peptide and protein PEGylation: a review of problems and solutions. *Biomaterials*, 22, 405-417.
- Vivancos, A. P., Castillo, E. A., Biteau, B., Nicot, C., Ayté, J., Toledano, M. B. & Hidalgo, E. 2005. A cysteine-sulfinic acid in peroxiredoxin regulates H₂O₂-sensing by the antioxidant Pap1 pathway. *Proceedings of the National Academy of Sciences*, 102, 8875-8880.
- Vivancos, A. P., Jara, M., Zuin, A., Sansó, M. & Hidalgo, E. 2006. Oxidative stress in *Schizosaccharomyces pombe*: Different H₂O₂ levels, different response pathways. *Molecular Genetics and Genomics*, 276, 495-502.

- Wadley, A. J., Chen, Y. W., Bennett, S. J., Lip, G. Y. H., Turner, J. E., Fisher, J. P. & Aldred, S. 2015. Monitoring changes in thioredoxin and over-oxidised peroxiredoxin in response to exercise in humans. *Free Radical Research*, 49, 290-298.
- Wang, R.-S., Oldham, W. M., Maron, B. A. & Loscalzo, J. 2018. Systems biology approaches to redox metabolism in stress and disease states. *Antioxidants & Redox Signaling*, 29, 953-972.
- Watson, W. H., Chen, Y. & Jones, D. P. 2003. Redox state of glutathione and thioredoxin in differentiation and apoptosis. *BioFactors*, 17, 307-314.
- Weiss, M. C., Preiner, M., Xavier, J. C., Zimorski, V. & Martin, W. F. 2018. The last universal common ancestor between ancient Earth chemistry and the onset of genetics. *PLOS Genetics*, 14, e1007518.
- Wiedemann, C., Kumar, A., Lang, A. & Ohlenschläger, O. 2020. Cysteines and disulfide bonds as structure-forming units: Insights from different domains of life and the potential for characterization by NMR. *Frontiers in Chemistry*, 8, 1-8.
- Wiederhold, N. P., Patterson, T. F., Srinivasan, A., Chaturvedi, A. K., Fothergill, A. W., Wormley, F. L., Ramasubramanian, A. K. & Lopez-Ribot, J. L. 2017. Repurposing auranofin as an antifungal: *In vitro* activity against a variety of medically important fungi. *Virulence*, 8, 138-142.
- Williams, C. H., Arscott, L. D., Muller, S., Lennon, B. W., Ludwig, M. L., Wang, P. F., Veine, D. M., Becker, K. & Schirmer, R. H. 2000. Thioredoxin reductase two modes of catalysis have evolved. *European Journal of Biochemistry*, 267, 6110-6117.
- Winther, J. R. & Thorpe, C. 2014. Quantification of thiols and disulfides. *Biochimica et Biophysica Acta (BBA) - General Subjects*, 1840, 838-846.
- Wondafrash, D. Z., Nire'a, A. T., Tafere, G. G., Desta, D. M., Berhe, D. A. & Zewdie, K. A. 2020. Thioredoxin-interacting protein as a novel potential therapeutic target in diabetes mellitus and its underlying complications. *Diabetes, Metabolic Syndrome and Obesity: Targets and Therapy*, 13, 43.
- Wu, Y. X. & Kwon, Y. J. 2016. Aptamers: The “evolution” of SELEX. *Methods*, 106, 21-28.
- Wysocki, R. & Tamás, M. J. 2010. How *Saccharomyces cerevisiae* copes with toxic metals and metalloids. *FEMS Microbiology Reviews*, 34, 925-951.
- Yanagida, M. 2002. The model unicellular eukaryote, *Schizosaccharomyces pombe*. *Genome Biology*, 3, 1-4.

- Ye, S., Chen, X., Yao, Y., Li, Y., Sun, R., Zeng, H., Shu, Y. & Yin, H. 2019. Thioredoxin reductase as a novel and efficient plasma biomarker for the detection of non-small cell lung cancer: a large-scale, multicenter study. *Scientific Reports*, 9, 2652.
- Ying, J., Clavreul, N., Sethuraman, M., Adachi, T. & Cohen, R. A. 2007. Thiol oxidation in signaling and response to stress: detection and quantification of physiological and pathophysiological thiol modifications. *Free Radical Biology & Medicine*, 43, 1099-1108.
- Yoshida, S., Katoh, T., Tetsuka, T., Uno, K., Matsui, N. & Okamoto, T. 1999. Involvement of thioredoxin in rheumatoid arthritis: Its costimulatory roles in the TNF-alpha-induced production of IL-6 and IL-8 from cultured synovial fibroblasts. *Journal of Immunology*, 163, 351-358.
- Younis, W., Thangamani, S. & Seleem, M. 2015. Repurposing non-antimicrobial drugs and clinical molecules to treat bacterial infections. *Current Pharmaceutical Design*, 21, 4106-4111.
- Zeller, T. & Klug, G. 2006. Thioredoxins in bacteria: Functions in oxidative stress response and regulation of thioredoxin genes. *Naturwissenschaften*, 93, 259-266.
- Zhang, J., Li, X., Han, X., Liu, R. & Fang, J. 2017. Targeting the thioredoxin system for cancer therapy. *Trends in Pharmacological Sciences*, 38, 794-808.
- Zhang, X., Selvaraju, K., Saei, A. A., D'Arcy, P., Zubarev, R. A., Arnér, E. S. J. & Linder, S. 2019a. Repurposing of auranofin: Thioredoxin reductase remains a primary target of the drug. *Biochimie*, 162, 46-54.
- Zhang, Y., Lai, B. S. & Juhas, M. 2019b. Recent advances in aptamer discovery and applications. *Molecules*, 24, 941.
- Zhao, J., Wang, M., Yang, Z., Wang, Z., Wang, H. & Yang, Z. 2007. The different behaviors of three oxidative mediators in probing the redox activities of the yeast *Saccharomyces cerevisiae*. *Analytica Chimica Acta*, 597, 67-74.
- Zheng, C. Y., Ma, G. & Su, Z. 2007. Native PAGE eliminates the problem of PEG-SDS interaction in SDS-PAGE and provides an alternative to HPLC in characterization of protein PEGylation. *Electrophoresis*, 28, 2801-2807.
- Zhou, J., Damdimopoulos, A. E., Spyrou, G. & Brüne, B. 2007. Thioredoxin 1 and thioredoxin 2 have opposed regulatory functions on hypoxia-inducible factor-1 α . *Journal of Biological Chemistry*, 282, 7482-7490.

- Zou, L., Lu, J., Wang, J., Ren, X., Zhang, L., Gao, Y., Rottenberg, M. E. & Holmgren, A. 2017. Synergistic antibacterial effect of silver and ebselen against multidrug-resistant Gram-negative bacterial infections. *EMBO Molecular Medicine*, 9, 1165-1178.
- Zuin, A., Gabrielli, N., Calvo, I. A., García-Santamarina, S., Hoe, K.-L., Kim, D. U., Park, H.-O., Hayles, J., Ayté, J. & Hidalgo, E. 2008. Mitochondrial dysfunction increases oxidative stress and decreases chronological life span in fission yeast. *PLOS One*, 3, e2842-e2842.

Appendix

Supplementary material – Appendix 1:

[https://github.com/Chepillay/Tejal-MSc-thesis/blob/main/Supplementary%20material%20-%20Appendix%201%20\(Tejal\).zip](https://github.com/Chepillay/Tejal-MSc-thesis/blob/main/Supplementary%20material%20-%20Appendix%201%20(Tejal).zip)

Computational model script S1:

Keywords

Description: NoName

Modelname: NoName

Output_In_Conc: True

Species_In_Conc: True

GlobalUnitDefinitions

UnitVolume: litre, 1.0, 0, 1

UnitLength: metre, 1.0, 0, 1

UnitSubstance: mole, 1.0, -6, 1

UnitArea: metre, 1.0, 0, 2

UnitTime: second, 1.0, 0, 1

Compartments

Compartment: vol_int, 5.2e-05, 3

Compartment: vol_ex, 0.05, 3

Function definitions

```
Function: function_5, k_hyp_ox , hyp_ox_param , Tpx1_ox_SOH , H2O2_int {  
k_hyp_ox*hyp_ox_param*Tpx1_ox_SOH*H2O2_int  
}
```

```
Function: function_4, V_basal {  
V_basal  
}
```

```
Function: function_3, substrate , Km , V {  
V*substrate/(Km+substrate)  
}
```

```
Function: function_2, k_H2O2_perm , H2O2_ex , vol_ex {  
k_H2O2_perm*H2O2_ex*vol_ex  
}
```

```
Function: function_1, k_H2O2_perm , vol_ex , vol_int , H2O2_int {  
k_H2O2_perm*(vol_ex/vol_int)*H2O2_int*vol_int  
}
```

```
# Reactions
```

```
# disulph_red1
```

```
re8:
```

```
Trx1SH + Tpx1_ox1 > {2.0}Tpx1SH + Trx1_ox
```

```
vol_int*k_disulph_red1*Tpx1_ox1*Trx1SH
```

```
# re8 has modifier(s): Trx1SH
```

```
# H2O2_metab
```

```
reaction_10:
```

```
H2O2_int > $pool
```

```
vol_int*function_3(H2O2_int,Km_H2O2_metab,Vmax_H2O2_metab)
```

```
# H2O2_basal
```

```
reaction_11:
```

```
$pool > H2O2_int
```

```
vol_int*function_4(V_basal)
```

```
# hyp_ox
```

```
reaction_12:
```

```
Tpx1_ox_SOH + H2O2_int > Tpx1_ox_SOOH
```

```
vol_int*function_5(k_hyp_ox,hyp_ox_param,Tpx1_ox_SOH,H2O2_int)
```

Trx1_reduction

reaction_13:

$\text{Trx1}_{\text{ox}} > \text{Trx1SH}$

$\text{vol_int} * k_{\text{Trx_red}} * \text{Trx1}_{\text{ox}}$

Cysp_ox

reaction_6:

$\text{Tpx1SH} + \text{H2O2}_{\text{int}} > \text{Tpx1SOH}$

$\text{vol_int} * k_{\text{cys_ox}} * \text{Tpx1SH} * \text{H2O2}_{\text{int}}$

disulph_form1a

reaction_7:

$\text{Tpx1SH} + \text{Tpx1SOH} > \text{Tpx1}_{\text{ox1}}$

$\text{vol_int} * k_{\text{disulph_form1}} * \text{Tpx1SOH} * \text{Tpx1SH}$

disulph_red3

reaction_4:

$\text{Trx1SH} + \text{Tpx1}_{\text{ox_SOOH}} > \text{Tpx1SH} + \text{Trx1}_{\text{ox}} + \text{Tpx1SOOH}$

$\text{vol_int} * k_{\text{disulph_red3}} * \text{Tpx1}_{\text{ox_SOOH}} * \text{Trx1SH}$

reaction_4 has modifier(s): Trx1SH

disulph_red2

reaction_2:

$\text{Trx1SH} + \text{Tpx1}_{\text{ox2}} > \text{Trx1}_{\text{ox}} + \text{Tpx1}_{\text{ox1}}$

$\text{vol_int} * k_{\text{disulph_red2}} * \text{Tpx1}_{\text{ox2}} * \text{Trx1SH}$

reaction_2 has modifier(s): Trx1SH

disulph_form2

reaction_3:

$\text{Tpx1}_{\text{ox_SOH}} > \text{Tpx1}_{\text{ox2}}$

$\text{vol_int} * k_{\text{disulph_form2}} * \text{Tpx1}_{\text{ox_SOH}}$

```

# disulph_form1b
reaction_1:
    {2.0}Tpx1SOH > Tpx1_ox_SOH
    vol_int*k_disulph_form1*pow(Tpx1SOH,2.0)

# H2O2_efflux
reaction_8:
    H2O2_int > H2O2_ex
    function_1(k_H2O2_perm,vol_ex,vol_int,H2O2_int)

# H2O2_influx
reaction_9:
    H2O2_ex > H2O2_int
    function_2(k_H2O2_perm,H2O2_ex,vol_ex)

# Fixed species

# Variable species
Tpx1SOH@vol_int = 0.0          # uM
Tpx1_ox_SOOH@vol_int = 0.0    # uM
Trx1SH@vol_int = 0.7          # uM
Tpx1SH@vol_int = 4.0          # uM
Trx1_ox@vol_int = 0.0         # uM
Tpx1_ox_SOH@vol_int = 0.0     # uM
Tpx1_ox1@vol_int = 0.0        # uM
Tpx1_ox2@vol_int = 0.0        # uM
H2O2_ex@vol_ex = 500.0        # uM
Tpx1SOOH@vol_int = 0.0        # uM
H2O2_int@vol_int = 0.0        # uM

```

Parameters

k_H2O2_perm = 0.000344145752146 # l s⁻¹
Vmax_H2O2_metab = 59.1101286989 # uM s⁻¹
Km_H2O2_metab = 0.00727013132059 # uM
k_cys_ox = 20.0 # uM⁻¹ s⁻¹
k_disulph_form1 = 1.00755933105 # uM⁻¹ s⁻¹
k_disulph_form2 = 3.43491295032 # s⁻¹
k_disulph_red1 = 0.189972075394 # uM⁻¹ s⁻¹
k_disulph_red2 = 0.142827879843 # uM⁻¹ s⁻¹
k_disulph_red3 = 0.029420345318 # uM⁻¹ s⁻¹
k_Trx_red = 33.6 # s⁻¹
k_hyp_ox = 0.012 # uM⁻¹ s⁻¹
V_basal = 5.27874025944 # uM s⁻¹
hyp_ox_param = 1.0